REPORT ON GEOLOGICAL SURVEY OF THE SULTANATE OF OMAN

CONSOLIDATED REPORT

MAY. 1983

JAPAN INTERNATIONAL COOPERATION AGENCY
METAL MINING AGENCY OF JAPAN

REPORT ON GEOLOGICAL SURVEY OF THE SULTANATE OF OMAN

CONSOLIDATED REPORT

MAY, 1983

JAPAN INTERNATIONAL COOPERATION AGENCY

METAL MINING AGENCY OF JAPAN

PREFACE

The Government of Japan, in response to the request of the Government of the Sultanate of Oman, decided to conduct of geological survey for mineral exploration in the Sultanate of Oman, and commissioned its implementation to Japan International Cooperation Agency.

Considering its technical aspects, the agency sought collaboration of Metal Mining Agency of Japan to accomplish the task within a period of three years.

This survey has been carried out for three years from 1980 to 1982, and it was able to accomplish on schedule under close cooperation with the Government of the Sultanate of Oman and its various authorities.

This report submitted hereby summarizes the results of the various survey performed during three years.

We wish to express our heartfelt gratitude to the Government of the Sultanante of Oman and other authorities concerned for their kind cooperation and support extended to the Japanese survey team.

March 1983

Keisuke Arita
President
Japan International Cooperation Agency

Masayuki Nishiie
President
Metal Mining Agency of Japan

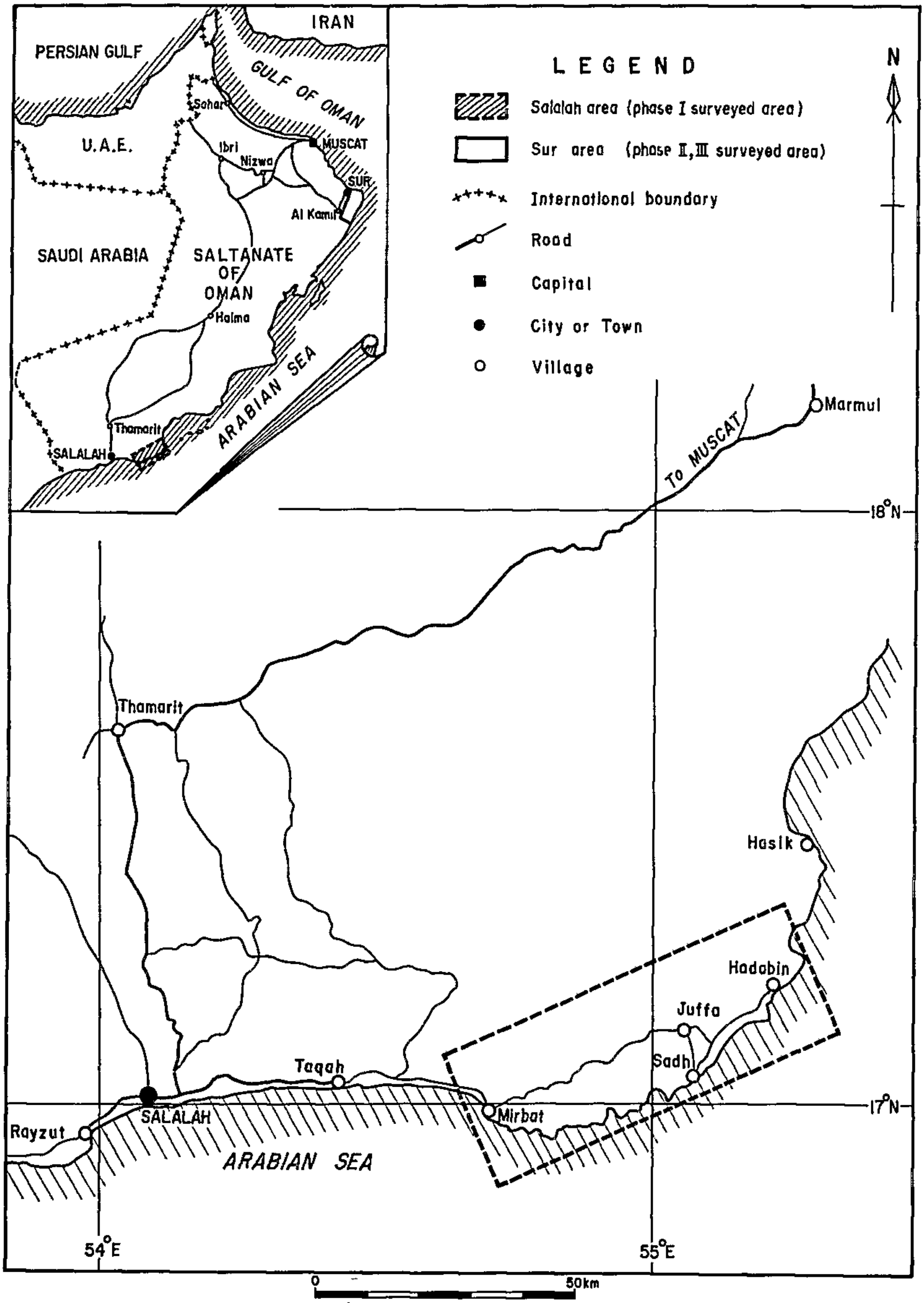

Fig. 1 Location Map of the Salalah Area

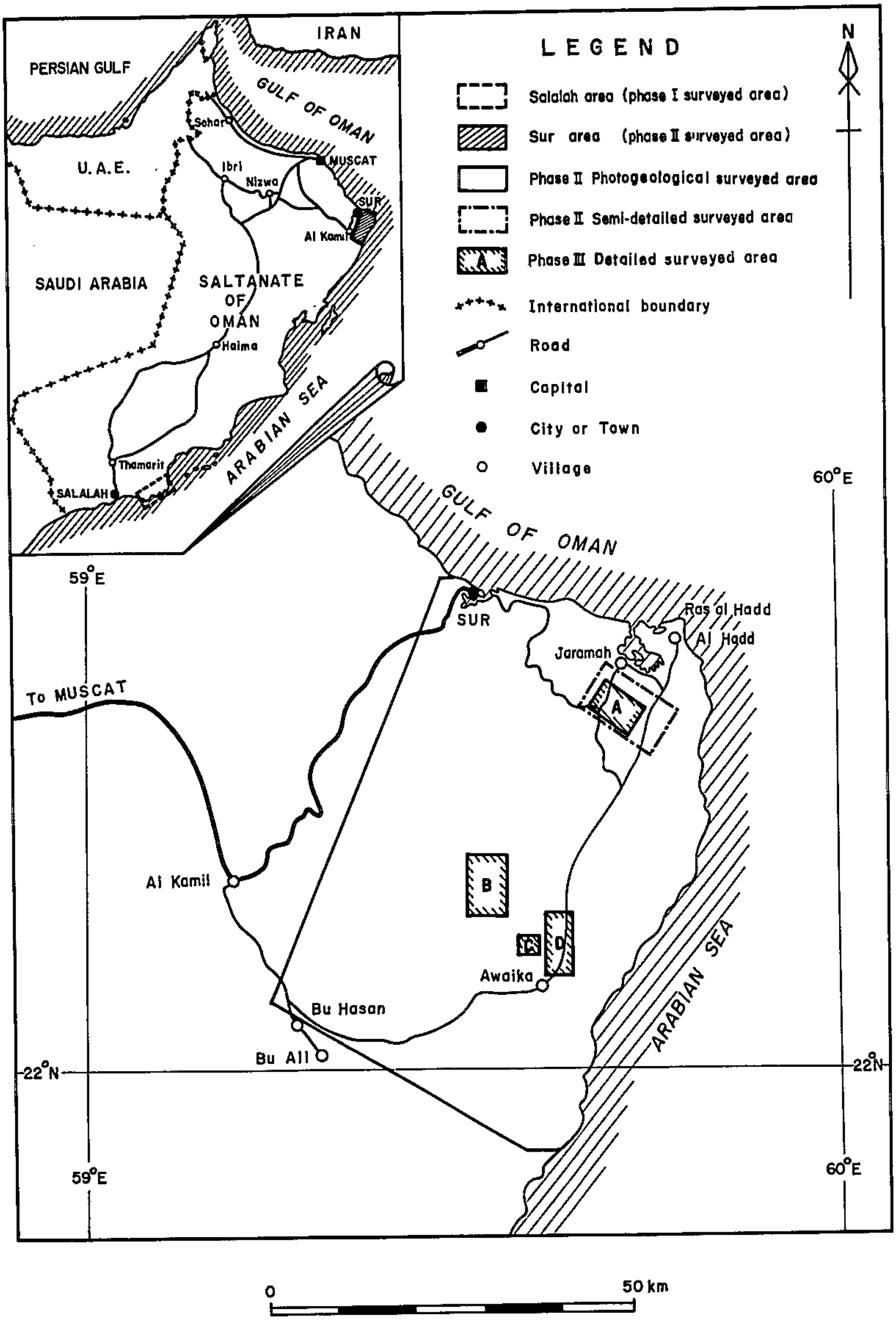

Fig. 2 Location Map of the Sur Area

CONTENTS

CHAPTER III. SUR AREA

CHAPTER IV. CONCLUSION AND EVALUATION

LIST OF ILLUSTRATION

ABSTRACT

This report summarizes the results of mineral exploration in the surveyed areas, Salalah area and Sur area, of the Sultanate of Oman which has been carried out for three years from 1980 to 1982.

The survey was conducted to investigate the possibility of ore deposits by revelation of the stratigraphy, geologic structure, igneous activity and mineralization of the area as well as the mutual relation between them.

The survey has been carried out in the Salalah area in 1980, and the Sur area in 1981 and 1982.

Salalah area is located south of Muscat, capital of Oman, about 1,000 km facing the Arabian Sea and total area is 1,500 km^2.

In the Salalah area, geological survey and measurement of radioactivity were conducted.

As the result of the survey, stratigraphy, geologic structure and igneous activity of the area were clarified, and only small copper occurrences in pegmatite veins and weak lead mineralization in barite veins were confirmed. Also the possibility of uranium deposit could not be recognized in the Mirbat Sandstone Formation. The survey for next year in the Salalah area, therefore, has been suspended.

Sur area is located southeast to Muscat about 150 km facing the Arabian Sea and the Gulf of Oman, has whole area of 3,400 km^2.

In 1981, photogeology on whole area and geological survey on the known manganese outcrops were carried out in the Sur area.

As the result of the survey, outline of the stratigraphy and geologic structure were clarified and many new manganese outcrops were found in the area.

In 1982, geological survey including trenching survey and drilling exploration have been conducted in the area where manganese outcrops distribute relatively dense, and occurrences, scale and continuity of the manganese deposits were clarified.

The manganese deposits are embedded in the Halfa Formation, Jurassic to Early Cretaceous, which is composed of chert and shale alternation.

The deposits particularly dominated in the Middle Member of the Halfa Formation.

The Halfa Formation shows very complicated geologic structure, folded and faulted, caused by Late Cretaceous thrust movement and Middle Tertiary uprift movement.

Three to six ore horizons have been confirmed in the area and many outcrops can be recognized in the whole area of the Halfa Formation.

Ore genesis is considered that stratiformed sedimentary ore deposit originates volcanism, and ore deposits are composed of several small ore beds.

The continuity of ore bodies was confirmed until thirty meters depth by the drilling exploration.

As a result of discussion and evaluation based on the numerous data, although manganese ore deposits are recognized in the Sur area, it seems that the development of ore deposits is not profitable at the present time because of their small scale, thin bed type, low grade and sporadic distribution.

CHAPTER I. GENERAL DESCRIPTION

1. The Purpose of the Survey

This survey has been conducted in the Salalah area and the Sur area having the purpose of the survey as follows.

In the Salalah area, investigation of stratigraphy and mutual relation between geologic structure and mineralization of the Precambrian and Paleozoic rocks, distributing in the small area of southeast of the Arabian Peninsula, were carried out in order to clarify a possibility of ore deposits.

In the Sur area, investigation of stratigraphy and geologic structure of the Halfa Formation of Triassic to Cretaceous age, embedding manganese ore deposits, was conducted in order to clarify the embedded situation of manganese ore deposits.

2. Outline of the Survey

This survey has been carried out for three years from 1980 to 1982, and the substances of the survey are shown in the Table 1.

3. Member of the Survey Team

Field work and laboratory work were carried out by Metal Mining Agency of Japan (MMAJ) with cooperation of the Ministry of Petroleum and Minerals of Oman.

The Members of the survey team of each year are shown in the Table 2.

4. Location and Access

4–1 Salalah Area

The survey area is 1,500 km^2 and located east to Salalah, capital city of Dhofar state of southern Oman (Fig. 1).

Muscat, capital of Oman, and Salalah are connected with international and domestic airlines and highway road.

Distance between Salalah and Mirbat, base camp point and located in the western part of the survey area, is about 70 km and it takes two hours by car.

Mirbat and Hadabin, eastern part of the area, are connected with truck road about 50 km.

4–2 Sur Area

The survey area, about 3,400 km^2, is located southeast of Muscat and southeastern end of

Table 1 Outline of the Field Survey in Phase Ⅰ, Ⅱ, Ⅲ

		1980	1981	1982
Period		Salalah Area 26 Sept. 1980 | 25 Dec. 1980	Sur Area 23 Oct. 1981 | 28 Dec. 1981	Sur Area 8 Nov. 1982 | 28 Dec. 1982
Geological survey and Photo-interpretation		Geo. – 1,500 km^2 (1/50,000) Photo. – 1,500 km^2 (1/50,000)	Geo. – 77 km^2 (1/20,000) Photo. – 3,400 km^2 (1/50,000)	Geo. – 95 km^2 (1/10,000) Trench – 375m (1/200)
Drilling Exploration				17 holes Total length 300 m
Laboratory Work	Thin Section	65	37	30
	Polished Section	6	26	16
	Assay	ore 20 rock 10	ore 206	ore 254
	X-ray	10	30	17
	K-Ar dating	5	–	–
	Fossil	12	26	20
	Spectrographic Analysis	–	50	–

Table 2 Member of the Survey Team in Phase Ⅰ, Ⅱ, Ⅲ

		1980	1981	1982
Japanese Member	Team Leader	Tsuyoshi Suzuki	Hirofumi Taniguchi	Haruo Kousaka
	Planning and Organization	Kyuzo Tadokoro Katsuzo Sawaya Kazunori Kano Hisamitsu Moriwaki	Hisamitsu Moriwaki Toshio Koizumi Tadaaki Ezawa	Hiroshi Iwasaki Takahisa Yamamoto
	Geologist	Kenji Wakita Akitsura Shibuya Kenichi Takizawa Yoshiaki Shibata	Masahiko Nouno Atsumu Nonami Masaaki Matsuoka Tadashi Yamakawa Yoshiaki Shibata	Masahiko Nouno Akio Abe Yoshiaki Shibata Norifumi Ushirone
	Drilling Operator			Yuuji Narita Kyozo Obara
Omani Member	Planning and Organization	Mohammed Kassim	Mohammed Kassim	Mohammed Kassim
	Geologist	Dr. Leif Carlson Hilal Mohammed Al Ezri Mohammed I. Khalifa	Naser Saleem Hareb Hamad	Mohammed El Hassan Rugheim Cherian Zachariah Adil Mansoor Mahfoodh

the Oman Mountains (Fig. 2).

Between Muscat and Jaramah, base camp point, is connected with pavement road and gravel road, about 360 km long, via Bid Bid, Ibra, Al Kamir and Awaika taking eight hours by car.

5. Topography and Climate

5–1 Salalah Area

The topography of the survey area is divided roughly into two types reflecting geology of the area.

From Mirbat to Hadabin, main part of the survey area, shows a peneplane topography with 0 ~ 300 m altitude.

Jabal Samhan area, north of the peneplane area, shows a wide tableland accompanying with escarpment of 1,000 ~ 1,500 m altitude.

In the peneplane area, NW–SE system ridges and drainages are formed by dyke swarm and mesa-shape topography, with Cretaceous to Tertiary sediments as same as the Jabal Samhan, are recognized near the shore.

5–2 Sur Area

The topography in the survey area is characterized by flat and/or moderate hills of chert and shale, and high land and/or tableland of limestone associated with escarpment.

Northern periphery shows 100 ~ 200 m altitude, and western periphery, 500 ~ 1,400 m altitude, of the survey area are formed high land and/or tableland of limestone. From the central area surrounded by limestone to the coast area of the Arabian Sea, moderate hill topography of 50 ~ 150 m height, composed of chert and shale alternation, are recognized.

CHAPTER II. SALALAH AREA

1. Summary of the Project Area

As the result of geological survey and mineral exploration, many basic data on stratigraphy, igneous activity and mineralization were obtained.

Stratigraphy of the several rocks in the area was established compared with geochronologic data. In particular, those facts have been clarified that the Precambrian rocks are equivalent to the Arabian Shield and that the Mirbat Sandstone Formation is not terrestrial sediments but shallow-sea sediments.

Mineral occurrences in the area are observed such as small amount of chalcopyrite, malachite and pyrite within pegmatite veins and a few galena in barite veinlets embedded in the Mirbat Sandstone: therefore these mineral occurrences can not be considered as economical targets.

As the result of the detailed survey on the Mirbat Sandstone Formation in order to investigate a possibility of uranium deposits, the possibility could not be obtained.

2. Geology

2–1 Outline of Geology

The Precambrian rocks are thought to be a part of the southern Arabian complex, which distribute in south of Saudi Arabia, Yemen and Aden, and consist of the Juffa Gneiss and Sadh Gneiss (770 ~ 610 m.y.), granodiorite (760 ~ 600 m.y.) intruding the gneisses, pegmatite (570 m.y.) and quartz monzonite (530 m.y.).

The Mirbat Sandstone Formation distributes in the western area covering dolerite dykes (440 m.y.) unconformably, and can be recognized to have similar characteristics as the Wadid Sandstone which is Carboniferous to Lower Permian and distributes from Saudi Arabia to Yemen.

The Umm er Radhuma Formation, Cretaceous to Tertiary sediments, rests unconformably upon the Precambrian rocks and Mirbat Sandstone Formation forming tableland and/or mesa.

2–2 Stratigraphy

Geologic stratigraphy of the survey area is divided from the bottom to upward as follows (Fig. 6).

Precambrian (Juffa and Sadh gneisses)	gneiss, granodiorite, pegmatite vein and quartz monzonite
Lower Paleozoic (dyke)	basic dyke (dolerite, basalt and andesite) acidic dyke (quartz porphyry, rhyolite and dacite)

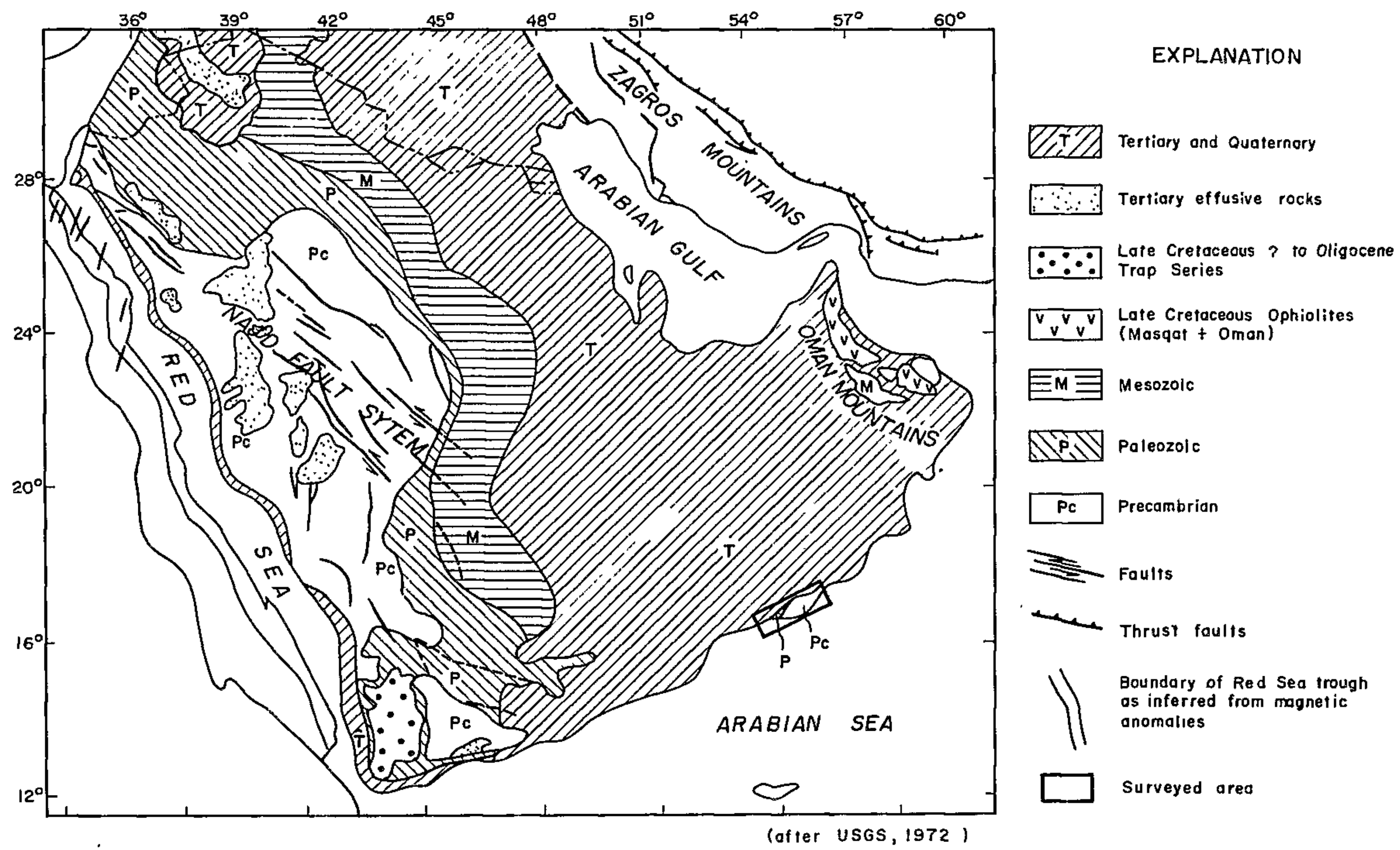

Fig. 3 Geologic Framework of the Arabian Peninsula

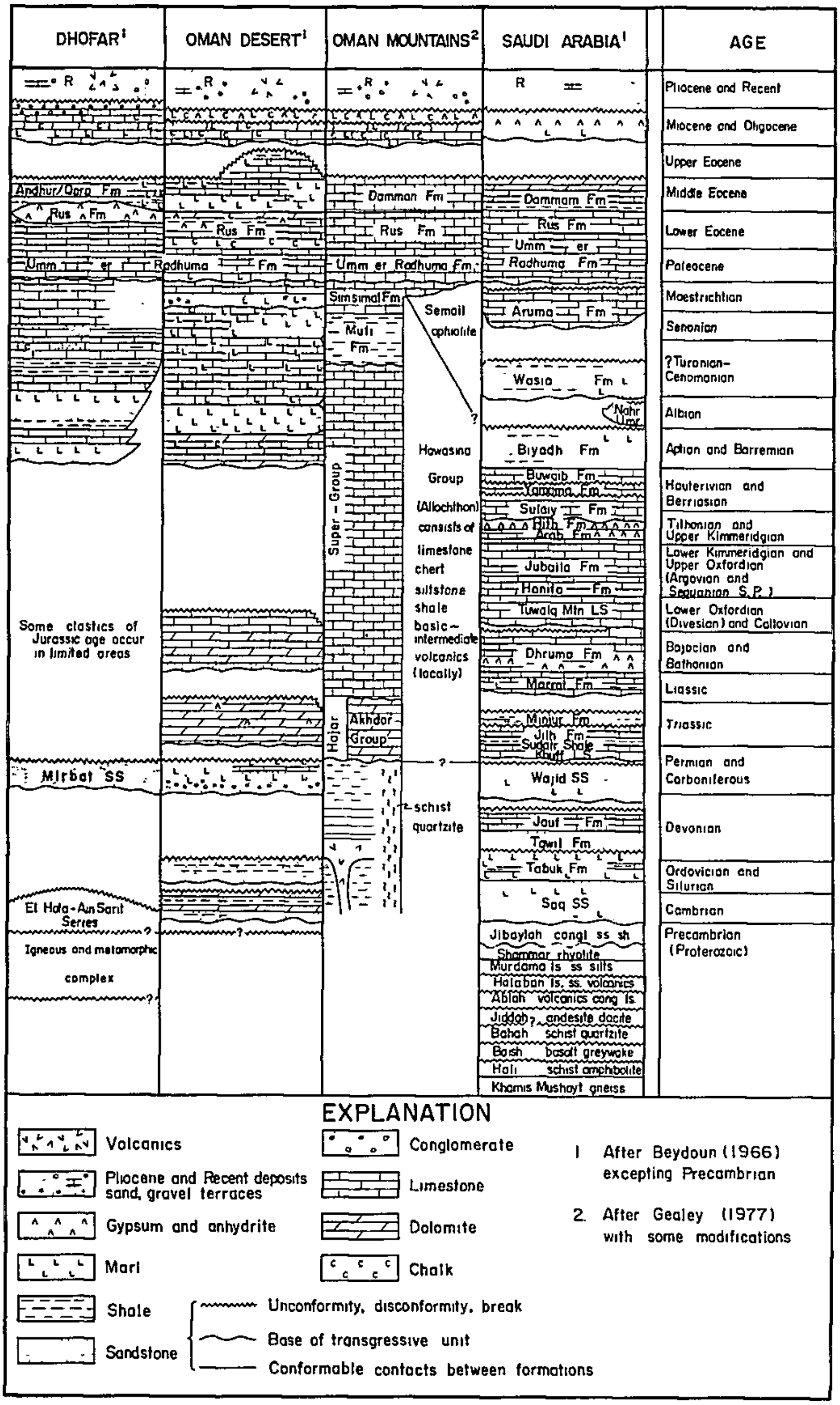

Fig. 4 Schematized Correlation of Stratigraphic Units in Oman and Saudi Arabia

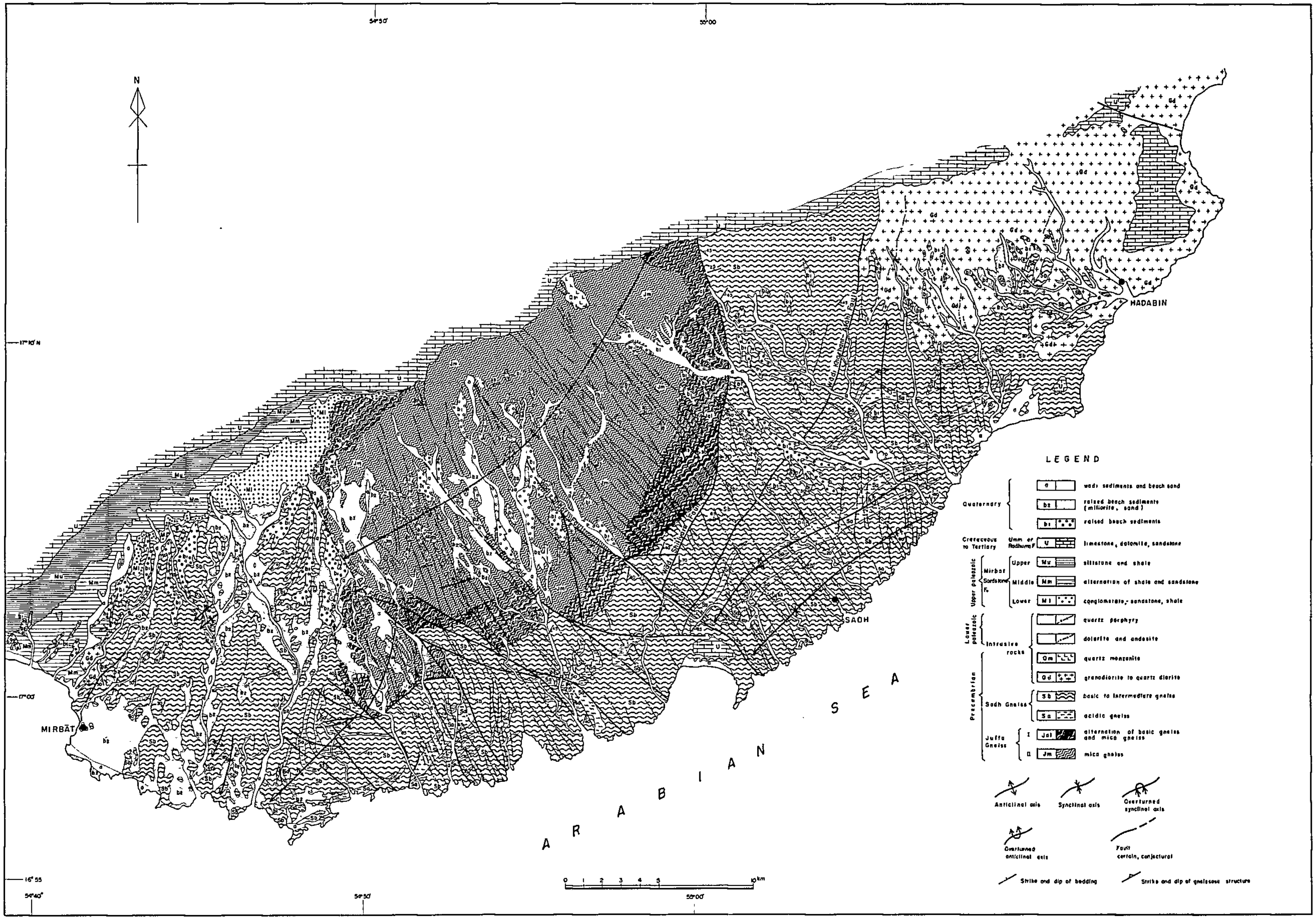

Fig. 5 Geological Map of the Salalah Area

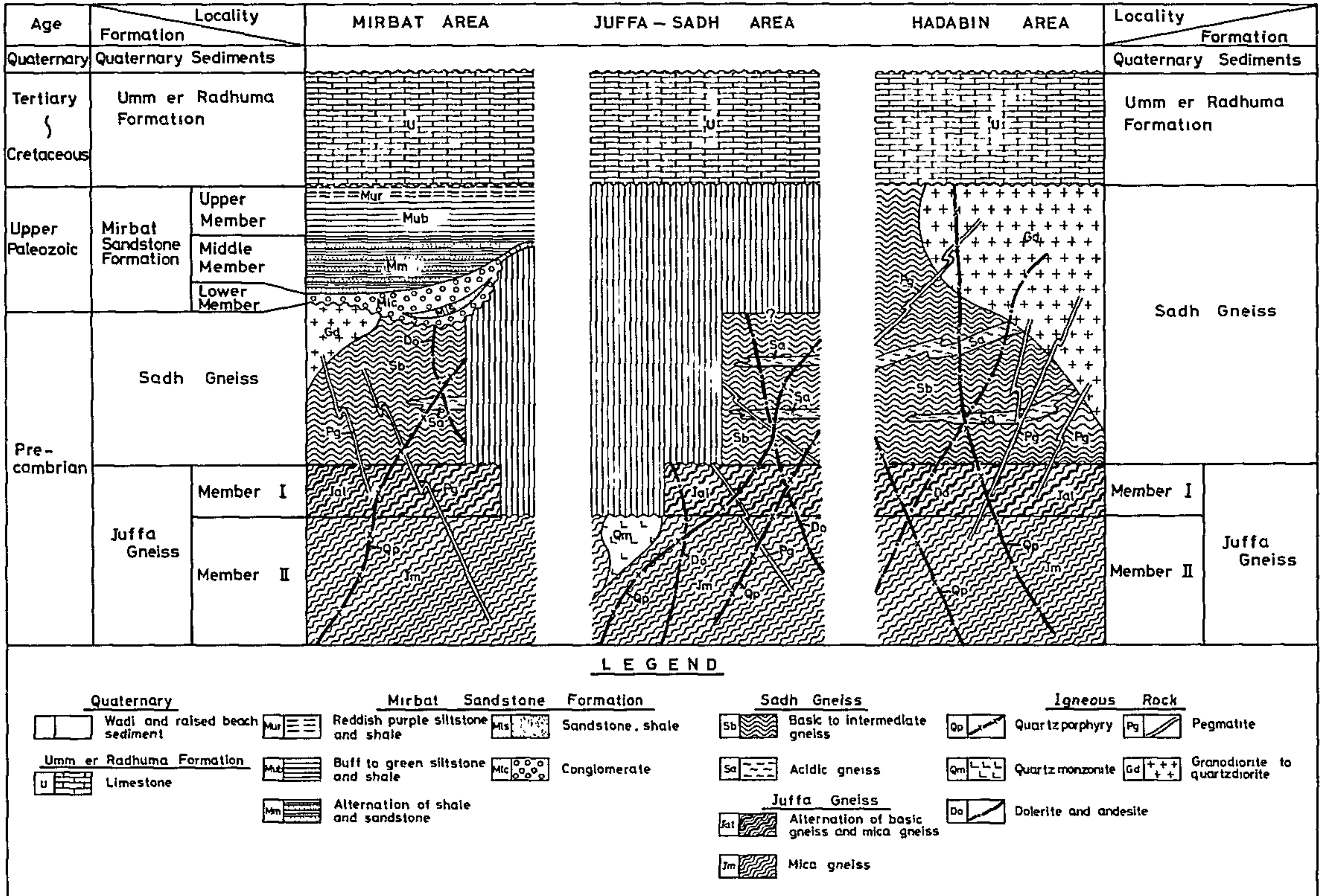

Fig. 6 Schematic Geological Columnar Section of the Salalah Area

Upper Paleozoic (Mirbat S.F.)	conglomerate, sandstone, siltstone, shale and limestone
Cretaceous ~ Tertiary (Umm er Radhuma F.)	limestone, dolomite, siltstone and santstone
Quaternary	raised beach sediments and fluvial sediments

2–2–1 Precambrian

(1) Juffa gneiss

This gneiss composes the lowest part of the areal geology, and is divided into two members, the II member and the I member from the bottom. The former consists of mica gneiss and the latter consists of mica gneiss and basic gneiss.

a) II Member

This member distributes in the central part of the survey area forming NE–SW anticlinal core (Fig. 5).

The dominant rock facies are graysh white mica gneiss composed mainly of muscovite, biotite, quartz, feldspar and garnet originating from pelitic and/or psammitic sediments.

b) I Member

This member overlies and surrounds the II member, and the main rock facies are gray to pinkish mica gneiss and black to dark green basic gneiss alternation.

Although constituent minerals of the mica gneiss are same as the II member, the minerals of the basic gneiss are composed of hornblende, feldspar, epidote, quartz and garnet.

Chemical assay values of the Juffa gneiss explain that the mica gneiss originated from pelitic and/or psamitic sediments, and the basic gneiss originated from basic igneous rocks or volcanic rocks.

(2) Sadh gneiss

Sadh gneiss comformably overlies Juffa gneiss, and distributes widly surrounding Juffa gneiss.

Main rock facies consist of basic to intermediate gneiss. The gneiss intercalates locally acidic gneiss.

Constituent minerals of basic to intermediate gneiss are composed mainly of hornblende, plagioclase, epidote, quartz, biotite and garnet.

Quartz, plagioclase and biotite are dominant minerals and hornblende decreases in the intermediate gneiss. Acidic gneiss does not include hornblende, but pottash feldspar is included.

Sadh gneiss is composed mainly of basic volcanic-origin gneiss and pelitic and/or psammitic

Table 3 Chemical Composition and C. I. P. W. Norm

Formation Name	Juffa Gneiss			Sadh Gneiss				Intrusive rocks: Mirbat stock	Intrusive rocks: Hadabin body		Intrusive rocks: Arzaq stock		Intrusive rocks: Acidic dike			Intrusive rocks: Basic dike		Intrusive rocks: Pegmatite dike
Sample No.	D-072	25-1-1*	25-2*	A-008	A-021	28-A-109*	28-A-110*	D-026	C-204	22-6*	B-028	22-2*	A-020	D-073	25-3-1*	D-071	26-B-102*	D-045
Location	Wadi Khorhant	Main Road	Wadi Shaat	Wadi Bayt Said	Wadi Shaat	Wadi Shaat	Wadi Adin	Wadi Ercahol	Wadi Anib	Wadi Hadabin	Wadi Arzaq	Wadi Arzaq	Wadi Khorhant	Wadi Khorhant	Main Road	Wadi Khorhant	Wadi Khorhant	Wadi Khorhant
Rock Name	Epidore hornblende gneiss	Biotite gneiss	Biotite gneiss	Biotite gneiss	Biotite hornblende gneiss	Hornblende gneiss	Hornblende gneiss	Grano-diorite	Grano-diorite	Grano-diorite	Quartz monzonite	Quartz monzonite	Quartz porphyry	Quartz porphyry	Quartz porphyry	Dolerite	Dolerite	Pegmatite
Chemical composition																		
SiO_2 %	46.49	65.26	68.86	73.18	47.98	49.80	37.16	70.44	71.07	70.39	74.58	74.29	73.84	73.76	78.99	49.35	54.62	73.34
TiO_2	1.24	0.61	0.60	0.25	1.17	1.35	3.21	0.14	0.19	0.21	0.08	0.14	0.05	0 06	0.06	0.76	0.95	0.06
Al_2O_3	16.11	17.54	14.70	13.82	20.41	14.08	12.63	16.27	15 72	15.55	13.56	13.27	13.48	13 60	12.93	16.60	16 44	14.49
Fe_2O_3	4.17	1.40	0.96	0 60	4.03	3.54	10.88	0.32	0.76	0.76	0.64	1.03	0.43	0.79	0.52	1.55	3.23	0.32
FeO	6.93	3.70	3.92	1.69	6.43	9.56	11.68	1.58	1.54	1.85	1.51	1.11	2.01	2.44	1.26	6.93	4.92	1.54
MnO	0.25	0.11	0.14	0.04	0.23	0.22	0.55	0 05	0.06	0.06	0 01	0.02	0 04	0.03	0.01	0.19	0.11	0 04
MgO	7.78	1.98	1.56	0.41	4.14	6.99	8.76	0.67	0.51	0.65	0 09	0.34	0.12	0.11	0.12	8 98	3 41	0.25
CaO	12.47	1.33	1.85	1.58	7.71	10 19	9.36	2.29	1.91	2 10	0.42	0.48	0 85	0.68	0 20	7 49	6.82	1.33
Na_2O	2.39	3.25	3 76	3.51	4.12	2.03	1.32	4.80	4.20	4 67	3.51	3.81	3 83	3.37	0 13	2 39	2.99	4.51
K_2O	0.27	2 97	2.35	3.56	1 07	0.86	0.77	1.58	2 88	2.41	4.67	4.85	4.02	4 42	3.80	1.67	2.10	2.56
P_2O_5	0.11	0.15	0 18	0.11	0.59	0.15	0.51	0.07	0 12	0.11	0.03	0 06	0 04	0 03	0 06	0.12	0.19	0.05
CO_2	-	-	-	-	-	-	-	0 53	-	-	-	-	-	-	-	0.79	1.94	0.50
$H_2O(+)$	1 09	1.07	0 83	0.28	1.48	0.38	2 48	0.59	0.30	0.14	0.30	0 09	0.36	0.32	1.21	2.47	1.82	0.53
$H_2O(-)$	0.12	0 22	0.12	0.26	0.04	0 18	0.08	0.26	0.18	0 23	0.18	0.24	0 28	0.14	0.52	0.26	0.18	0.14
Total	99.42	99.59	99.83	99.29	99.40	99.33	99.39	99.59	99.44	99 13	99.58	99.73	99.35	99.75	99 81	99.55	99.72	99.66
CIPW norm																		
Q		27.3	29 4	34.2		1 9		30 9	30.0	27.8	34 1	32.0	32.5	34.1	62.3		13 0	34.2
C		6.8	2.9	1.6				3 8	2 4	1 8	1.9	0 9	1.2	2.0	8.3		1.6	3.0
or	1.7	17.8	13.9	21.1	6 1	5.0	4.5	9.5	17.3	14.5	27.8	28 4	23.9	26 2	22.3	10.0	12 2	15.0
ab	20.4	27.3	32 0	29.9	34.6	17.3	11 0	40 4	35.7	39.3	29.9	32.0	32.5	28.3	1 0	20.4	25.2	38 3
an	32.3	5 8	8.3	7 0	34.2	26.7	26.4	8.1	8 6	9.5	1.9	2.5	4.2	3.3	1.1	29.5	20.9	3 6
di wo	12 0				0.2	9 6	7.0									0 8		
di en	8.0				0.1	5.3	4.7									0.5		
di fs	3.1				0.1	3.9	1 8									0.2		
hy en	1.5	4.9	3.9	1 0	1.3	12 0	3.9	1.7	1.3	1 6	0.2	0.8	0 3	0.3	0.3	15.8	8.5	0.6
hy fs	0 6	4.9	5 7	2.4	0 9	8.9	1 5	2.5	2.0	2.5	2.1	0.9	3.3	3.7	1.8	7.3	5.0	2.5
fo	6.9				6.2		9.3									4.3		
fa	3.0				4.6		3.9									2.2		
mt	6.0	2.1	1.4	0.9	5.8	5.1	15.7	0.5	1.2	1.2	0 9	1.4	0 7	1.2	0 7	2.3	4.6	0.5
il	2.4	1.2	1.2	0.5	2 3	2.6	6.1	0.3	0.3	0.5	0.2	0 3	0 2	0.2	0.2	1.5	1.8	0.2
ap	0.3	0.3	0.3	0 3	1.3	0.3	1.3		0 3	0 3						0.3	0.3	
cc								1.2								1.8	4.4	1.1
Total	98.2	98.4	99 0	98.9	97 7	98.6	97.1	98 9	99.1	99.0	99.0	99.2	98.8	99.3	98.0	96.9	97.5	99.0
Q+or+ab	22.1	72 4	75 3	85.2	40.7	24.2	15.5	80 8	83.0	81.6	91.8	92.4	88.9	88.6	85.6	30 4	50.4	87.5
D.I.	22.5	73.6	76.1	86.1	41.7	24 5	16.0	81.7	83.8	82.4	92.7	93.1	90.0	89 2	87.3	31.4	51.7	88.4

* ... JICA (1979)

Table 4 Chemical Composition of Various Rocks

Composition \ Sample No.	1	2	3	4	5	6	7	8	9	10	11	12	13	14	15
SiO_2	63.50	69.60 ~ 77.74	79.03	49.06	50.48	45.31 ~ 47.63	66.34 ~ 74.12	70.18	73.30	70.8	56.5	48.7	45.0	64.43	66.70
TiO_2	0.71	0.18 ~ 0.50	0.40	1.36	1.45	1.51 ~ 3.37	0.15 ~ 0.39	0.39	0.11	0.45	-	2.5	2.6	0.68	0.42
Al_2O_3	16.88	7.29 ~ 11.32	10.81	15 70	15.34	13.33 ~ 16.94	13.18 ~ 16.92	14.47	12.33	12.9	18.5	20.6	19.8	15.51	16.20
Fe_2O_3	2.18	0.73 ~ 1.05	0.55	5.38	3.84	3.98 ~ 6.67	0.62 ~ 2.14	1.57	2.58	3.1	4.4	1.1	1.1	1.73	0.92
FeO	3.25	0.66 ~ 2.62	1.63	6.37	7.78	4.69 ~ 7.97	0.70 ~ 2.81	1.78	1.28	0.2	0.7	8.35	9.9	3.12	2.80
MnO	0.05	0.01 ~ 0.07	0.04	0.31	0.20	0.16 ~ 0.21	0.01 ~ 0.02	0.12	0.02	-	-	-	-	0.09	0.10
MgO	2.23	0.72 ~ 1 94	0.94	6.17	5.79	5.34 ~ 7.67	0 51 ~ 2.33	0.88	0.26	0.2	0.2	4.3	5.6	3.27	2.10
CaO	0.64	1.57 ~ 4.23	1.68	8.95	8.94	7.09 ~ 11.59	2.08 ~ 5.85	1.99	0.46	1.2	0.9	6.6	7.8	4.98	4 60
Na_2O	1.97	1.56 ~ 2.96	3.08	3.11	3.07	2.33 ~ 3.38	3.09 ~ 5.10	3.48	4.55	5.85	4.6	4.03	4.65	4.02	3.80
K_2O	4.00	2.14 ~ 3.16	1.43	1.52	0.97	0.52 ~ 0.67	0.24 ~ 2.45	4.11	4.20	7.73	10.2	1.4	1.55	1.29	1.30
P_2O_5	0.18	0.07 ~ 0.18	0.08	0.45	0.25	0.04 ~ 0.27	0.02 ~ 0.06	0.19	0.05			n d	n.d	0.25	0.10
H_2O+	2.70	0.73 ~ 2.00	0.39	1.62	1.89	3.03 ~ 4.15	0.58 ~ 1.62	0.84	0.86	1.35	3.9	1.8	1.6	1.12	1.03
$H_2O\_$	0.53	0.01 ~ 0 40	0.01				0.11 ~ 0.66								
Total	98.82		100.10							100.00	99.9	99.65	99.75	100.5	100.2

1. Average of 17 slates and their metamorphosed equivalents in the northern Kiso district in Japan [Katada M. (1967)]
2. Range in Compositions of 7 non-metamorphosed sandstone [ditto]
3. Biotite-gneiss [ditto]
4. All basalt (198 samples) [Daly, R.A. (1933)]
5. All diabase (90 samples) [ditto]
6. Actinolite epidote schist (4 samples) [Shibata H. (1968)]
7. Trondjemite (9 samples) [ditto]
8. All granite (546 samples) (Daly)
9. Alkaline granite (12 samples) (Daly)
10. Rhyolite [USGS 1966 after Barthoux 1922]
11. Granular leucocratic microsyenite [ditto]
12. Basalt of Gabal El Abd [ditto]
13. Basalt of Wadi Masour [ditto]
14. Hornblende quartz diorite of Arabian plutonics [Green Wood and Brown 1973]
15. Quartz diorite " [ditto]

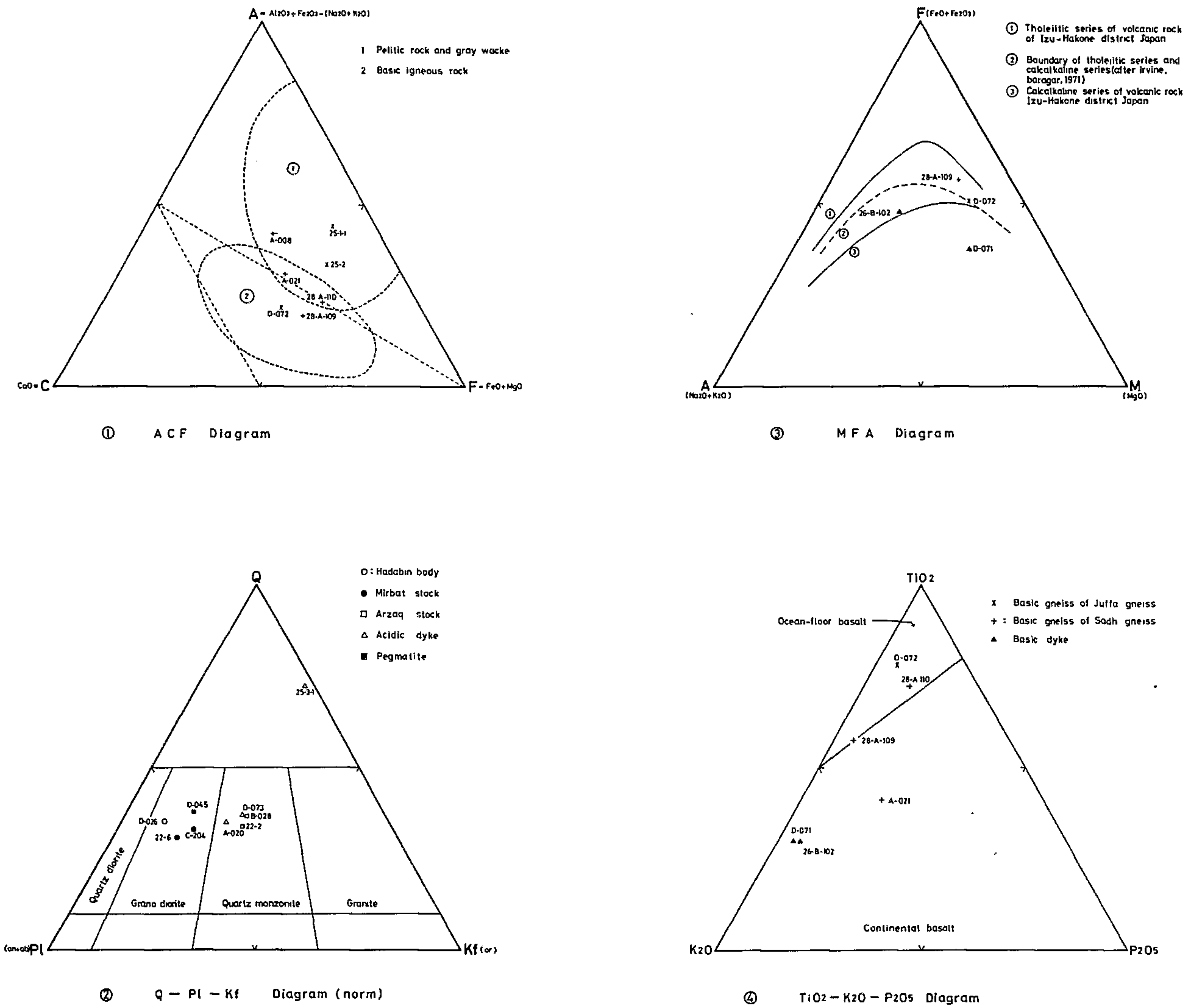

Fig. 7 Diagram of Chemical Composition

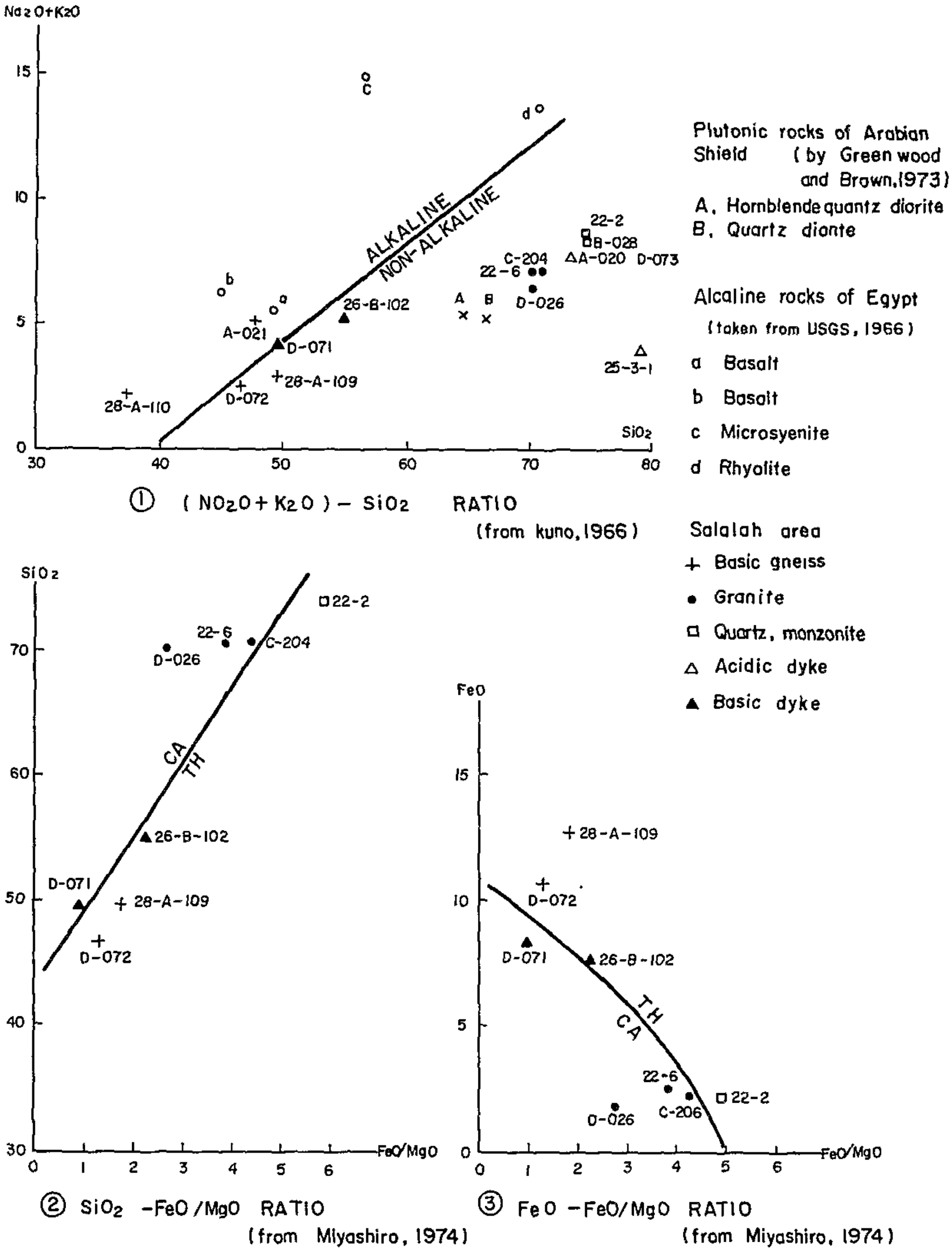

Fig. 8 Ratio of Chemical Composition

sediments-origin gneiss such as Juffa gneiss.

(3) Granodiorite

Hadabin mass in the northeastern area and Mirbat body in the western area are recognized.

These intrusive mass show the rock facies, composed mainly of granodiorite and localy quartzporphyry with gneissose structure.

Hadabin mass particularly dominate a gneissose rock facies in the marginal zone of it showing irreguralar shape and changes to homogeneous rock facies towards the inner zone.

Mirbat mass is a small, extending N–S and gneissose structure is vague.

(4) Pegmatite vein

Pegmatite veins in the survey area are observed in the precambrian gneisses and granodiorite mass, particularly dominant in the gneiss, and are recrystalline pegmatite composed mainly of quartz, potash feldspar and muscovite without rare elements nor uranium minerals.

(5) Quartz monzonite

A quartz monzonite stock is observed in the north-central part of the survey area.

The rock facies are reddish grey to reddish brown tint holocrystalline rock, and it is megascopically similar to acidic dykes but results of K-Ar dating give different ages.

Constituent minerals are composed mainly of quartz, plagioclase, potash feldspar, biotite and muscovite.

2–2–2 Lower Paleozoic (dyke rocks)

A numerous basic and acidic dyke swarms which intrude the Precambrian rocks tending NW–SE, N–S and NE–SW direction can be observed widespread in the survey area.

1) Basic dykes

Basic dykes trend NW–SE predominantly, and have 3 to 5 meters width extending from a few to several tens killometers.

Dolerite and basalt are main rock facies and andesite to diorite porphyry can be partially recognized. Constituent minerals are composed mainly of plagioclase, pyroxene, biotite, quartz and sericite, and chloritization can be partially observed.

These dykes intruded in the Precambrian rocks and some of them are unconformably overlain by Mirbat Sandstone Formation and Umm er Radhuma Formation. K-Ar dating resulted Ordovician to Silurian age.

2) Acidic dykes

Acidic dykes trend NW–SE, intruding Precambrian rocks, and dominate in the central area.

Width of the dyke is 2 to 3 meters extending tens kilometers continuously.

Reddish gray to reddish brown tint quartz porphyry is the main rock facies grading into rhyolite towards the marginal part.

Constituent minerals consist mainly of plagiocalse, quartz and potash feldspar with sericitization dominantly.

The acidic dykes cut basic dykes and is unconformably overlain by Mirbat Sandstone Formation and Umm er Radhuma Formation.

2–2–3 Upper Paleozoic (Mirbat Sandstone Formation)

Mirbat Sandstone Formation, distributed in the western area, is composed mainly of conglomerate, sandstone, siltstone, shale and limestone, and is divided into three members from the bottom as lower, middle and upper member.

Lower member consists mainly of conglomerate, interbedding conglomeratic sandstone and alternation of sandstone and shale, accompanying the thick basal conglomerate at the base of the formation.

Middle member consists dominantly of alternation of sandstone and shale, and intercalates a limestone bed at the boundary with lower member.

Sandstone is pale yellow to yellowish brown tint well bedded quartzose sandstone and/or arkosic sandstone showing ripple mark and cross bedding.

The formation trends NE–SW and dips $10^\circ \sim 15^\circ$ northwest. As the sedimentary environment, relative subsidence and rapid sedimentation took place in the early stage and changed to calm subsidence and sedimentation in the middle to later stage under the shallow sea environment.

Although the correlation of sedimentary age of the formation is difficult, the later Paleozoic – Carboniferous to early Permian – is thought to be correlated.

2–2–4 Cretaceous ~ Tertiary (Umm er Radhuma Formation)

This formation extends widespread in the Jabal Samhan tableland of the northern area accompanying escarpement, and shows mesa topography in the coast area.

Pale yellow to white tint limestone and/or marl, well-bedded and intercalated locally with dolomitic limestone beds, are main rock facies accompany some sandstone beds and conglomerate

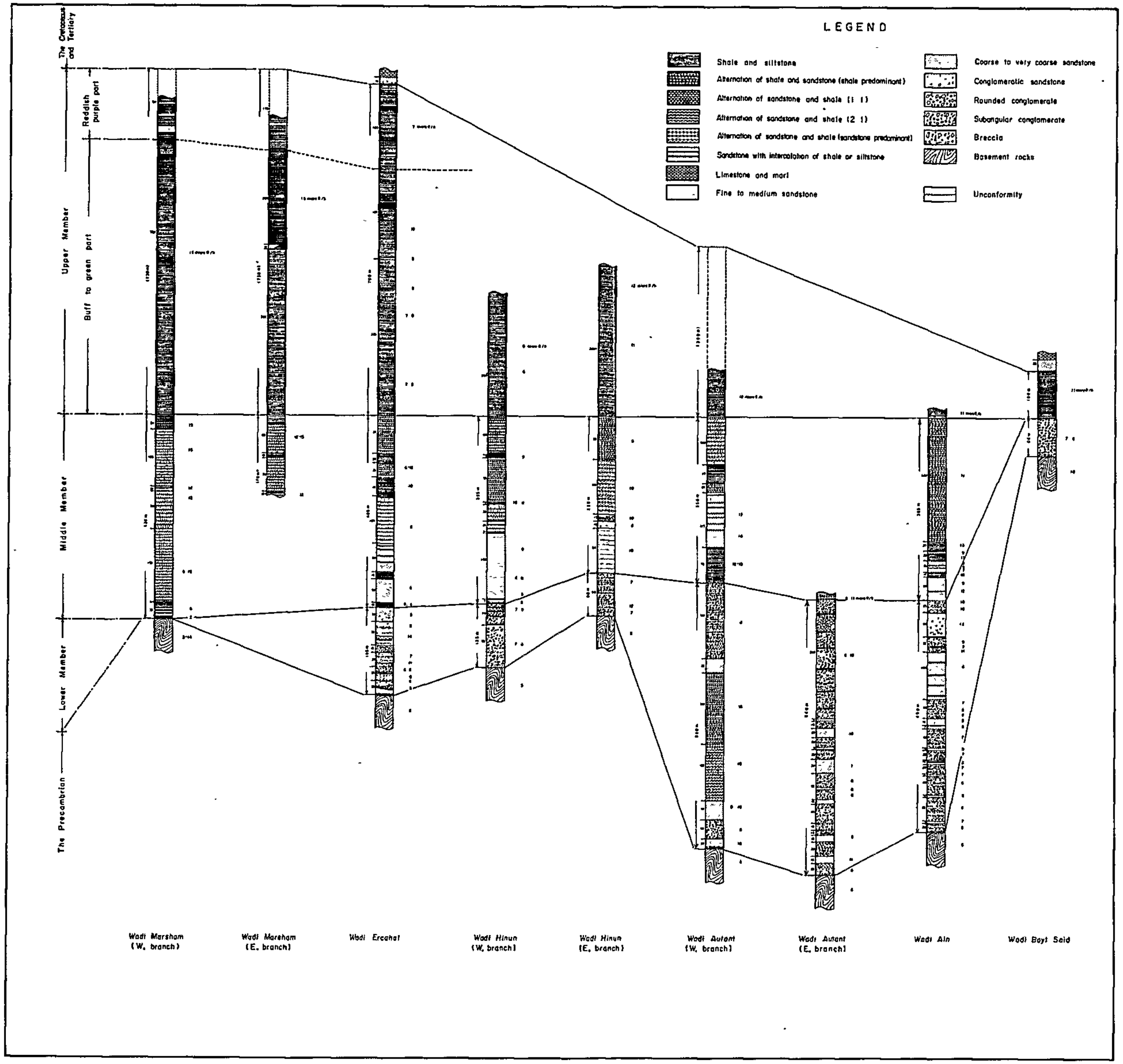

Fig. 9 Geological Columnar Section of Mirbat Sandstone Formation

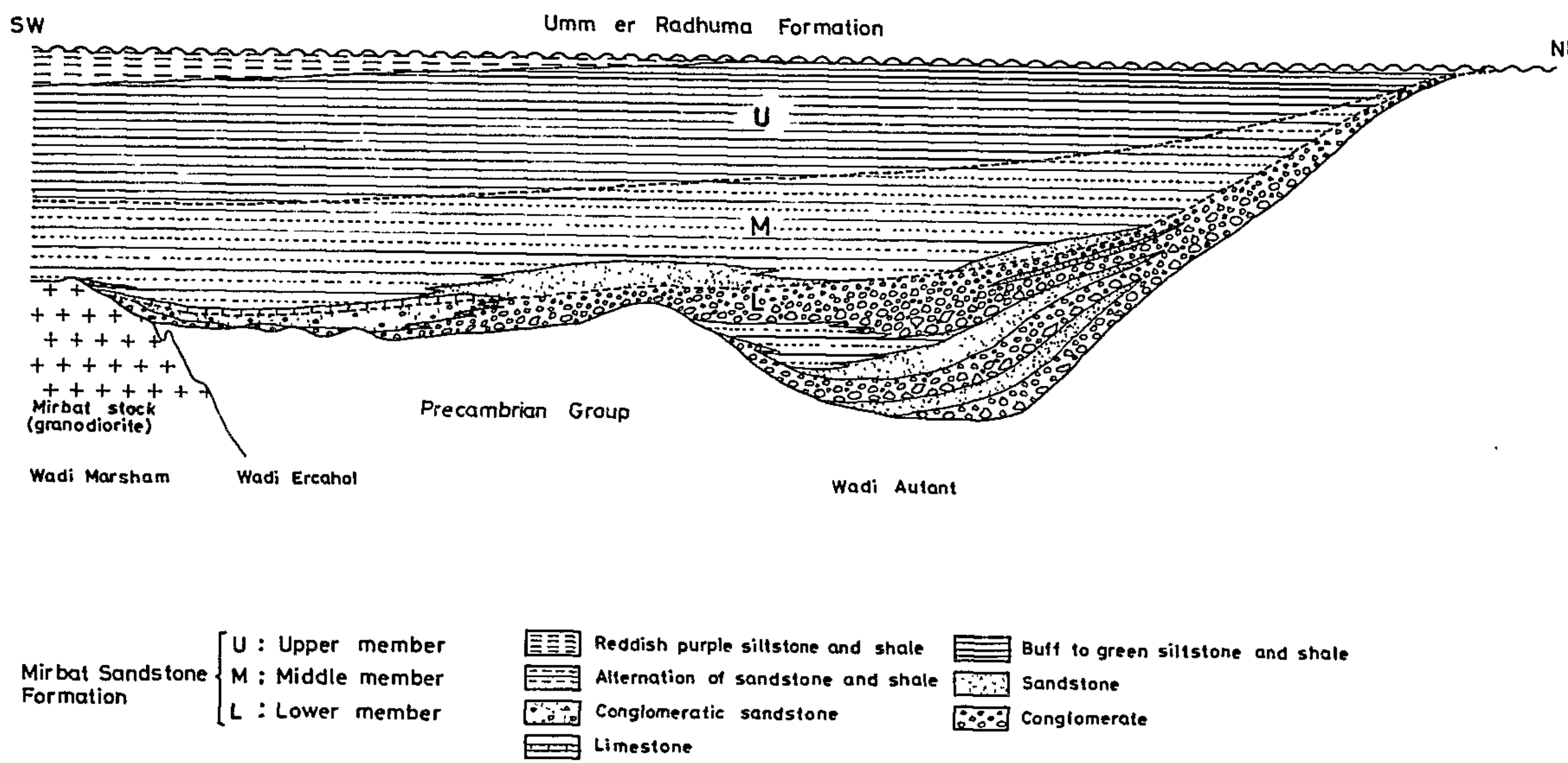

Fig. 10 Schematic Profile of Mirdat Sandstone Formation

beds at the bottom.

Fossils in limestone such as *Nummulites globulus Leymerie,* 1846, one of the larger foraminiferas and *Soritunae, Cyclamminae and Alvealinidae* of the smaller foraminiferas were obtained and can be correlated with lower to middle Eocene stage.

As the result of the identification of the fossils and situation of the sandstone beds at the bottom, this limestone formation though to be considered Cretaceous to Tertiary.

2–2–5 Quaternary Sediments

The Quaternary sediments consist mainly of raised sediments, beach sand and gravel of the major rivers.

The raised beach sediments are divided into poor-sorted coarse sediments which consist of gravel, sand and silt, and fine sediments which consist of miliolids and sand bearing abundant shells.

Beach sand and aeolian sand distribute along part of the coast line.

The river sediments consist mainly of sand and gravel showing poor grading and lacking fine sediments because of scarce water flow and short length of the rivers in the area.

2–3 The Results of Geochronology

The result of K-Ar measurement of the metamorphic and igneous rock are shown as follows (Table 5),

Mica gneiss	(Juffa gneiss)	734 ± 36 m.y.
Hornblende gneiss	(Sadh gneiss)	662 ± 33 m.y.
Acidic gneiss	(〃)	638 ± 32 m.y.
Granodiorite	(Hadabin mass)	713 ± 36 m.y.
〃	(〃)	640 ± 32 m.y.
〃	(Mirbat body)	727 ± 36 m.y.
Pegmatite		576 ± 28 m.y.
Quartz monzonite		537 ± 26 m.y.
Dolerite dyke		438 ± 22 m.y.
Quartz porphyry		374 ± 19 m.y.

These rocks are divided into three groups, such as

(1) group 770 ~ 600 m.y.

Juffa gneiss, Sadh gneiss and granodiorite

(2) group 600 ~ 510 m.y.

Pegmatite and quartzmonzonite

Table 5 Result of K—Ar Dating

Rock	Sample No	Age (m.y.)
JICA 1979		
① Mica gneiss in Juffa Gneiss	25-1-1	734.7 ± 36.7
② Hornblende gneiss in Sadh Gneiss	28-A-109	662.8 ± 33.1
③ Granodiorite (Hadabin body)	22-6	640.2 ± 32.1
④ Perthite in pegmatite	27-A-105	576.7 ± 28.8
⑤ Quartz monzonite	22-2	537.5 ± 26.9
MMAJ 1980		
⑥ Acidic gneiss in Sadh Gneiss	A—008	638 ± 32
⑦ Quartz porphyry dyke	A—020	374 ± 19
⑧ Granodiorite (Hadabin body)	C—204	713 ± 36
⑨ Granodiorite (Mirbat body)	D—026	727 ± 36
⑩ Dolerite dyke	D—076	438 ± 22

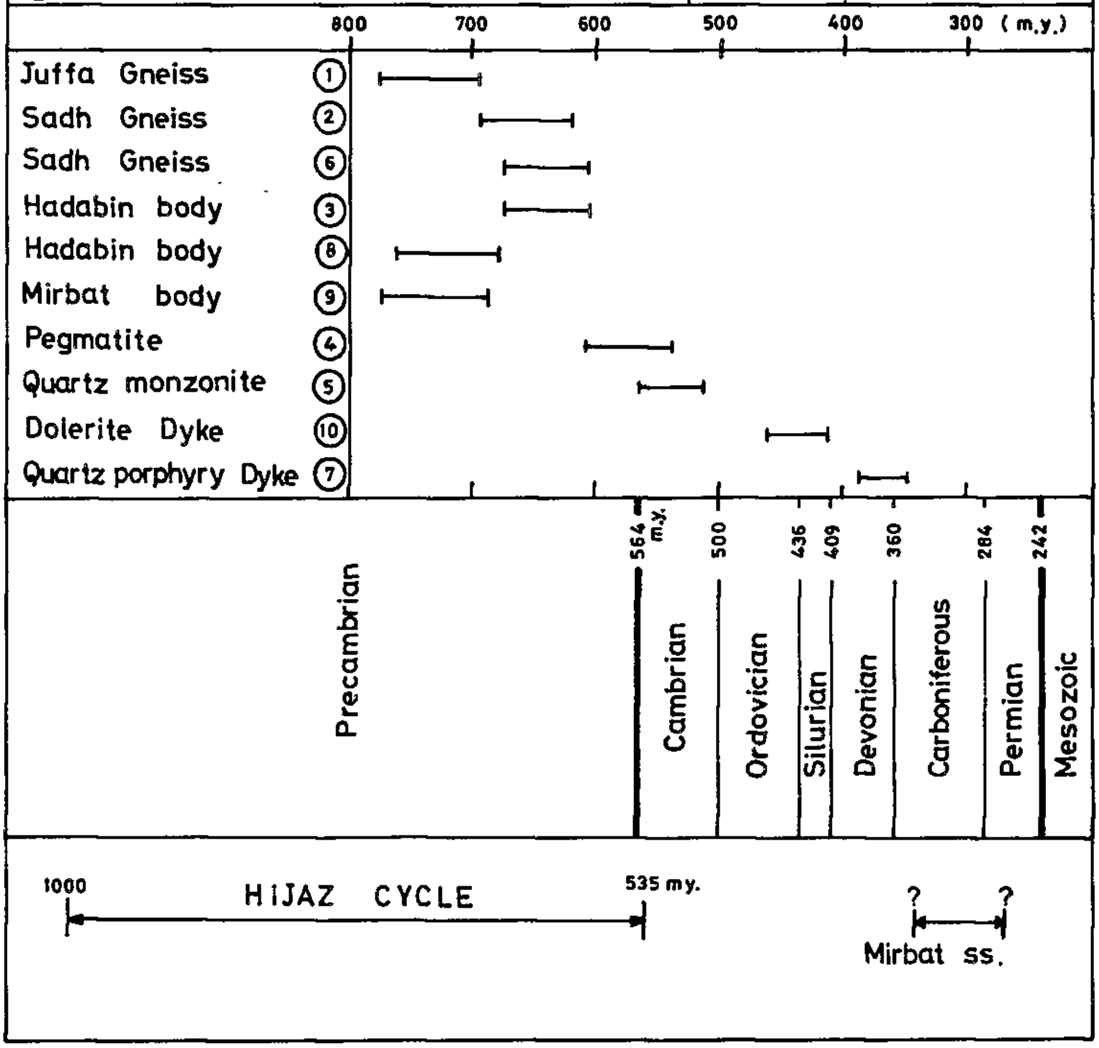

[illegible]

(3) group 460 ~ 350 m.y.

Basic and acidic dykes

On the group (1), Juffa gneiss conformably underlies Sadh gneiss and both gneisses are subjected to same regional metamorphism. Then the age of 720 to 600 m.y. shows a range of metamorphism.

Granodiorite masses, intruded into the metamorphic rocks in the end of metamorphism, are subjected to same regional metamorphism as the metamorphic rocks.

On the group (2), pegmatite veins were formed as the products of the final stage of granodiorite intrusion or recrystalline gneiss of regional metamorphism.

Quartz monzonite is appearently quite similar with quartz porphyry dyke. It is clarified that the quartzmonzonite intruded at the final stage of the granitic magmatism as the result of the geochronology.

On the group (3), dolerite and quartz porphyry dykes intruded in the rock of group (1) and (2), and quartz dyke also cuts the dolerite dyke. The result of geochronology is corresponded with the result of field survey.

The ages (770 to 510 m.y.) of group (1) and (2) are coincident with the age (1,000 to 510 m.y.) of the Hijaz orogeny that formed the Arabian Shield.

On the other hand, although no fossil has been found and radiometric age determination is not available, the Mirbat Sandstone Formation is presumed to be the periods of from Carboniferous to Early Permian because the formation overlies uncomformably the dolerite and quartz porphyry dykes of Late Ordovician to Early Carboniferous age and because the formation is probably equivalent to the Wajiel Sandstone Formation (Early Permian or older) of the Arabian Shield.

2–4 Metamorphism of Precambrian Rocks

The metamorphic rocks in the area consist of mainly mica gneiss, basic gneiss, acidic gneiss and intermediate gneiss.

Constituent minerals under the microscopic observation are shown as follows.

Mica gneiss – muscovite, biotite, quartz > plagioclase > garnet, epidote and K-feldspar
Basic gneiss – hornblende> plagioclase, epidote > quartz, garnet and biotite
Acidic gneiss – quartz, plagioclase > biotite, K-feldspar > muscovite, garnet and epidote
Intermediate gneiss – quartz, plagioclase, biotite > hornblende > garnet

Juffa gneiss is composed mainly of mica gneiss and intercalates basic gneiss beds.

Sadh gneiss is composed mainly of basic gneiss and intermediate gneiss intercalating acidic gneiss.

As mentioned above, Juffa gneiss consists of dominant pelitic components and Sadh gneiss consists of mainly mafic components.

General components of the both gneisses are quartz, plagioclase, biotite, epidote and garnet. This mineral assemblage is characteristic of the metamorphic facies of epidote-amphibolite to lowei part of amphibolite.

2–5 Geologic Structure

Principal geologic structure in the survey area trends NE–SW, NW–SE and N–S.

2–5–1 Fold Structure of the Precambrian Rocks

A basic geologic structure of the Precambrian rocks in the area is an anticlinal structure trending NE–SW.

Juffar gneiss located in the axial part of the anticline and Sadh gneiss is distributed surrounding the Juffa gneiss.

Small anticlines and synclines trending N–S are distributed in the northeastern and southwestern areas.

2–5–2 Geologic Structure of Intrusive Rocks

1) Granodiorite

Hadabin mass, over 20 km of diameter, showing batholith shape and Mirbat body, 2 km of diameter, is stock like intrusion. Intrusive trend of the former is vague and later is extended N–S.

2) Quartz monzonite

Quartz monzonite stock, 2 km of diameter, trends NW–SE extention.

3) Dyke swarm

Principal trend of the dyke swarm is NW–SE, otherwise N–S trend can be observed in the northeastern area and southwestern area.

2–5–3 Fault Structure

Principal trends of the fault are shown as NW–SE and NE–SW systems.

1) NW–SE system fault

Wadi Ain fault, Wadi Bayt Said fault and Wadi Shaat fault are arranged in parallel from western area to eastern area.

2) NE–SW system fault

Wadi Shiliyarn fault and Wadi Khorhant-Atah fault are recognized in the area from northeast to southwest.

NW–SE faults cut folding structure of the Precambrian rocks and NE–SW faults show characteristic of strike fault.

Dolerite intruded in the fault crucks and is crushed marginal part and dislocated. These fault were formed at the folding stage of the Precambrian rocks and the fault activity was removed after dyke intrusion.

2–5–4 Sedimentary Structure of Mirbat Sandstone Formation

Mirbat Sandstone Formation trends NE–SW and dips moderately NW as monoclinal distribution.

The other hand, basal part, refracting the original shape of basement rocks, shows an irregular form and thick conglomerate deposited in the basement depression.

Lower member and middle member show an abut sedimentary structure, and cross lamina which shows very shallow environment can be observed in the beds. Upper member, which consist of fine sediments, shows statical conditions.

2–5–5 Umm er Radhuma Formation

This formation lies horizontally and/or dips moderately north or northeast covering the Jabal Samhan tableland.

The escarpements were formed by the uplift movement probably after the Miocene period.

3. Ore Deposits

3–1 Metallic Mineral Deposits

Information on metallic mineral deposits in the Salalah area are very few so far.

The known mineral occurrences in the past, are as follows.

Quartz veins with small amount of galena along acidic dykes intruded into Juffa gneiss, and secondary goethite crystal from pyrite and/or pegmatite veins with rare malachite, limonite and goethite were reported.

Some mineral occurrences are confirmed as the result of present geological survey as follows.

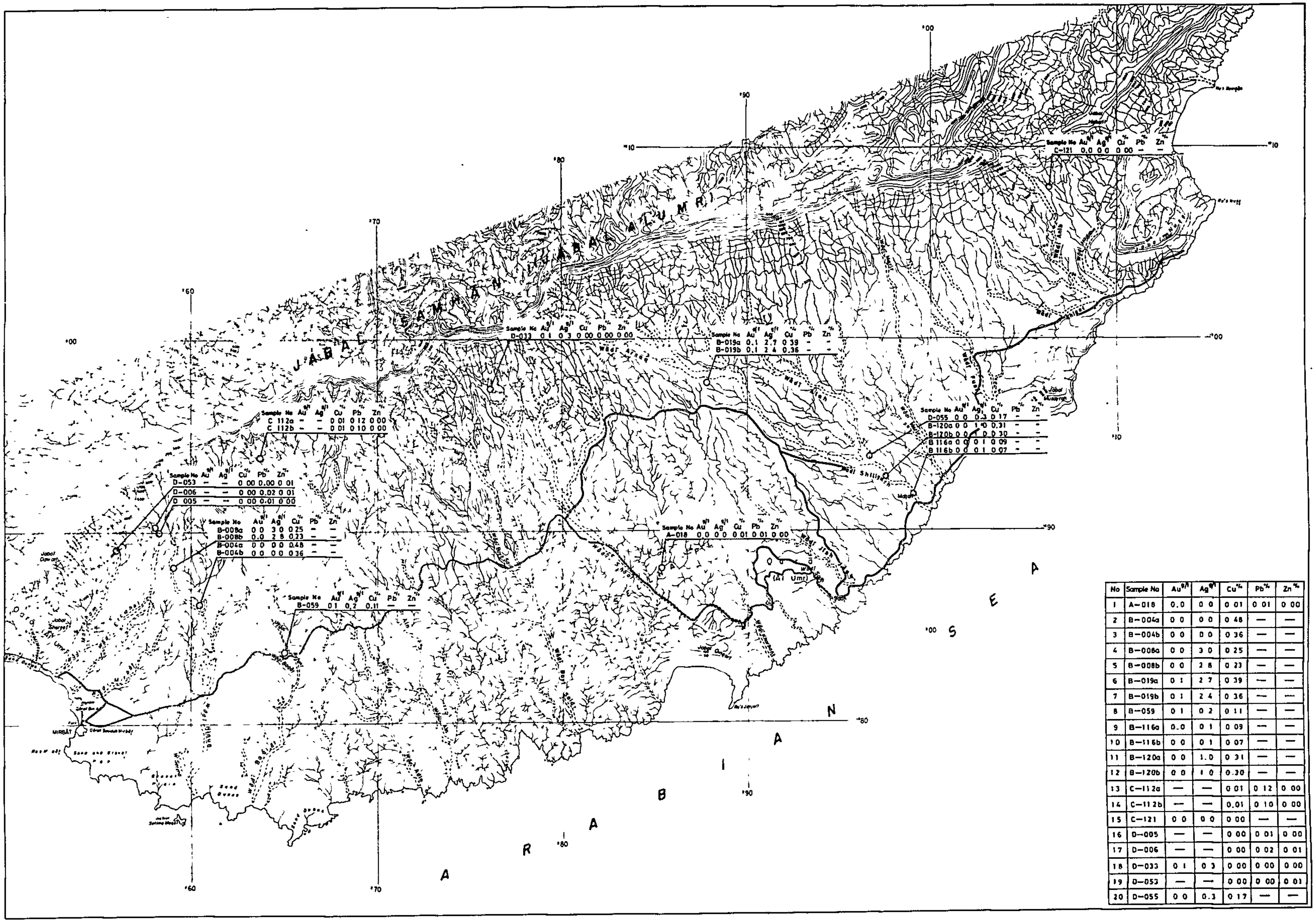

No	Sample No	Au g/t	Ag g/t	Cu %	Pb %	Zn %
1	A−018	0.0	0 0	0 01	0 01	0 00
2	B−004a	0 0	0 0	0 48	—	—
3	B−004b	0 0	0 0	0 36	—	—
4	B−008a	0 0	3 0	0 25	—	—
5	B−008b	0 0	2 8	0 23	—	—
6	B−019a	0 1	2 7	0 39	—	—
7	B−019b	0 1	2 4	0 36	—	—
8	B−059	0 1	0 2	0 11	—	—
9	B−116a	0.0	0 1	0 09	—	—
10	B−116b	0 0	0 1	0 07	—	—
11	B−120a	0 0	1.0	0 31	—	—
12	B−120b	0 0	1 0	0.30	—	—
13	C−112a	—	—	0 01	0 12	0 00
14	C−112b	—	—	0.01	0 10	0 00
15	C−121	0 0	0 0	0 00	—	—
16	D−005	—	—	0 00	0 01	0 00
17	D−006	—	—	0 00	0 02	0 01
18	D−033	0 1	0 3	0 00	0 00	0 00
19	D−053	—	—	0 00	0 00	0 01
20	D−055	0 0	0.3	0 17	—	—

Fig. 11 Distribution of Mirbat Occurrences and Chemical Analysis

1) Wadi Shiliyarn copper occurrence

Six copper occurrences were recognized in the area where about 3 km upstream from the junction of Wadi Shiliyarn and Sadh-Hadabin road.

The geology of the area is composed of intermediate gneiss and acidic gneiss. Pegmatite veins associate with pyrite, limonite, chalcopyrite and its secondary mineral such as bornite and malachite are recognized.

In the Juffa gneiss at midstream of the Wadi Shiliyarn a pegmatite vein accompanied with rare malachite and chalcopyrite is found.

General width of these pegmatite veins is 10 cm to 2 meters.

Assay result of the mineral occurrence in the downstream shows 0.07 ~ 0.3% Cu and the other occurrence in the midstream shows 0.39% Cu.

2) Wadi Hinun copper occurrence

Pegmatite veins accompanying small amount of malachite are recognized in the points of 4.5 km and 7.5 km upstream from the junction of Wadi Hinun and Mirbat-Juffa road.

Assay result of the malachite-concentrated part shows 0.25 ~ 0.38% Cu.

3) Wadi Baqlat copper occurrence

There are a small amount of malachite and limonite in the pegmatite vein at the junction of Wadi Baqlat and Mirbat-Juffa road. Assay result is 0.11% Cu in the malachite-concentrated part.

Copper minerals of the survey area are recognized only in the pegmatite vein except marginal part of igneous rocks.

Assay results of mentioned above are of the copper mineral-concentrated parts in a few centimeters, and the copper grade in the total width of the veins is very low. Then the size and grade of these occurrences are not considered to be economic.

4) Galena in barite vein

Some barite-calcite veinlets, bearing galena crystals, trend E–W in the lower member of Mirbat Sandstone Formation. Size of the galena crystals is 0.5 ~ 2 mm and any other sulphide minerals or secondary minerals can not be recognized.

Assay of the galena-concentrated part is 0.12% Pb.

3–2 Uranium

As the result of radiometric measurement, U_3O_8 = 0.003% Th = 0.001% in the Sadh gneiss

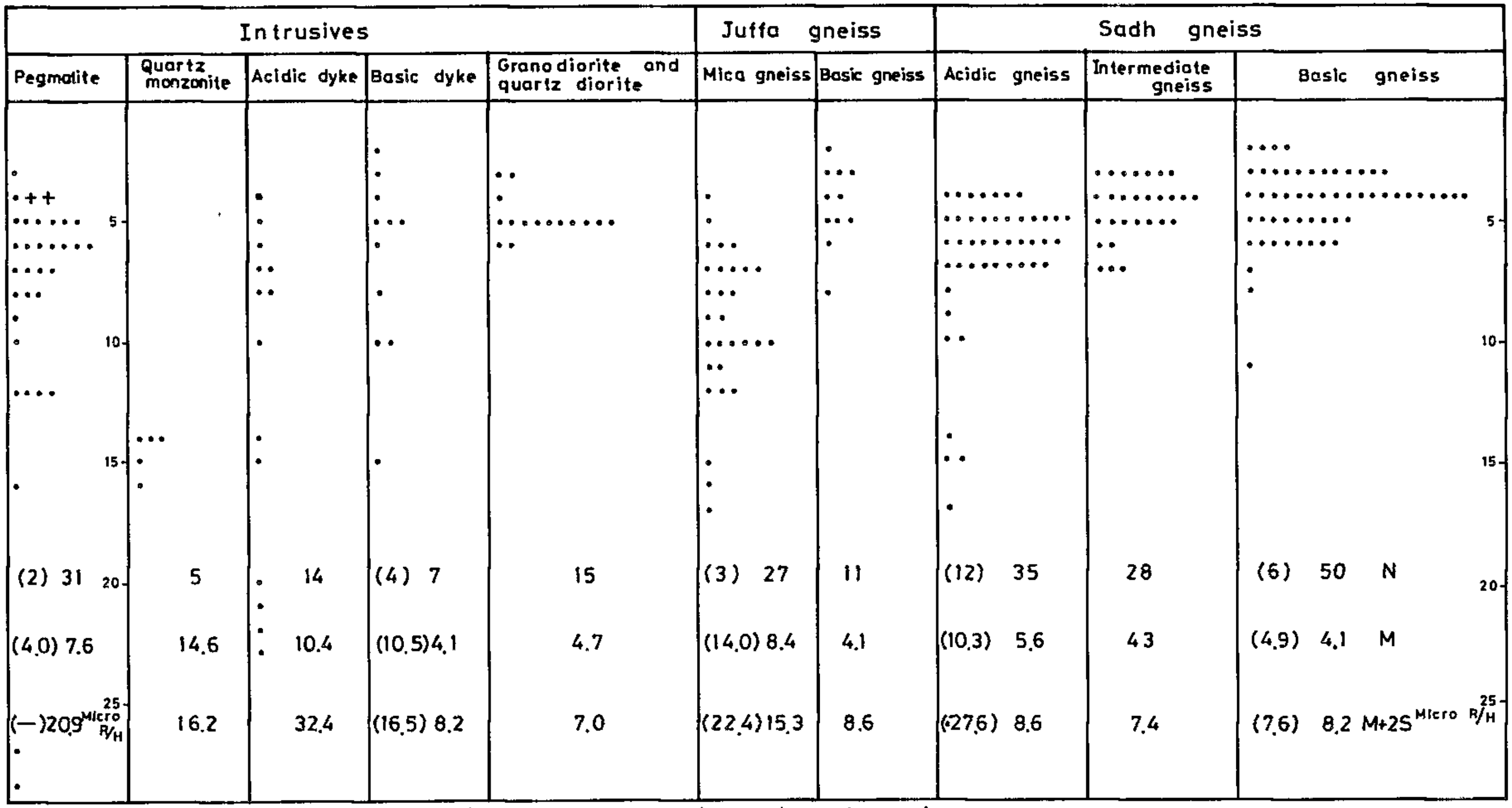

Note : Symbole + shows quartz vein. bracked number means the number of samples

Fig. 12 Histogram of Radioactivity on the Basement Rocks

Radio-activity Micro R/H	Upper Member of Mirbat Sandstone Formation					
	Conglomerate	Very coarse sandstone	Coarse sandstone	Medium ~ fine sandstone	Siltstone ~ shale	Limestone
2						
3						
4						
5			•			
6					••••	
7			•		•	
8					•	
9					•••	
10					•	
11					•••••	
12					••	
13						
14						
15					••	
16						
Log. mean	Micro R/H		5 9 (2)		9 4 (19)	
M + 2 σ	Micro R/H		8.2		16.8	

Radio-activity Micro R/H	Middle Member of Mirbat Sandstone Formation					
	Conglomerate	Very coarse sandstone	Coarse sandstone	Medium ~ fine sandstone	Siltstone ~ shale	Limestone
2						
3						
4	•		•			
5		•	••••			
6				••		
7		•	••	•		
8		••			••••	
9			•	••••	•••••	
10			•	•••	•••••	
11				••	••••	
12				••	•••••	
13					••	
14					••	
15				•	•••••	
16					•	
Log mean	4.0 Micro R/H (1)	6 9 (4)	6.1 (9)	9.5 (15)	11.1 (33)	29 (3)
M + 2 σ	— Micro R/H	10.1	10.8	15 5	16 8	51

Radio-activity Micro R/H	Lower Member of Mirbat Sandstone Formation					
	Conglomerate	Very coarse sandstone	Coarse sandstone	Medium~ fine sandstone	Siltstone~ shale	Limestone
2						
3						
4		•				
5	••••	••	••	•		
6	••••••	•				
7	•••••••••••••••		•	•		
8	•••••	•	•	••••		
9	•		•			
10	••			••••	•	
11	•		•	•	••	
12				•	•	
13	•					
14						
15						
16						
Log. mean	7 1 Micro R/H (35)	5 5 (5)	7.2 (6)	8.7 (12)	11.0 (4)	
M+2 σ	10.8 Micro R/H	8 6	12 9	13.6	12.5	

Note: Bracketed number shows number of samples

Fig. 13 Histogram of Radioactivity on the Each Rock Facies of Mirbat Sandstone Formation

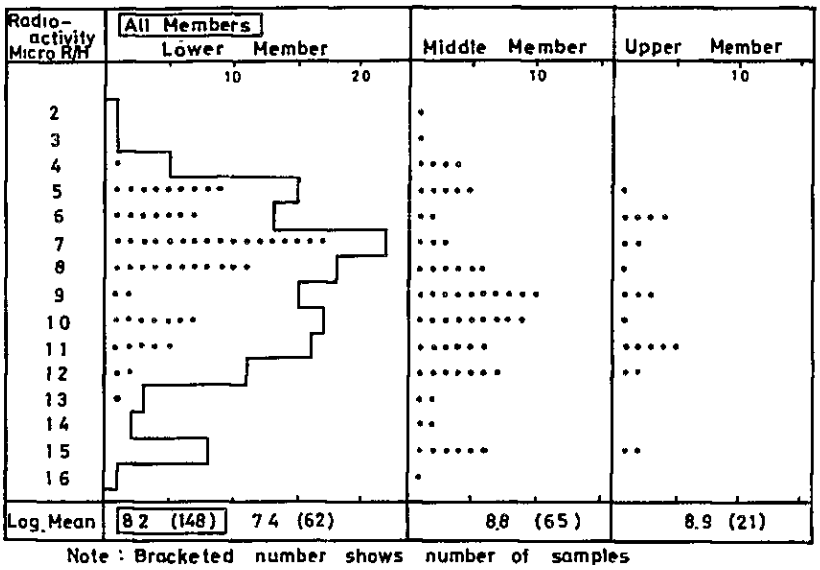

Fig. 14 Histogram of Radioactivity on Mirbat Sandstone Formation

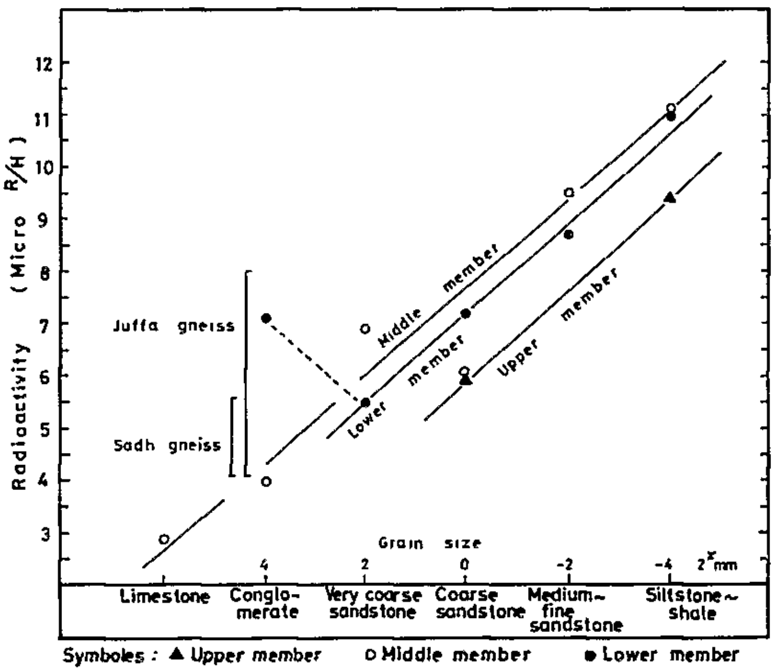

Fig. 15 Comparison of Radioactivity and Grain Size on Mirbat Sandstone Formation

and U_3O_8 = 0.04% in the siltstone of the Mirbat Sandstone Formation were reported in the past.

Detailed stratigraphical survey and radiometric survey in Mirbat Sandstone Formation and radiometric survey in Precambrian rocks and intrusive rocks have been carried out in order to clarify the possibility of the sandstone-type or vein-type uranium deposit.

3–2–1 Radiometric Result of Mirbat Sandstone Formation

Mirbat Sandstone Formation consists of three members from the bottom; lower, middle and upper. These members have sedimentary structure indicating shallow-sea deposition.

Radiometric values of these sandstones are shown as 2 ~ 16 μR/h (Table A–5, A–6), and peak of the histogram show 7 ~ 10 μR/h.

Radiometric values in the different grain size of sandstones tend to increase as the size decreases.

Average logarithmic values of radiometric values of each grain size of sandstone have a linear correction (Fig. 13).

Although channel structures in the basal part of Mirbat Sandstone Formation were recognized and expected concentration of uranium, measured values are 2 ~ 16 UR/h and can not be recognized in that structures.

Anomalous values, therefore, have not been detected in the Mirbat Sandstone Formation and the possibility of uranium deposits is considerably low.

3–2–2 Radiometry of the Precambrian Rocks and Intrusive Rocks

Histogram of radiometry of the Precambrian rocks and intrusive rocks are shown as Fig. 12 and 13.

Precambrian gneiss, basic dyke and granodiorite show low value of 5 μR/h.

Acidic dyke, quartz monzonite and mica gneiss show 7 ~ 15 μR/h effected by high quantity of potassium.

Pegmatite shows 6 μR/h peak which indicates that the pegmatite does not include any uranium minerals.

3–3 Other Minerals

Recrystallized pegmatite veins can be observed widespread in the survey area. These pegmatite veins are small size, a few centimeter to two meter width and 150 meter maximum length, composed mainly impure quartz and feldspar with no economical values.

JICA (1979) reported that the result of emission spectrographic analysis of Wadi sediments

did not detect any element of rare metal.

Although titanium minerals are sparsely present in the boundary area of Juffa gneiss and Sadh gneiss, quantity of the minerals is very small.

Seashore in the survey area has not beach sand bearing rutile and/or ilmenite, therefore, there is no possibility of beach sand doposits.

CHAPTER III. SUR AREA

1. Summary of the Project Area

This area was surveyed geologically in years of 1981 and 1982. In 1981, it was mainly tried to make clear the regional geological structure, the stratigraphy and geological structure in the vicinity of the known ore deposits. And also, the geological survey, the aerial photo-interpretation, and the field verification of the study were carried out in order to find out new manganese ore deposits. In 1982, the geological survey and the drilling survey were conducted to make the evaluation of manganese ore deposits in four areas selected by the results of the abovementioned work in 1981.

Numerous basic data on geology, stratigraphy and ore deposits were obtained during two years.

Manganese ore deposits embed in the Triassic to Early Cretaceous Halfa Formation, the structure and stratigraphy of the Halfa Formation are made clear. Also, ore horizon and characterics and scale were clarified in detail.

2. Geology

2–1 Outline of Geology

The surveyed area is located in the southeastern part of the Oman Mountains, and a part of the formations composing the Oman Mountains is distributed in this area.

This surveyed area consists of basements of Precambrian age, the Halfa Formation from Triassic to lower Cretacious ages, and Limestone Formation from Maastrichtian to Middle Tertiary age. The rocks are covered with sediments of Quaternary age. And also, basic and acidic intrusive rocks are observed in a small scale.

The basement consisting of amphibolite, gneiss and numerous intrusive rocks occurs in Jabar Jaalan. The intrusive rocks are composed of granite, basic and acidic intrusive rocks which penetrated the amphibolite and gneiss.

The Halfa Formation distributes widely in this area, and consists of the alternation of chert and shale. The formation is divided into three members of the Lower, Middle, and Upper. The Middle Member intercalating the manganese ore deposits is also subdivided into three or four submembers.

The Limestone Formation cover the basements and the Halfa Formation with an uncomformity, and includes many relatively large foraminifera. The limestones intercalate arkose sandstones and psammitic limestone.

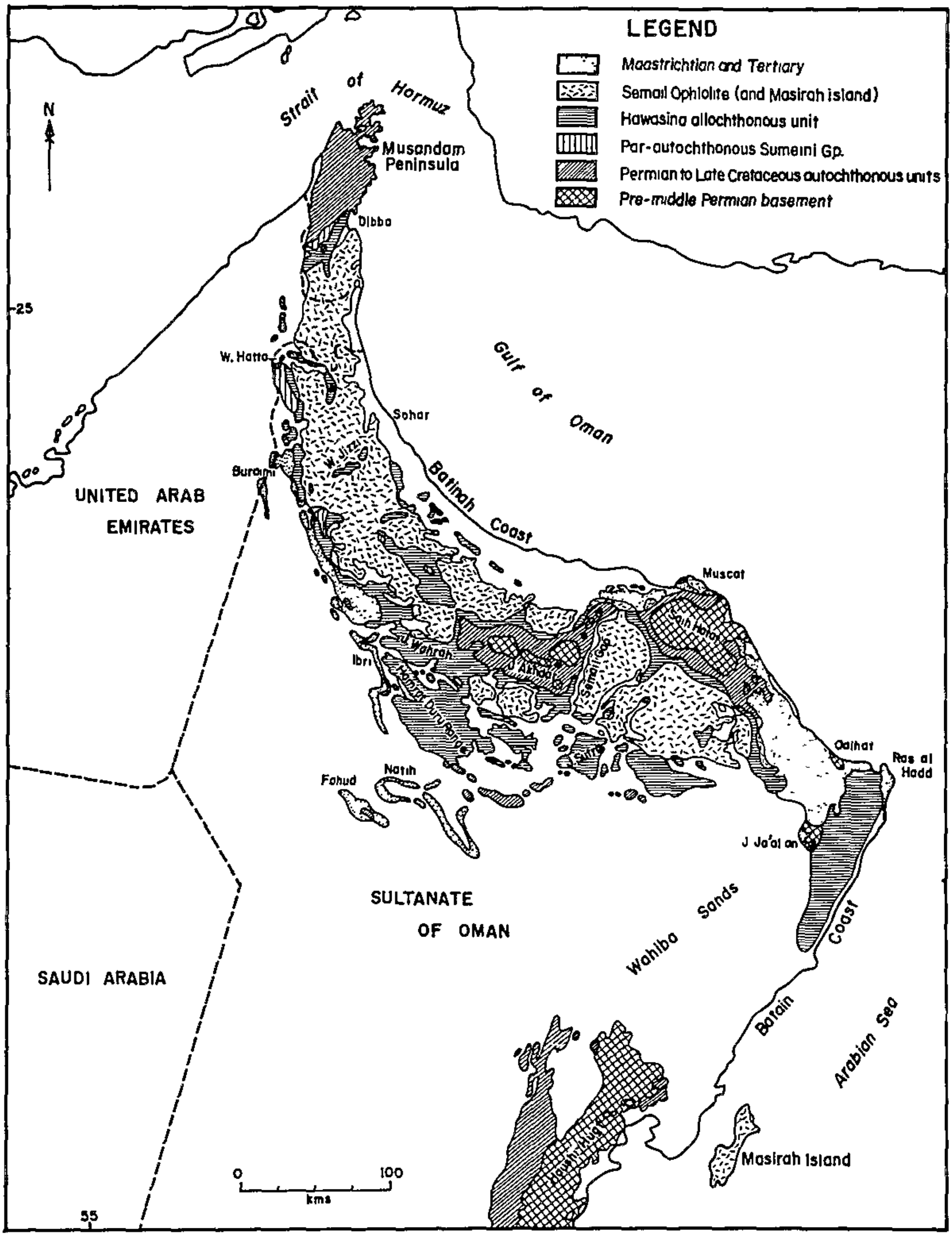

(after K.W. Glennie et al, 1974)

Fig. 16 Geological Map of the Northern Oman

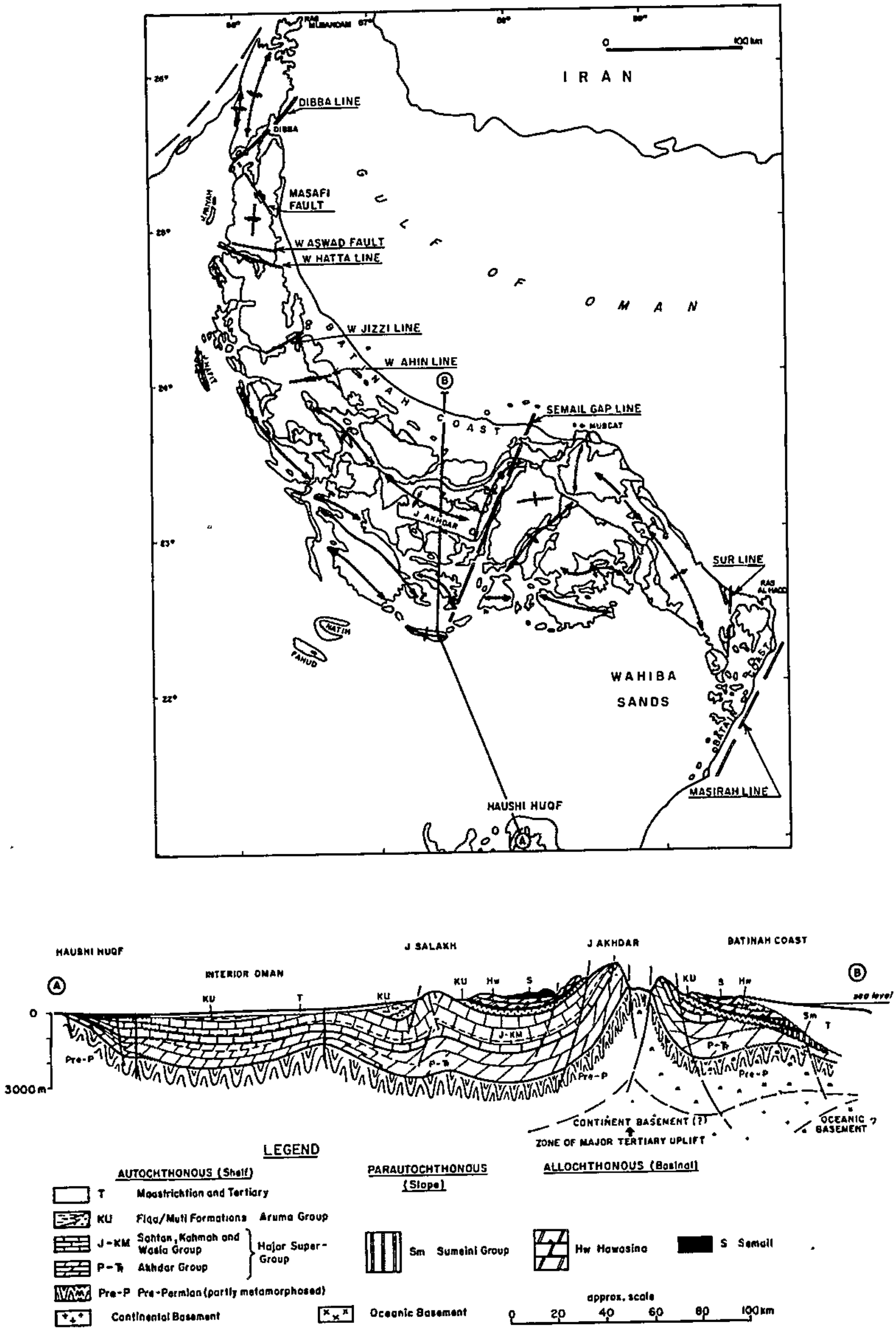

(after K.W. Glennie et al, 1974)

Fig. 17 Geological Framework of the Northern Oman

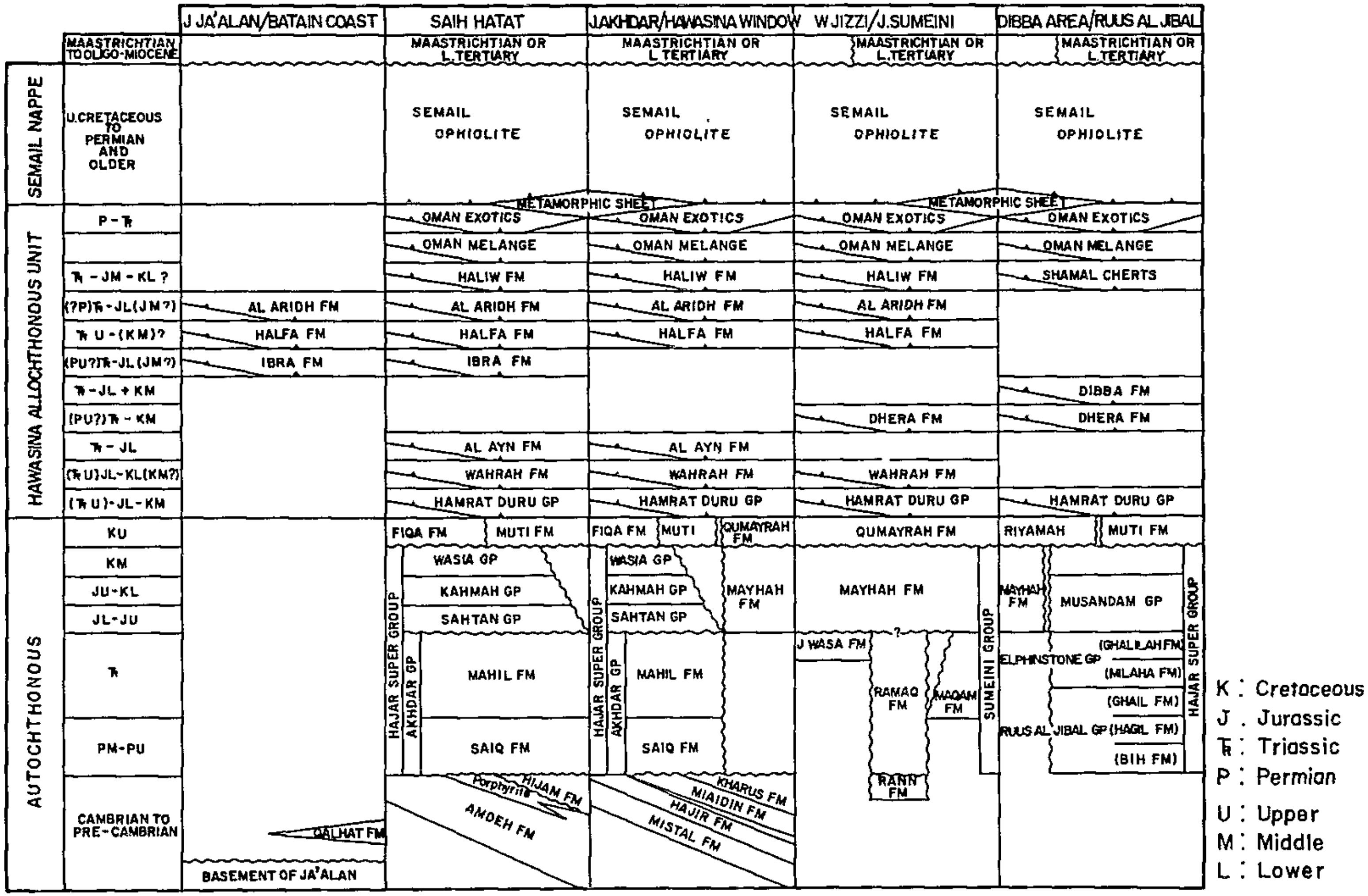

(after K.W. Glennie et al, 1974)

Fig. 18 Schematized Correlation of the Stratigraphic Units in the Oman Mountains

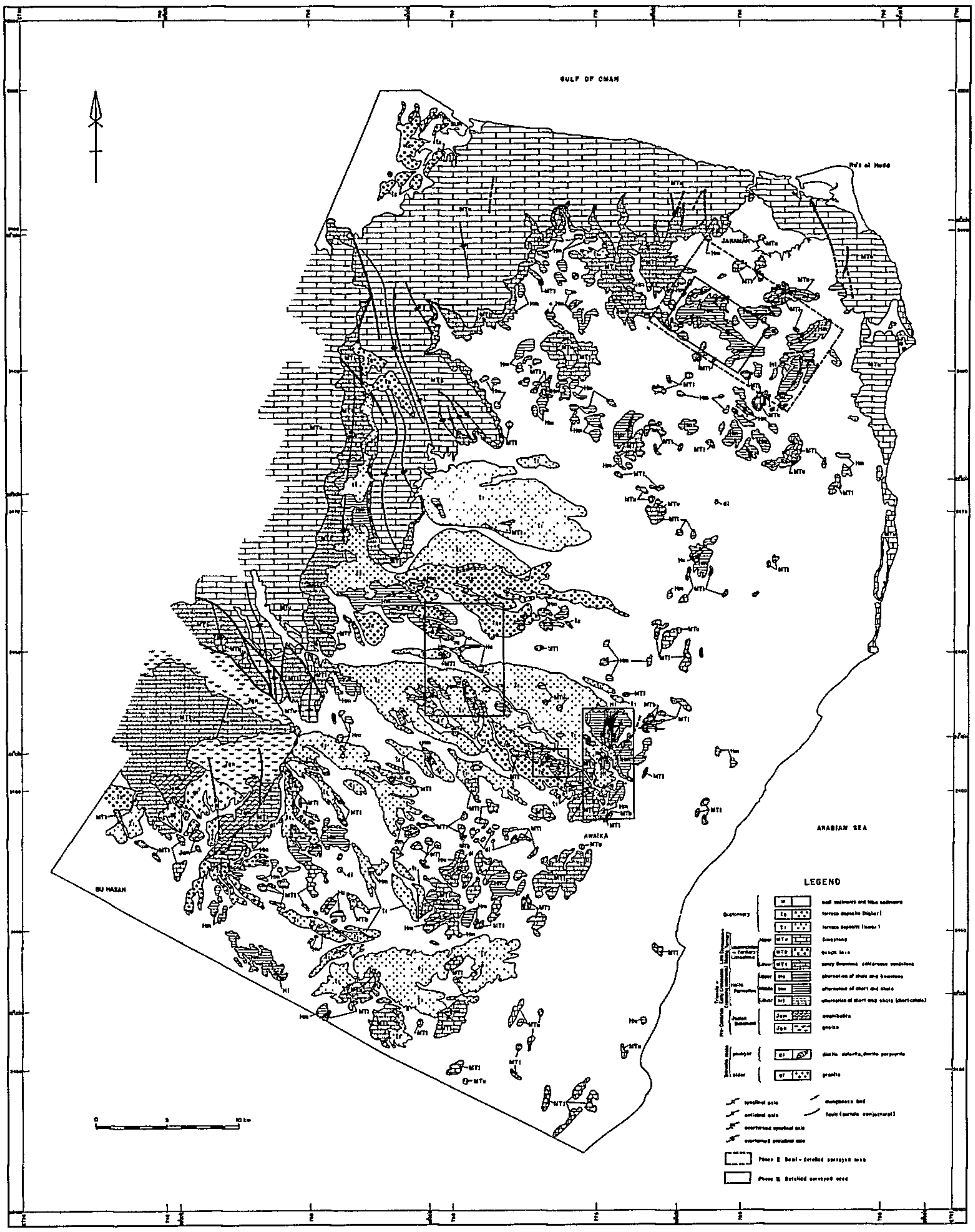

Fig. 19 Geological Map of the Sur Area

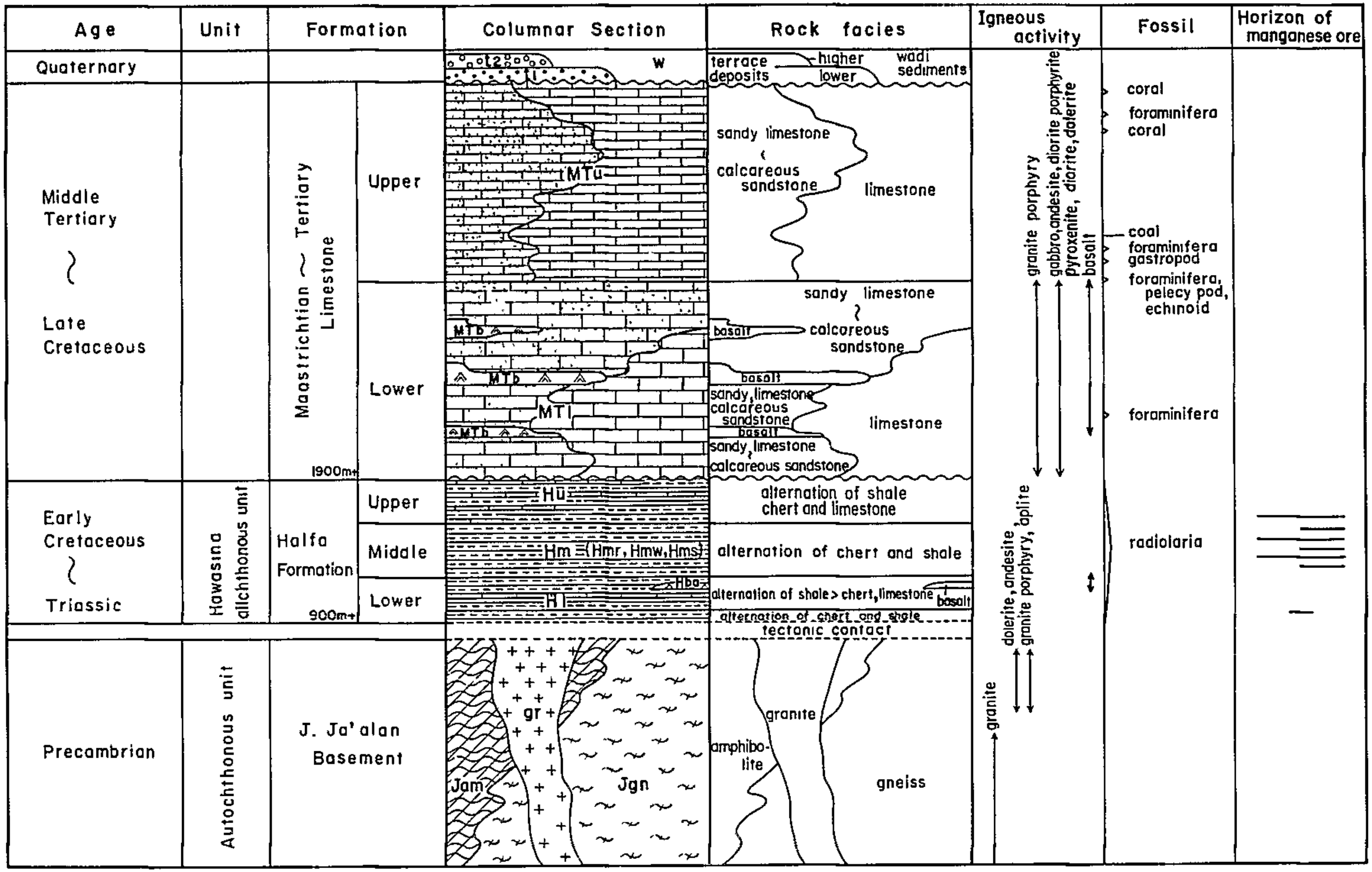

Fig. 20 Schematic Geological Columnar Section of the Sur Area

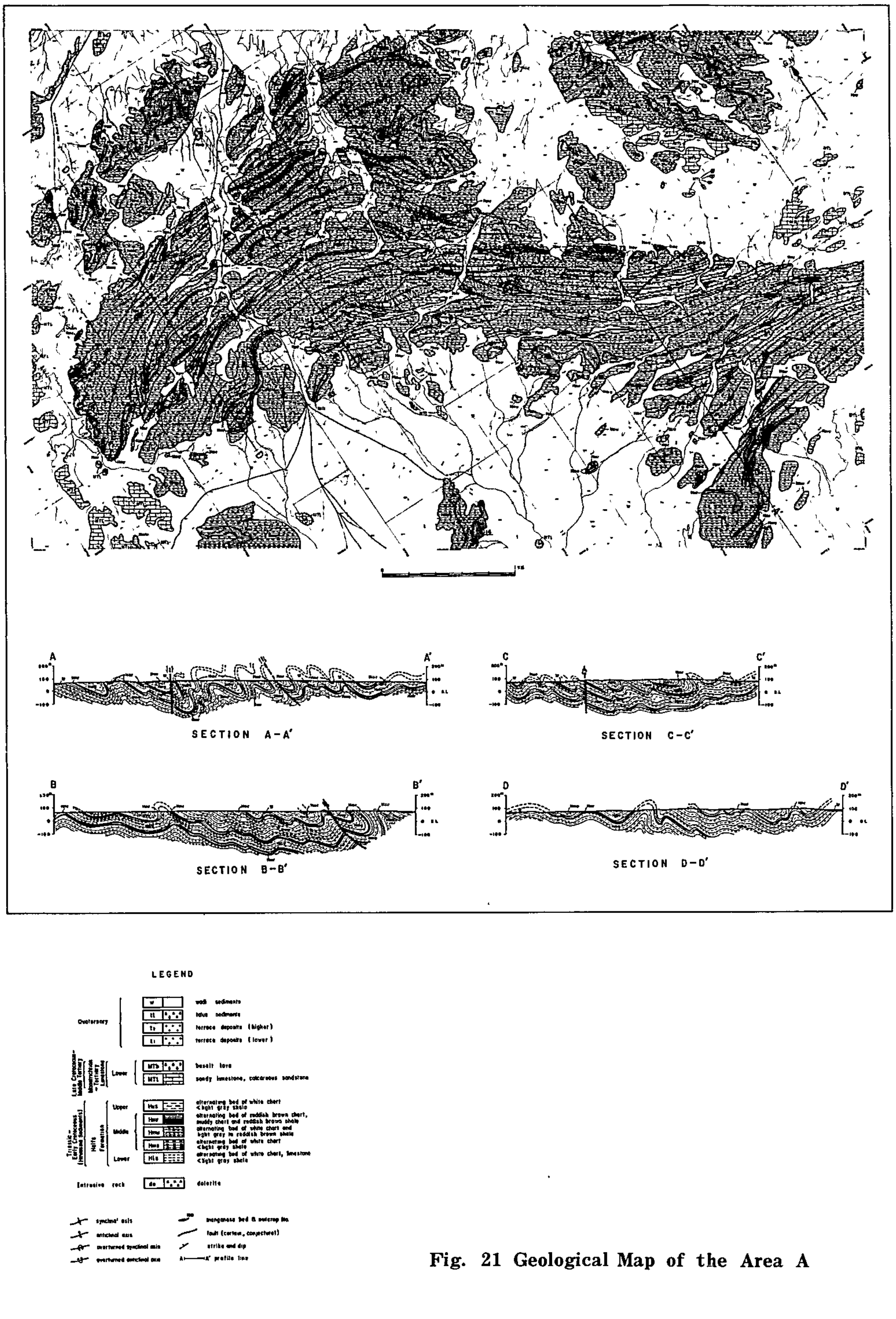

Fig. 21 Geological Map of the Area A

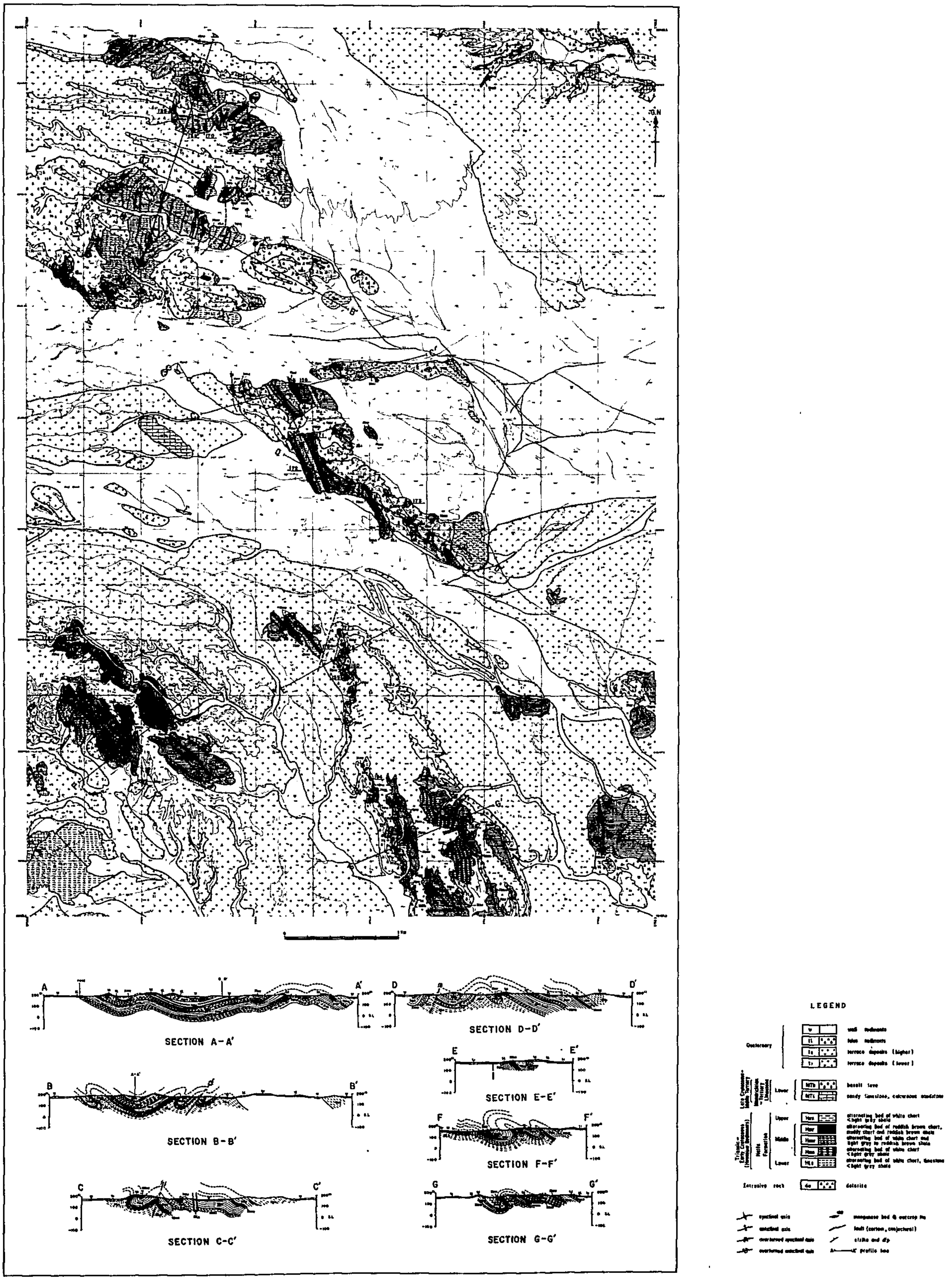

Fig. 22 Geological Map of the Area B

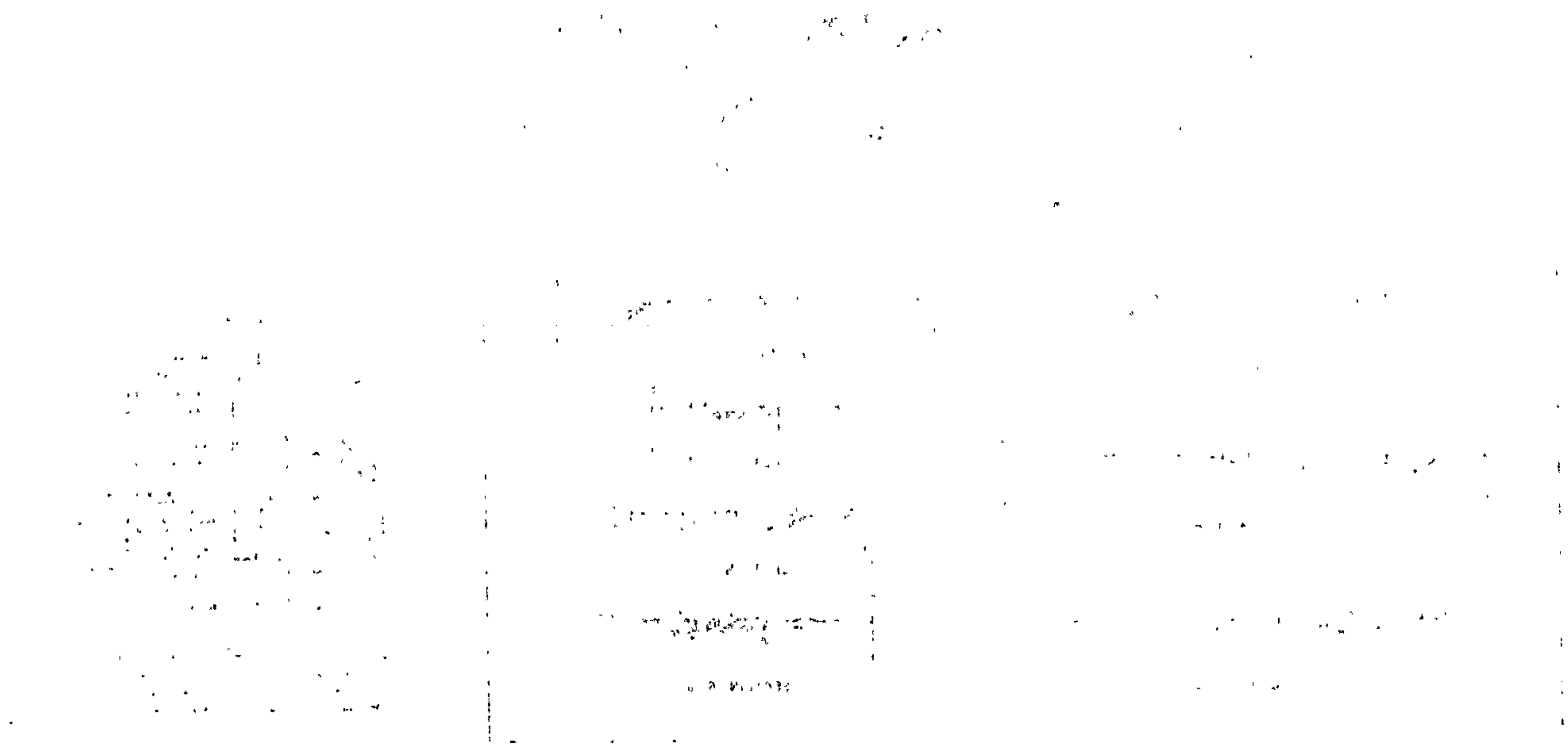

Fig. 2.[illegible] Geological Map of the Area B

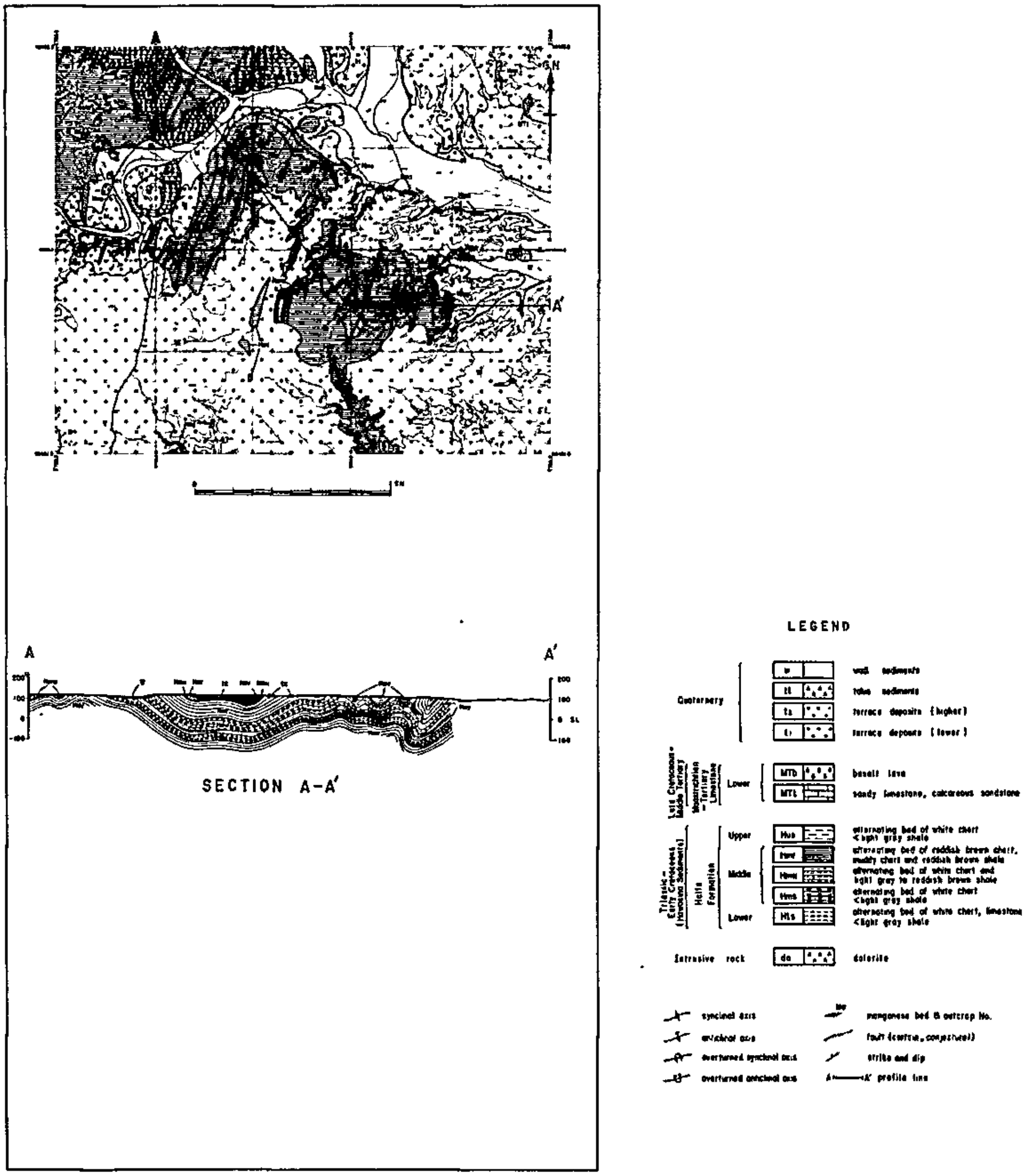

Fig. 23 Geological Map of the Area C

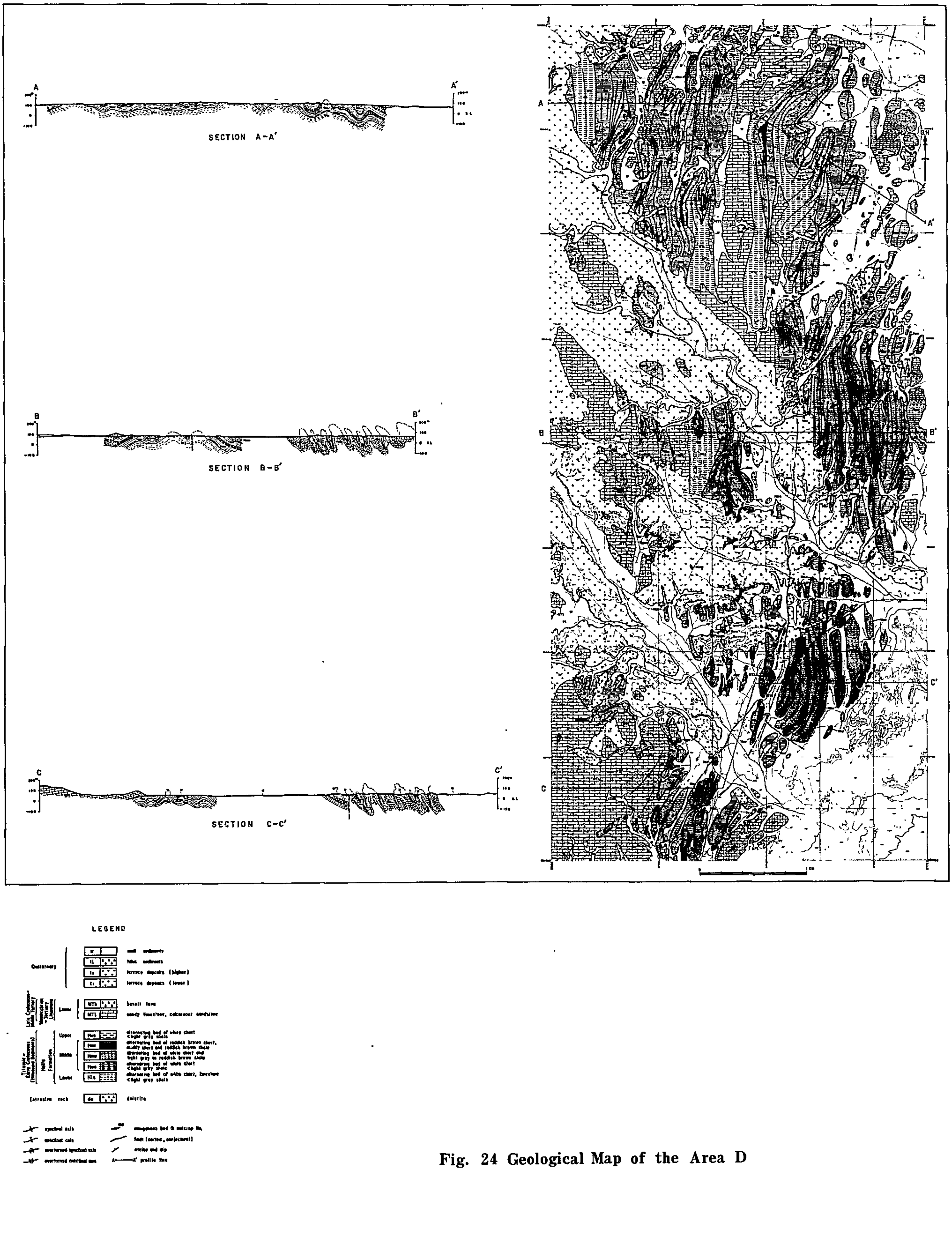

Fig. 24 Geological Map of the Area D

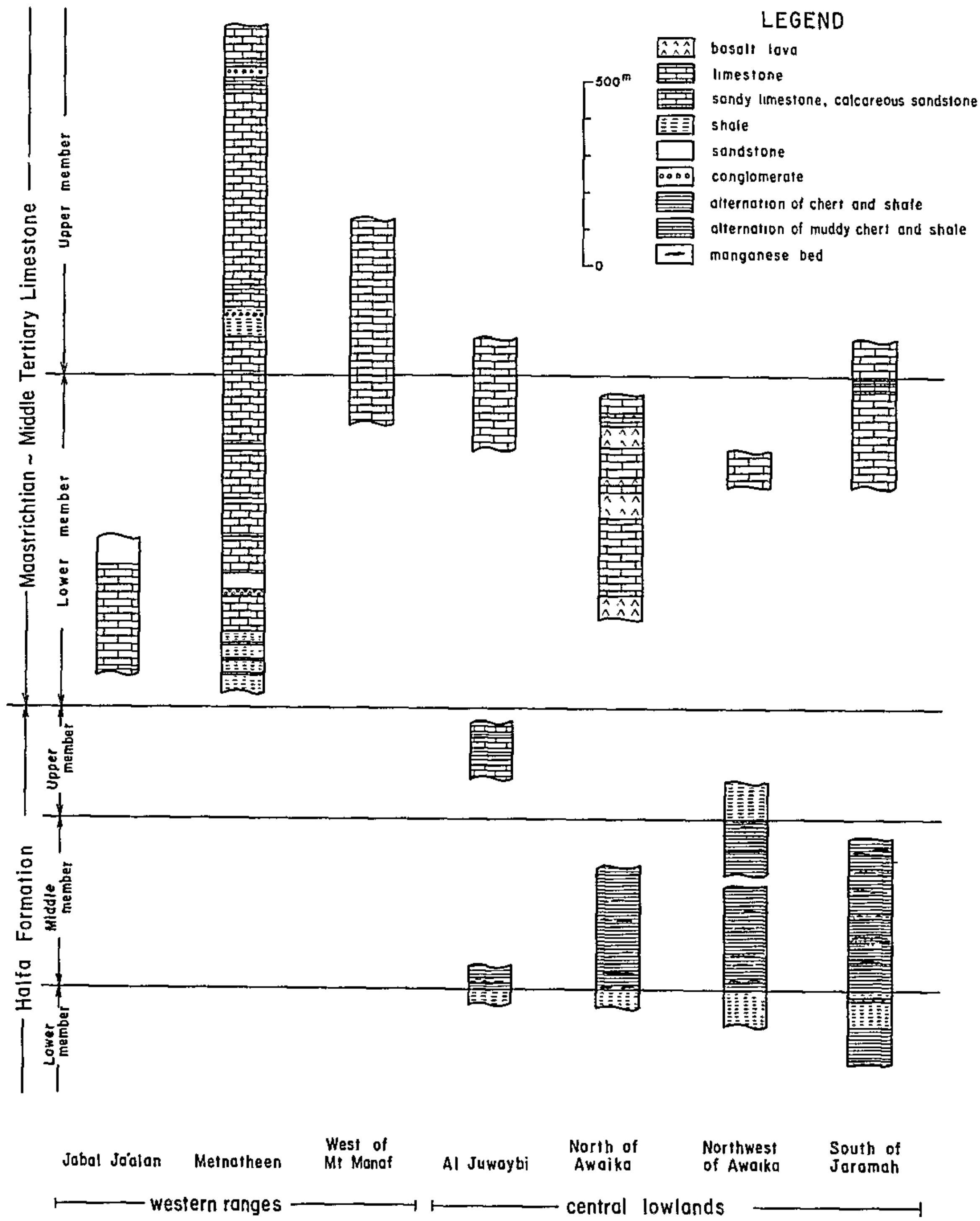

Fig. 25 Geological Columnar Sections in the Sur Area

The sediments of Quaternary age consists of the terrace deposit, littoral sediments and aeolian deposit.

The intrusive rocks such as basalt, andesite and granite porphyry exist penetrating the metamorphic rocks of Precambrian age. And basalt, ardesite and diorite also exist penetrating the Halfa Formation and some of the Limestone Formation.

The gologic structure is very complicated under the influence of the thrust movement of the Halfa Formation in the Late Cretaceous age and the upheaval movement in the Middle Tertiary. Therefore, faults and folds develop considerably in this area. The fold structure shows usually combination of second or third folds, the principal fold axes in the direction of E–W, NW–SE, NE–SW and N–S. The faults show two tendencies of the strikes which consists with the fold axses and intersect obliquely the axses.

2–2 Stratigraphy

The geological stratigraphy at the principal districts in the surveyed area is established by the Halfa Formation, Tertiary Limestone Formation and Quaternary sediments.

2–2–1 Halfa Formation

The Halfa Formation distributes around the hilly regions in this surveyed area, and is consisted chiefly of the alternating bed of chert and shale. The formation is classified into three members of the lower, middle and upper by means of photogeology, and the alternating bed of chert and limestone is also divided into the red, white and transitional alternating beds.

1) Lower Member

This member distributes at the Area A and B. This member is consisted mainly of shale of yellowish white to pale purple grey, and establishes the alternation bed with grey chert in a part. At the area B, the calcareous nodule of black to blackish brown is intercalated, at the area D, the thin bed of pale pinkish siliceous limestone is intercalated. It is considered that the member has the relationship of tectonic contact with the lower formation (Glennie et al., 1974).

2) Middle Member

This member distributes around all area where manganese ore deposits exist and consists mainly of the red, white alternating bed of chert and shale and transitional alternating beds.

The red alternating bed is the alternation of red, reddish brown or greyish brown chert and

reddish brown or pale brown shales. The chert and shale which establish the red alternation bed represent respectively 1 to 20 cm in thickness. The quantitative ratio of chert to shale is about 2 to 10, and chert is thicker than shale.

The red alternating bed is very important key bed that explorates the manganese ore deposits in this surveyed area. Five, four, four and three alternating beds are found at area A, B, C and D, respectively and each thickness is 5 to 30 m, 30 to 90 m, 20 ~ 90 m and 30 to 50 m, respectively.

The white alternating bed is the alternation of white, pale yellow, greyish white or pale purple chert and shale. Each bed is about 2 to 20 cm in thickness. The ratio of chert to shale is approximately unity, or shale is more abundant than chert. The white alternating bed in the area A, does not have the manganese ore deposits. While, in the area B the manganese ores of lens shape below 5 m in thickness are sometimes observed.

It shows 10 m, 10 to 60 m, 40 m and 50 m, and 5 to 40 m in thickness at the area A, B, C and D, respectively.

The transitional alternating bed consists of the alternation of pale pink chert and reddish brown and pale brown shale. The ratio of chert to shale is approximately unity. In this bed at the area A, the manganese ores of the nodule texture below 1 cm in thickness are scarcely found. This bed shows 10 to 50 m and 10 m in thickness at the area A and B, respectively. While, the bed does not distribute at the area C. At the area D, two or three beds are found, and their thickness ranges from 5 to 40 m. This transitional alternating beds have the gradual relationship to the white alternating beds in any case. The geological map represents the two kinds of alternating beds as a white alternating bed. And also, at the area A, B and C, the shale bed distributes.

3) Upper Member

This member is found only at the area B. The rock facies show no difference from the Lower Member, and are mainly composed of shale of yellowish white. At the area B, this member is distinguished from the Upper Member, because it intercalates the Middle Member.

According to biostratigraphic consideration for the radiolarian chert, age of chert in this area shows from Tithonian to Aptian.

2–2–2 Tertiary Limestone Formation

The Limestone Formation is divided into the Lower and Upper Members due to the rock facies.

The Lower Member distributes at the eastern, southern and western districts in the surveyed

area. And small outcrops of the limestone are also observed generally at the lower level in all the surveyed area. The Limestone Formation at the lowland of the area A, B, C and D is equivalent to the Lower Member.

This Limestone Formation is mainly composed of psammitic limestone of pale to dark grey, and sometimes intercalates sandstone and shale. The psammitic limestone includes generally medium to coarse grains of quartz, and scarcely calacareous breccias. It has been considered that the Limestone Formation has the relationship of uncomformity to the Halfa Formation. The Upper Member distributes around the plateau and the hill at the northern and western districts in the surveyed area.

The rock facies of limestone are not consolidated, porous and white to pale grey colored. In the pore, many calcite crystals are observed.

2–2–3 Quaternary Sediments

Quaternary sediments are composed of sand and gravel, and distributes widely around the lowland in the surveyed area. The distribution area is over 50% in the surveyed area. At the eastern district, a dune develops in a small scale.

At the area A, only wadi sediments distribute. While, the area B, C and D show the distribution of talus deposits, wadi sediments, and terrace deposit which consist of sand and gravel.

2–3 Intrusive Rocks

Intrusive rocks such as dolerite, basalt and pyroxenite are intruded in the surveyed area. Dolerite distributes as dykes or sills in a small scale penetrating the Halfa Formation and a part of the Limestone Formation at the area B and D. Basalt is small dykes in the Halfa Formation at the area D. Pyroxenite is found as a small outcrop only in the terrace deposit at the area B.

2–4 Geologic Structure and Geological History

2–4–1 Geologic Structure

The geologic structure in the surveyed area is controled by the thrust movement of later Cretaceous and the upheaval movement of middle Tertiary. The fold axses represent the directions of N–S, NE–SW and E–W systems. The Limestone Formation shows the folds of long wavelength of N–S and NNW–SSE systems. The principal faults are N–S and NW–SE systems in the direction.

Intrusive rocks develop as dykes in the NE–SW direction at the eastern part of surveyed area, and also as sills in the Halfa Formation.

The area A, B, C and D surveyed in detail show mainly the distribution of the Halfa Formation, and a little different geologic structure with each area.

Area A ... three fold systems exist.

1) The main folding structure has the wavelength ranging from 100 to 500 m. The fold axes represent the NW–SE, E–W, and NE–SW systems in direction.

2) The wavelength ranges between 1 to 3 m. This type shows the open fold intersects at right angles to the tight fold having the same fold axis as 1).

3) This type represents the wavelength of a several centimeters, and constructed by the fold, of type 2). In this folds, many small faults develop trending ENE–WSW and NE–SW systems in directions.

Area B ... main folding axes are NE–SW and or NNE–SSW systems. And also, the folding axes such as the E–W, NW–SE, and NE–SW systems are found at the southern area. There exist the thrust parallel to the bedding, and fault intersecting obliquely the bedding.

Area C ... main folding axes are N–S and NNE–SSW systems, and the small folds having folding axes of NNE–SSW are also found. There exist many small faults of E–W direction at this area.

Area D ... main folding axes are the N–S and NNE–SSW systems having the wave length of 50 to 100 m, and also the fold having the folding axis of NE–SW system. The repetition of the Halfa Formation is recognized because of the folding. The faults of the NE–SW system are developed remarkably, and also small faults of N–S and E–W systems exist in this area. The intrusive rocks show the N–S and NNE–SSW direction.

2–4–2 Geological History

The geology in the Sur area constitutes a part of one in the Oman mountains, that is, the geotectonic history in the Oman mountains means one in this surveyed area.

The neritic limestone, and the calicareous neritic sediments (Ibra Formation) originating into immixture of clastics from the continent from Permian to Triassic age. At the period of later Jurassic to early Jurassic, the Hawasina Basin was formed due to subsidence in this area, and the Halfa Formation began to be deposited. At this period, the formation of oceanic ridge and extensive submarine volcanic activities occured.

The thick sediments (Hawasina Group) representing many types of rock facies from Jurassic to middle Cretaceous were formed. The Halfa Formation is one part of the Group, and is composed of the alternating bed of chert and shale of pelagic sediments. It has been considered that the manganese ore deposits were formed relating to the volcanic activities at this period.

The extentive thrust movement occurred due to the collision of the Arabian plate to the Iranian plate which began from the later Cretaceous. Consequently, the Halfa Formation was thrust over the existing Arabian Platform, and also ophiolite was thrust over the Hawasina Group. The extensive fold and fault were formed in the Halfa Formation due to the thrust movement. This area was the sedimentary environment of land and/or submarine, and consequently the thick limestone bed was formed.

3. Manganese Ore Deposits

3–1 General Description

Even though the existence of the manganese ore deposits had been known in the Sur Area, many outcrops of the deposits were found still more by the geological survey at the second year. The occurrence, continuity and scale of the ore deposits were also made clear by the survey at the third year.

The ore deposits mainly occur in the red alternating bed of the Middle Member of the Halfa Formation forming the several manganese ore beds. The ore bed zone is able to be tracked along the strike direction, sometimes over 1,500 m, though each ore bed is on a small scale and intermittent.

Manganese ore is composed mainly of pyrolusite and small amount of cryptomelane and manganite. The ore grade is low, it ranges from 20 to 40% (MnO_2).

Three to six beds including the ore deposits are embedded in the Middle Member, and the repetition of the ore is recognized on the surface due to the folding.

It is considered that the ore deposits have a genetical relation to submarine volcanic activity.

The results of the survey are mentioned as follows.

3–2 Distribution of Ore Deposits

The manganese ore deposits exist extensively over the Middle Member of the Halfa Formation in the Sur area.

The areas where the ore deposits are relatively centralized are the objective areas of the third-year survey. In particular, many outcrops of ore deposits are found at the area A, which is 5 km south of Jaramah, and the area B, 16 km northerwest of Awaika. The distribution of ore outcrops over the whole Sur area is shown in Fig. 19, plate 1. The distribution of ore outcrops at each area is shown in Figs. 21, 22, 23 and 24, respectively. Data of the principal ore outcrops are summarized in Table 6.

Table 6 List of Manganese Outcrops

(Area A)

Outcrop No.	Location		Strike dip	Lateral Length (m)	Average Thickness (m)	Mode of Ore	Host Rock	Ore Sample No.	Average Grade	
	Latitude	Longitude							MnO_2(%)	Mn(%)
56	N2482	E781	E–W 85S~85N	50	0.30	layer	muddy chert/ shale	A068 A069	19.95	12.84
59	N2482	E781	N65W 65~70N	150	0.20	do	do	A009 A014 A012	21.17	13.55
60	N2482	E781	N65W 85S~60N	80	0.15	do	do	A016 A018	27.26	17.98
64	N2482	E780	N80W~E–W 55~65S	140	0.20	do	do	A070 A071	27.83	18.12
68	N2484	E780	N70E 25S	150	0.40	do	do	D026A D030A D028A D032A	21.17	13.98
69	N2481	E780	N80E 90	300	0.61	do	do	F056A~F058A F060A, F061A	19.69	12.87
71	N2481	E780	N80E 55N	350	0.50	do	do	H070A~H076A H078A, H079A F063A~F068A H081A~H084A	24.70	15.21
72	N2481	E780	N45E 60N	140	0.30	do	do	F074A~F076A	30.79	20.12
73	N2483	E780	N30W 50S	250	0.90	do	do	D034A	19.83	12.61
76	N2481	E770	N85E 80W	300	0.45	do	do	F077A~F080A	13.24	9.07
95	N2483	E779	N50W 45S	350	0.85	do	do	D039A~D042A D044A, D047A D049A	19.40	11.66
110	N2485	E778	E–W/75N N45W/30S	1510	0.60	do	do	B107A~B116A C063A~C074A F088A~F095A H085A~H143A	26.68	17.29
114	N2482	E778	N25W 70N	70	0.85	do	do	C047A~C049A	17.71	11.50
116	N2482	E777	E–W 50S	430	0.43	do	do	B137A B140A B139A	16.18	10.33
117	N2484	E777	N80W 55S	500	0.29	do	do	B141A~B145A	19.94	12.84
120	N2485	E777	E–W 60S	50	0.62	do	do	A029A A032A A031A	12.26	8.01
121	N2485	E747	N75E 70~80N	140	0.30	do	do	A034A A038A A036A A039A	16.65	10.73
123	N2484	E777	N75W 40S	650	0.34	do	do	B043A~B045A B120A~B124A	31.57	20.39
124	N2483	E777	N65E 70S	65	0.40	do	do	B136A	58.15	36.74
132	N2484	E777	N30~60E 70N	160	0.30	do	do	A043A~A045A	11.95	7.68
133	N2483	E777	N40E 70N	200	0.24	layer lens	do	B103A B106A B105A	19.35	12.43
136	N2485	E776	N70E 80S	500	0.84	layer	do	D054A D058A D055A D061A D063A D067A D066A	23.67	15.00
140	N2484	E776	E–W/50S N50E/55N	500	0.47	do	do	J087A~J107A B092A B096A B095A B098A~B101A J073A~J075A	27.68	17.54
142	N2484	E776	N45E 50S	300	0.29	do	do	B084A~B086A B091A	26.59	17.51

(Area B)

Outcrop No.	Location		Strike dip	Lateral Length (m)	Average Thickness (m)	Mode of Ore	Host Rock	Ore Sample No.	Average Grade	
	Latitude	Longitude							MnO_2(%)	Mn(%)
155	N2463	E759	N22W 56S	50	0.65	layer	gray chert/ purple shale	H045A	41.11	25.92
158	N2460	E760	N10W 73S	150	2.37	lens	muddy chert/ shale	H041A H044A H043A E026A	39.78	22.73
159	N2458	E761	N20~35W 45N	590	4.15	layer	do	E027A G045A~G048A G054A~G062A G065A~G067A G075A~G078A G080A~G083A G085A~G106A G112A~G115A K090A K091A	34.94	21.48
168	N2463	E759	N4E 76S	70	0.60	do	do	H046A	34.56	21.85
169	N2463	E760	N16E 46S	50	1.30	do	do	H049A	41.47	25.61
170	N2463	E760	N25E 56N	50	0.70	do	do	H047A	65.74	40.08
171	N2460	E760	folded	100	0.25	do	do	H040A	46.99	29.24
172	N2460	E760	N20W 75N	350	0.45	do	do	H038A H039A	47.16	29.01
173	N2459	E761	N25E 70S	40	0.80	lens	do	H033A	34.07	21.20
174	N2458	E758	N–S 40E	10	0.70	layer	do	K019A	71.29	44.37
175	N2458	E758	N20W 55N	40	0.20	do	do	K020A	24.74	14.71
176	N2458	E758	N25W 45N	30	0.30	do	do	K022A	45.14	28.55
177	N2458	E761	N10W 72N	20	0.15	do	do	G014A	31.72	20.06
178	N2458	E761	N40W 80S	50	0.70	lens	do	G009A	17.48	10.44
179	N2458	E761	N32W 80S	30	0.05	layer	do	G043A	28.95	18.34
180	N2458	E761	N18W 65S	20	0.20	do	do	G063A	85.14	52.97
181	N2457	E759	N30W 45N	60	0.40	do	do	K024A	35.44	22.48
182	N2457	E759	N38W 40N	130	0.28	nodule	do	K027A	71.49	44.61
183	N2457	E759	N55W 75S	40	0.70	layer	do	K026aA K026bA	34.94	22.04
184	N2457	E761	N15W 50N	370	1.30	do	do	G116A G119A G117A G121A G122A G123A	26.50	14.75
185	N2457	E763	N25E 45N	100	0.45	do	do	K016A K017A	36.42	22.22
186	N2456	E762	N15E 60S	40	0.30	do	do	G026A	23.49	13.29
187	N2456	E762	N70E/55N N60W/60N	110	0.30	do	do	G028A G029A	45.54	28.38

(Area C)

Outcrop No.	Location		Strike dip	Lateral Length (m)	Average Thickness (m)	Mode of Ore	Host Rock	Ore Sample No.	Average Grade	
	Latitude	Longitude							MnO_2(%)	Mn(%)
161	N2452	E767	N50W/40S N5W/65S	250	1.35	layer	muddy chert/ shale	J024A E076A J025A	13.90	8.71
188	N2452.5	E766.5	N12E/74S N5E/60S	70	0.50	do	do	H023A H028A	46.54	29.69
189	N2452.5	E767	N75W 23S	70	0.25	do	do			
190	N2452	E766.5	N30E 80S	80	0.30	do	do	H029A	47.07	29.68
191	N2451	E767	folded	100	0.30	do	do			

(Area D)

Outcrop No.	Location		Strike dip	Lateral Length (m)	Average Thickness (m)	Mode of Ore	Host Rock	Ore Sample No.	Average Grade	
	Latitude	Longitude							MnO_2(%)	Mn(%)
160	N2456	E771	N–S 80E	250	0.95	layer	muddy chert/ shale	K004A K050A~K052A K053aA K054A K053bA K055aA K0556A K55cA K060A~K064A E037A	40.77	25.58
192	N2456	E771	N–S 55E	110	0.50	do	do	K056A K057bA K057aA K058aA K058bA K059A	45.91	28.18
193	N2454.5	E770.5	folded	40	0.20	do	do			
194	N2453.5	E769	N60E 45S	100	0.30	do	do	H011A	20.35	12.60
195	N2452	E770.5	folded	50	0.25	do	do			
196	N2452.5	E771.5	N5E 85S	230	0.15	do	do			
197	N2452.5	E771.5	N15W~N10E 78E	260	0.25	layer lens	do			
198	N2448	E770	N–S~N10E 60W	250	0.20	layer	do			

3–3 Occurrence of Ore Deposits

The ore deposits occur in the Halfa Formation of Triassic to early Cretaceous age, especially in the red alternating bed of the Middle Member. And also the ore deposits scarcely occur in the white alternating bed of the Middle Member and the alternating bed of chert and shale of the Lower Member.

The red alternating bed is the alternation of reddish brown chert and muddy chert, and reddish brown shale. The bed shows the pale brown color in the vicinity of manganese ore bed. A chert bed is massive in the central and gradually changes to the muddy chert toward the margin. The microscopic studies give that the muddy chert contains the reddish lamination and clay mineral. The ratio of chert to shale ranges from 2:1 to 10:1. The red alternating bed generally contacts with the white alternating bed at the upper and lower margins. The white alternating bed is the alternation of greyish white chert and shale. The ratio of chert to shale is approximately unity or somewhat less.

The ore deposits are the ore bed zone which consists of several layer of a small-scale manganese ore beds developing in parallel to the bedding of the red alternating bed and the manganese nodule zone. The manganese ore bed represents the concentration of manganese ore minerals in the black massive siliceous layer. While, the manganese nodular zone shows the occurrence of manganese ores of spotted and lense shape in the country rock near the ore bed. The size of the ore bed is generally below 20 cm in width and below 10 ~ 20 m in length. It shows, however, 3 m in width and 120 m in length at the maximum. The manganese nodular zone shows scarcely above 10 m in width.

The beds including ore deposits extensively suffer from the folding. The ore deposits receive the folding with the alternating beds, and steep on the surface.

3–4 Continuity of Ore Deposits

The ore deposits occur as ore bed zone consisting of several thin ore beds. One bed is generally less than 10 ~ 20 m in the strike direction. It scarcely shows more than 100 m in length. One manganese ore bed is on a small scale and very poor in continuity. It, however, exists intermittently along the strike direction, and ore bed zone can be traced over 1,500 m at the maximum.

The extension in the dip direction was made clear by the drilling survey in the third year. The drilling survey showed that a bed was continuous by 30 m beneath the surface. Consequently, it is concluded that the extension along the direction of dip is the same tendency as the direction of strike on the surface.

3–5 Scale of Ore Deposit

The ore deposits above 15 cm in thickness and 20 cm in length of all are summarized in Table 6. The ore reserve is estimated by the ore estimation standard as stated later (Fig. 26).

Ore Estimation Standard

Length : The ore deposit is the ore bed zone consisting of a several ore beds. The length x 0.8 (due to the discontinuous feature)

Thickness : The average thickness of ore bed, the thickness at the sampling point x 0.8 (due to the lenticular shape)

Depth : The ore deposit is presumed to be continuous by the 30 m below the surface.

Specific gravity : On the hypothesis that the ore is composed of pyrolusite (specific gravity, 5.1) and quartz (specific gravity, 2.65), the ore specific gravity was estimated referring to the MnO_2 grade in the ore.

At the results of calculation, ore reserve 520,000 tons with average grade 29.57% (MnO_2), 19.92% (Mn), was obtained as the total ore reserve of this area.

The results of each area are as follows :

	Number of Ore Outcrops	Ore Reserve (T)	Average Grade (MnO_2%, Mn%)	
Area A	24	214,880	23.59	15.10
Area B	23	250,545	36.04	24.06
Area C	5	25,537	19.60	12.29
Area D	8	30,965	33.36	20.68
Total	60	521,927	29.57	19.92

The ore reserve of each outcrops is shown in Table 7. The outcrops having the maximum ore reserve is No.159 outcrop where trenching survey was conducted. It is estimated that the reserved ore is 155,601 T, and the average MnO_2 grade is 34.94%.

The other deposits, however, are very small and its calculated ore reserve is less than 5,000 tons. Then, it is concluded that there exist many samll manganese ore deposits in the Sur area.

3–6 Principal Ore Outcrops

The No.110 outcrops surveyed by drilling, and the No.159 outcrops trenched, are stated later.

Table 7 Ore Reserve of Manganese Outcrops

(Area A)

Outcrop No.	Lateral Length (m)	F_1	Thickness (m)	F_2	Dip Side Length (m)	Specific Gravity	Ore Reserve (t)	Average Grade MnO_2(%)	Contents MnO_2(t)	Number of Samples
56	50	80	0.30	80	30	3.00	864	19.95	172.4	2
59	150	80	0.20	80	30	3.04	1,751	21.17	370.7	3
60	80	80	0.15	80	30	3.15	725	27.26	197.6	2
64	140	80	0.20	80	30	3.16	1,698	27.83	472.6	2
68	150	80	0.40	80	30	3.04	3,502	21.17	741.4	4
69	300	80	0.61	80	30	3.00	10,540	19.69	2,075.3	15
71	350	80	0.50	80	30	3.10	10,416	24.70	2,572.8	10
72	140	80	0.30	80	30	3.37	2.717	30.79	836.6	3
73	250	80	0.90	80	30	3.00	12,960	19.83	2,570.0	1
76	300	80	0.45	80	30	2.87	7,439	13.24	984.9	5
95	350	80	0.85	80	30	3.01	17,193	19.40	3,335.4	7
110	1,510	80	0.60	80	30	3.07	53,403	23.01	12,288.1	121
114	70	80	0.85	80	30	2.96	3,381	17.71	598.8	3
116	430	80	0.43	80	30	2.94	10,437	16.18	1,688.7	3
117	500	80	0.29	80	30	3.01	8,379	19.94	1,670.8	4
120	50	80	0.62	80	30	2.87	1.708	12.26	209.4	3
121	140	80	0.30	80	30	2.95	2,378	16.65	395.9	4
123	650	80	0.34	80	30	3.24	13,747	31.57	4,339.9	5
124	65	80	0.40	80	30	3.85	1,921	58.15	1,117.1	1
132	160	80	0.30	80	30	2.86	2,635	11.95	314.9	2
133	200	80	0.24	80	30	3.00	2,764	19.35	534.8	2
136	500	80	0.84	80	30	3.08	24,837	23.67	5,878.9	26
140	500	80	0.47	80	30	3.16	14,258	27.68	3,946.6	10
142	300	80	0.29	80	30	3.14	5,245	26.59	1,394.6	3
						A Total	214,880	22.67	48,708.2	

(Area B)

Outcrop No.	Lateral Length (m)	F_1	Thickness (m)	F_2	Dip Side Length (m)	Specific Gravity	Ore Reserve (t)	Average Grade MnO_2(%)	Contents MnO_2(t)	Number of Samples
155	50	80	0.65	80	30	3.45	2,153	41.11	885.1	1
158	150	80	2.37	80	30	3.41	23,275	39.78	9,258.8	4
159	590	80	4.15	80	30	3.31	155,601	34.94	54,369.1	52
168	70	80	0.60	80	30	3.31	2,669	34.56	922.4	1
169	50	80	1.30	80	30	3.45	4,306	41.47	1,785.7	1
170	50	80	0.70	80	30	4.04	2,715	65.94	1,790.3	1
171	100	80	0.25	80	30	3.57	1,714	46.99	805.4	1
172	350	80	0.45	80	30	3.58	10,820	47.16	5,105.5	2
173	40	80	0.80	80	30	3.29	2,021	34.07	688.6	1
174	10	100	0.70	80	24	4.19	563	71.29	401.5	1
175	40	80	0.20	80	30	3.10	476	24.74	117.8	1
176	30	80	0.30	80	30	3.54	612	45.14	276.1	1
177	20	100	0.15	80	24	3.24	187	31.72	59.3	1
178	50	80	0.70	80	30	2.97	1,996	17.48	348.9	1
179	30	80	0.05	80	30	3.19	92	28.79	26.6	1
180	20	100	0.20	80	24	4.61	354	85.14	301.4	1
181	60	80	0.40	80	30	3.33	1,534	35.44	543.8	1
182	130	80	0.28	80	30	4.18	2,921	71.49	2,088.5	1
183	40	80	0.70	80	30	3.31	1,779	34.94	621.7	2
184	370	80	1.30	80	30	3.13	28,906	26.50	7,660.1	6
185	100	80	0.45	80	30	3.34	2,886	36.42	1,051.0	2
186	40	80	0.30	80	30	3.08	710	23.49	166.8	1
187	110	80	0.30	80	30	3.55	2,249	45.54	1,024.2	2
						B Total	250,545	36.04	90,298.6	

(Area C)

Outcrop No.	Lateral Length (m)	F_1	Thickness (m)	F_2	Dip Side Length (m)	Specific Gravity	Ore Reserve (t)	Average Grade MnO_2(%)	Contents MnO_2(t)	Number of Samples
161	250	80	1.35	80	30	2.90	18,792	13.90	2,612.1	2
188	70	80	0.50	80	30	3.51	2,359	46.54	1,097.9	2
189	70	80	0.25	80	30	3.0	1,008	19.0*	191.5	
190	80	80	0.30	80	30	3.58	1,650	47.09	776.7	1
191	100	80	0.30	80	30	3.0	1,728	19.0*	328.3	
						C Total	25,539	19.60	5,006.5	

(Area D)

Outcrop No.	Lateral Length (m)	F_1	Thickness (m)	F_2	Dip Side Length (m)	Specific Gravity	Ore Reserve (t)	Average Grade MnO_2(%)	Content MnO_2(t)	Number of Samples
160	250	80	0.95	80	30	3.44	15,686	40.77	6,395.2	15
192	110	80	0.50	80	30	3.55	3,748	45.91	1,720.7	6
193	40	80	0.20	80	30	3.0	460	19.0*	87.4	
194	100	80	0.30	80	30	3.02	1,740	20.35	354.1	1
195	50	80	0.25	80	30	3.0	720	19.0*	136.8	
196	230	80	0 15	80	30	3.0	1,987	19.0*	377.5	
197	260	80	0.25	80	30	3.0	3,744	19.0*	711.4	
198	250	80	0.20	80	30	3.0	2,880	19.0*	547.2	
						D Total	30,965	33.36	10,330.3	
						A,B,C,D Total	521,927	29.57	154,343.6	

*estimated grade

Schematized Distribution of Manganese Ore Beds

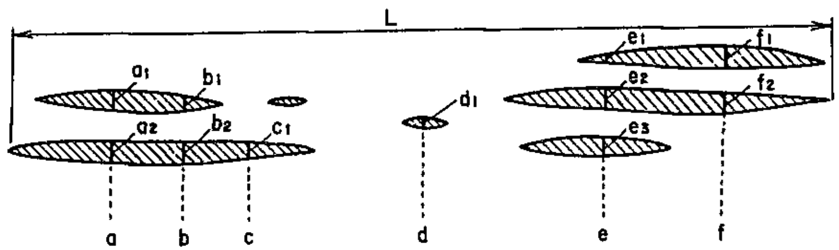

$Ta = a_1 + a_2$

$Tb = b_1 + b_2$

$Tc = c_1$

$Td = d_1$

$Te = e_1 + e_2 + e_3$

$Tf = f_1 + f_2$

} thickness of manganese layers in each sampling sites

Ore Reserve = $L \times F_1 \times T \times F_2 \times D \times S$

L length of strik side

F_1 : length factor (0.8)

T : average thickness

$T = Ta + Tb + Tc + Td + Te + Tf / n$

n number of sampling site

F_2 : shape factor (0.8)

D : length of dip side (30m)

S specific gravity

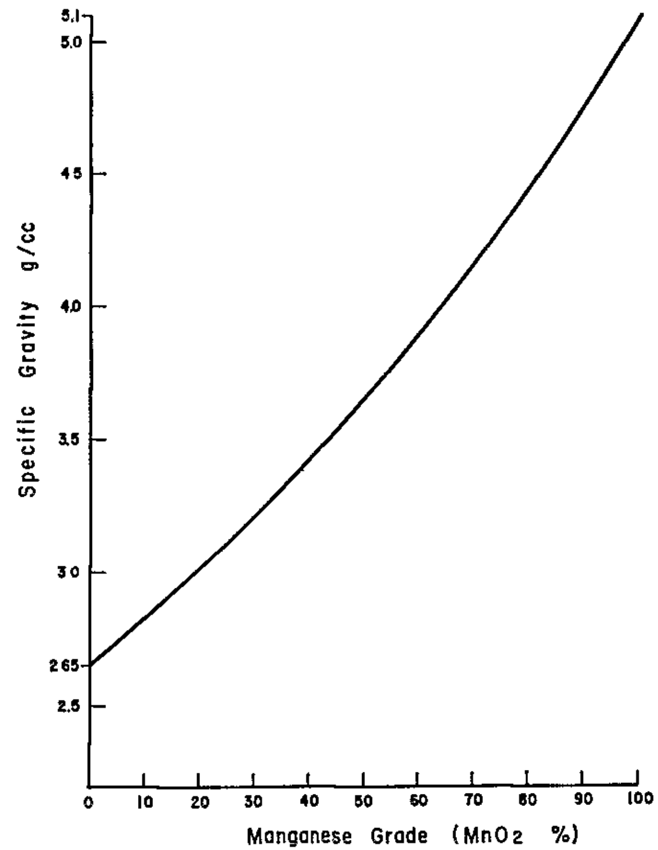

Correlation Curve between Manganese Grade (MnO_2) and Specific Gravity

Fig. 26 Calculation Method of Manganese Ore Reserve

3–6–1 No.110 outcrop

The No.110 outcrop exists at the hill of 75 ~ 95 m above sea level, locating from the center to the west in the area A. The outcrop occurs in the red alternating bed, which show the strike of N45°W and the dip of 30° ~ 80°S at the easternside, and the strike of E–W dipping north at the central part to western side (Fig. 27).

While, from the central part to westernside, there exist small anticlinal and synclinal structures parallel to the bedding, general dipping to the north. The faults of the NE– SE system intersecting the ore bed are found. The ore outcrops are composed of manganese ore bed of various size of large to small, and generally show the 10 ~ 20 cm in thickness, though there is the ore bed of 2 m in the maximum thickness. The extension shows generally below 10 ~ 30 m in length as it reaches to 100 m in length at the maximum. The number, thickness and extension of ore bed are predominant at the eastern outcrops. The manganese nodular zone develops around the ore beds.

The red alternating bed shows the reddish brown to pale brown color, and the alternation of muddy chert predominantly. The white alternating bed bordering to the red alternating bed at the north is found. The boundary of two beds is clear. The boundary becomes no clear at the south, and changes to the transitional alternating bed gradually. As the result of the biostratigraphic study for radiolarian chert, it is clarified that white alternating bed is overtuned and white alternating bed is younger than red alternating bed.

The drilling survey was carried out to make clear the continuity of the outcrops downwards. It is clarified that the outcrop is discontinuous along the direction of dip as well as along the direction of strike on the surface.

The ore reserve is estimated by taking 1,510 m in length toward the strike, 0.60 m in thickness and 30 m in length toward the dip to be 53,403 T. The average grade is 23.01% MnO_2. The results of drilling survey are shown later.

3–6–2 No.159 outcrop

The No.159 outcrop was discovered by the survey at the second year. The outcrop is exposed at the western cliff of the higher terrace in the southern part of the area B (Fig. 28).

The trench was carried out in order to make clear the southern and northern extension of the outcrop in this year. The trench was planned at the area of terrace deposits and talus deposite. Five trenches at intervals of 50 ~ 100 m were done at the southern part of the outcrop, while three trench at intervals of 100 m at the northern part. Total length of trenches is 375 m (Fig. 28).

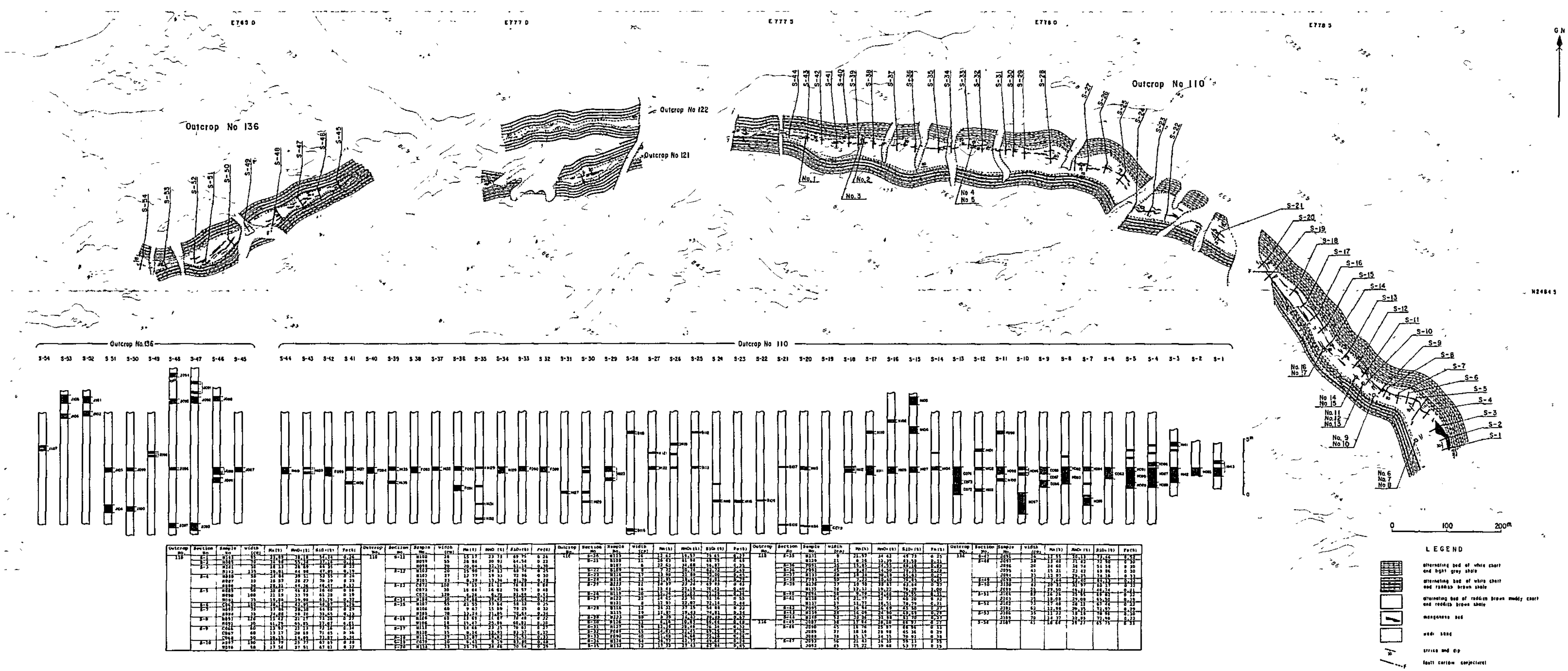

Fig. I—13 Geological Map of the Drilling Area (Manganse Outcrop No. 110, No. 136)

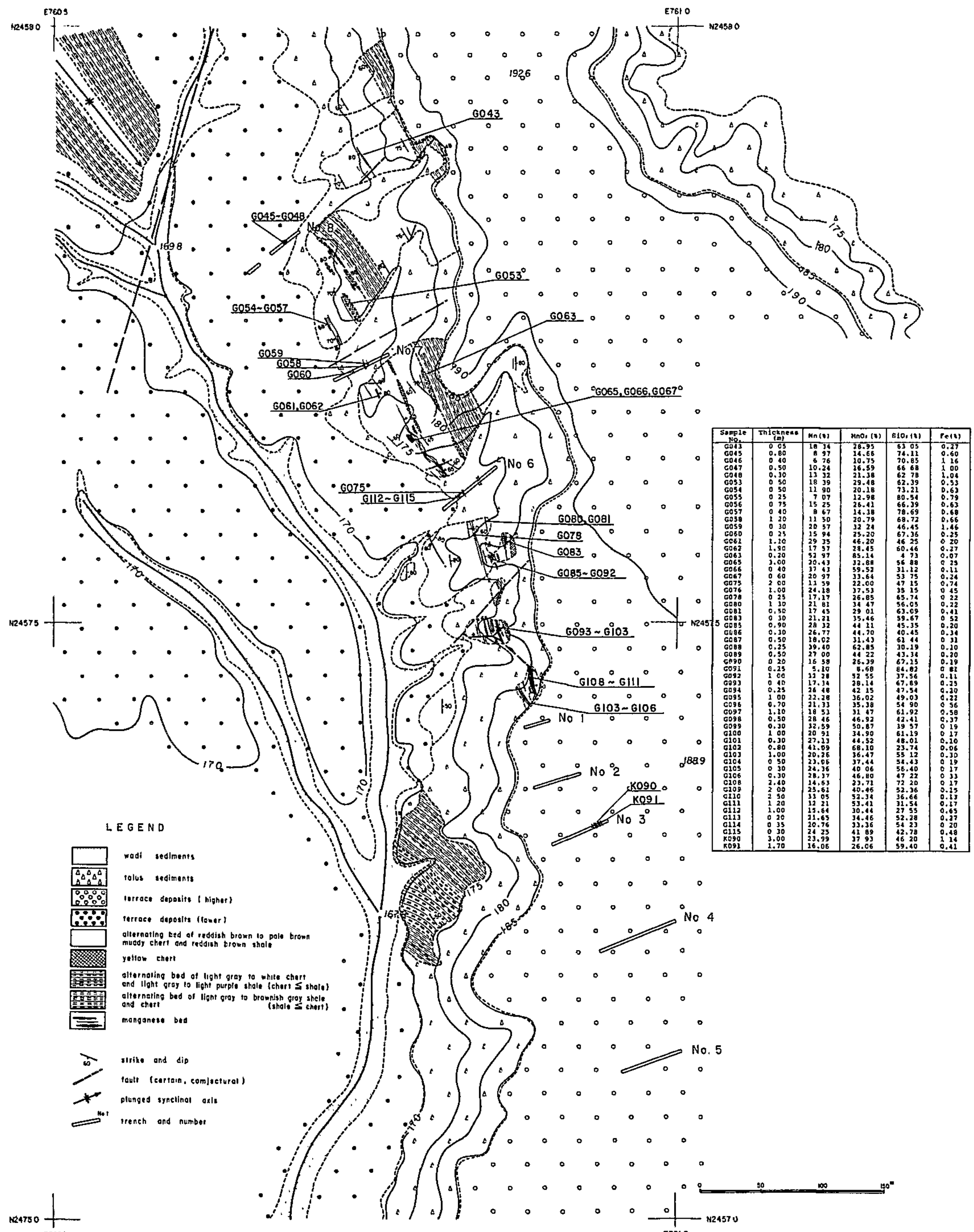

Sample No.	Thickness (m)	Mn (%)	MnO₂ (%)	SiO₂ (%)	Fe (%)
G043	0.05	18.34	28.95	63.05	0.27
G045	0.80	8.97	14.66	74.11	0.60
G046	0.40	6.76	10.75	70.85	1.16
G047	0.50	10.24	16.59	66.68	1.00
G048	0.30	13.32	21.38	62.78	1.04
G053	0.50	18.39	29.48	62.39	0.53
G054	0.50	11.90	20.18	73.21	0.63
G055	0.25	7.07	12.98	80.54	0.79
G056	0.75	15.25	26.41	66.39	0.63
G057	0.40	8.67	14.38	78.69	0.68
G058	1.20	11.50	20.79	68.72	0.66
G059	0.30	20.57	32.24	46.45	1.46
G060	0.25	15.94	25.20	67.36	0.25
G061	1.10	29.35	46.20	46.25	0.20
G062	1.90	17.57	28.45	60.46	0.27
G063	0.20	52.97	85.14	4.73	0.07
G065	3.00	20.43	32.88	56.88	0.25
G066	0.40	37.43	59.52	31.12	0.11
G067	0.60	20.97	33.64	53.75	0.24
G075	2.00	11.59	22.00	47.15	0.74
G076	1.00	24.18	37.53	35.15	0.45
G078	0.25	17.17	26.85	65.74	0.22
G080	1.30	21.81	34.47	56.05	0.22
G081	0.50	17.45	29.01	63.09	0.41
G083	0.30	21.21	35.46	59.67	0.52
G085	0.90	28.32	44.11	45.35	0.20
G086	0.30	26.77	44.70	40.45	0.34
G087	0.50	18.02	31.43	61.44	0.31
G088	0.25	39.40	62.85	30.19	0.10
G089	0.50	27.00	44.22	43.34	0.20
G090	0.20	16.58	26.39	67.15	0.19
G091	0.25	5.10	8.68	84.82	0.82
G092	1.00	33.28	52.55	37.56	0.11
G093	0.40	17.34	28.14	67.89	0.25
G094	0.25	26.48	42.15	47.54	0.20
G095	1.00	22.28	36.02	49.03	0.22
G096	0.70	21.33	35.38	54.90	0.56
G097	1.10	18.53	31.47	61.92	0.58
G098	0.50	28.46	46.92	42.41	0.37
G099	0.30	32.59	50.87	39.57	0.19
G100	1.00	20.91	34.90	61.19	0.17
G101	0.30	27.13	44.52	48.01	0.10
G102	0.80	41.09	68.10	23.74	0.06
G103	1.00	20.26	36.47	55.12	0.30
G104	0.50	23.06	37.44	54.43	0.19
G105	0.30	24.36	40.06	56.40	0.17
G106	0.30	28.37	46.80	47.22	0.33
G108	2.40	14.63	23.71	72.20	0.17
G109	2.00	25.61	40.46	52.36	0.15
G110	2.50	33.05	52.34	36.66	0.13
G111	1.20	32.21	53.41	31.54	0.17
G112	1.00	15.64	30.44	27.55	0.65
G113	0.20	21.65	34.46	52.28	0.27
G114	0.35	20.76	33.36	54.23	0.20
G115	0.30	24.25	41.89	42.78	0.48
K090	3.00	23.99	37.93	46.20	1.14
K091	1.70	16.06	26.06	59.40	0.41

Fig. 28 Geological Map of the Trenching Area (Manganese Outcrop No. 159)

The ore deposits are composed of many manganese ore beds occurring in the red alternating bed of the strike of N–S to N40°W in direction, and the dip of 50°N. Eleven manganese beds were recognized. This is traced toward the 440 m north from the terrace. The two ore beds were found at the trench No.3 in the southern extension which was presumed to be continuous over 150 m in length. The maximum thickness of the ore bed is 3 m and the maximum length is 50 m. The ore bed shows very variable thickness. The yellow chert (yellow siliceous rock) occurs as the lens shape at the boundary of the red alternating bed and white alternating beds. And the manganese ore bed is often found near the boundary. The yellow chert sometimes shows 3 m in thickness.

The geologic structure around this outcrop is considered to be the monoclinic structure of the NW–SW and NE–SE systems of strike direction, dipping gently towards the east with the wavy structure. There occur the faults of NW–SE and NE–SW systems in direction, which transfered the ore deposits.

The ore reserve was estimated to be 155,601 T (590 m with the strike extension, 4.15 m in thickness, and 30 m with the dip extension), and the average MnO_2 grade is 34.94%.

The ore reserve of the outcrop No.159 is the biggest in the Sur area.

There are the trenches whose extension was not wholly made clear by this operation due to the thick terrace deposit (above 3 m). The southern extension of this outcrop is presumed to connect with the manganese ore outcrop in the red alternating bed of the south cliff of the terrace.

3–7 Ore

Manganese ore is divided into the layered and nodular ores.

1) Layered ore

The layered ore is the principal ore in the manganese ore deposits in this area, representing the manganese concentration form of the layer and lens in the black and compact siliceous bed. The fine manganese ore minerals are disseminated in the black siliceous bed. The segregation quartz vein develops in the layered ore. Some ore shows the colloform texture.

2) Nodular ore

The nodular ore is found around layered ores and forms manganese nodular zone. Manganese minerals in a nodular ore concentrate in lenticular or spot form. The size of lenticular form ranges 0.5 cm ~ 2 cm in thickness and 3 cm ~ 10 cm in length. The plane shape of the lens is

irregular and sometimes amoebic. The veinlets of manganese minerals with segregation quartz are rarely observed in the fractures of chert.

3) Manganese ore minerals

The X-ray diffraction study and the microscopic observation of thin section gave mainly pyrolusite and minor cryptomelane and manganite as the constituent manganese minerals in this ore. A part or large part of pyrolusite may be the pseudomorph of manganite, judging from the feature of cleavage. The ore sample from cuttings gave the same manganese ore mineral assemblage as one on the surface.

3–8 Analysis of Ore

The ores in this area were analyzed chemically about Mn, MnO_2, SiO_2, Fe, P and S. Consequently it was shown that the MnO_2 is 20 ~ 40%. The values show that the ores in this area are the low grades. The average of the Fe, P and S contents is 0.33%, 0.03% and 0.12%, respectively, which shows very low content. This ores have the high SiO_2 content because of the quartz forming the black siliceous part.

3–9 Minor Element Analysis

The minor elements of ores and chert were analyzed by means of the spectrographic analysis. The number of sample is 50. The objective minor elements are 26. The analytical results exhibit little difference with samples and/or outcrops as shown in Figs. 29 and 30. The content of Co, Ba and Sr shows the same variation as Mn. It was proposed by Borchert (1970) and Zantop (1980) that Ba and Sr are the elements concentrating into the volcanogenic sedimentary deposit. Three samples were analyzed quantitatively about seven elements. The 50 samples were estimated quantitatively about the seven elements by using the above values. The analytical data are summarized in Fig. 31. Consequently, it is considered that the minor elements in the Sur area show the same feature as ones in the ores of Oligocene and volcanogenic ores, and are very close to the volcanogenic sedimentary ores having the same anomalies of Cu and Zn.

It is concluded that the manganese ore deposits in the Sur area were formed in close relation with volcanism, judging from the minor elements of ores and the wall rock.

3–10 Electric Characteristics of Ores.

The manganese ore is used as a important part of the dry cell. The electrical ability test was carried out in order to evaluate ores in the Sur area suitable as raw materials of the dry cell. The

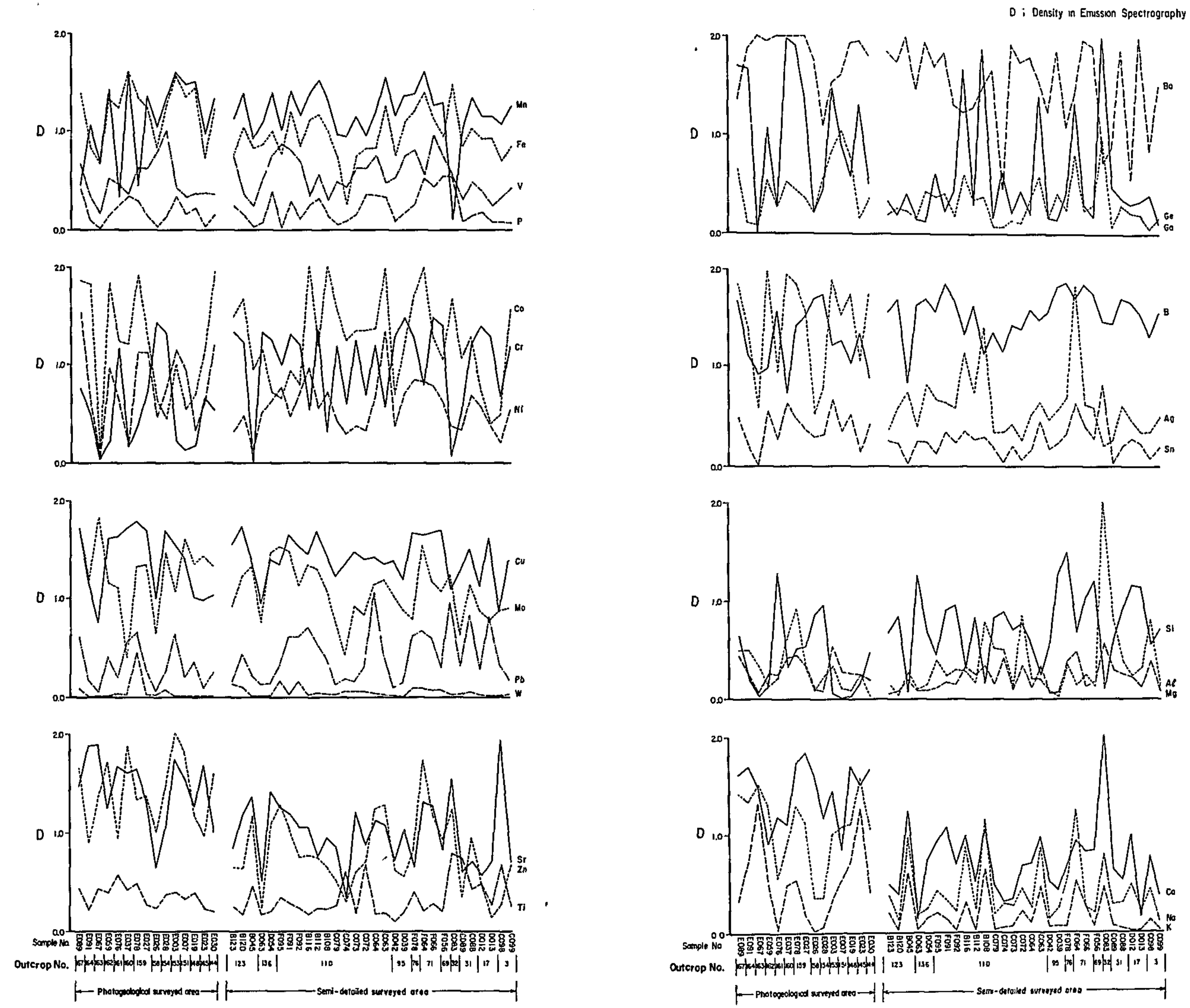

Fig. 29 Trend of Density in Emission Spectrography of Minor Elements in Manganese Ore

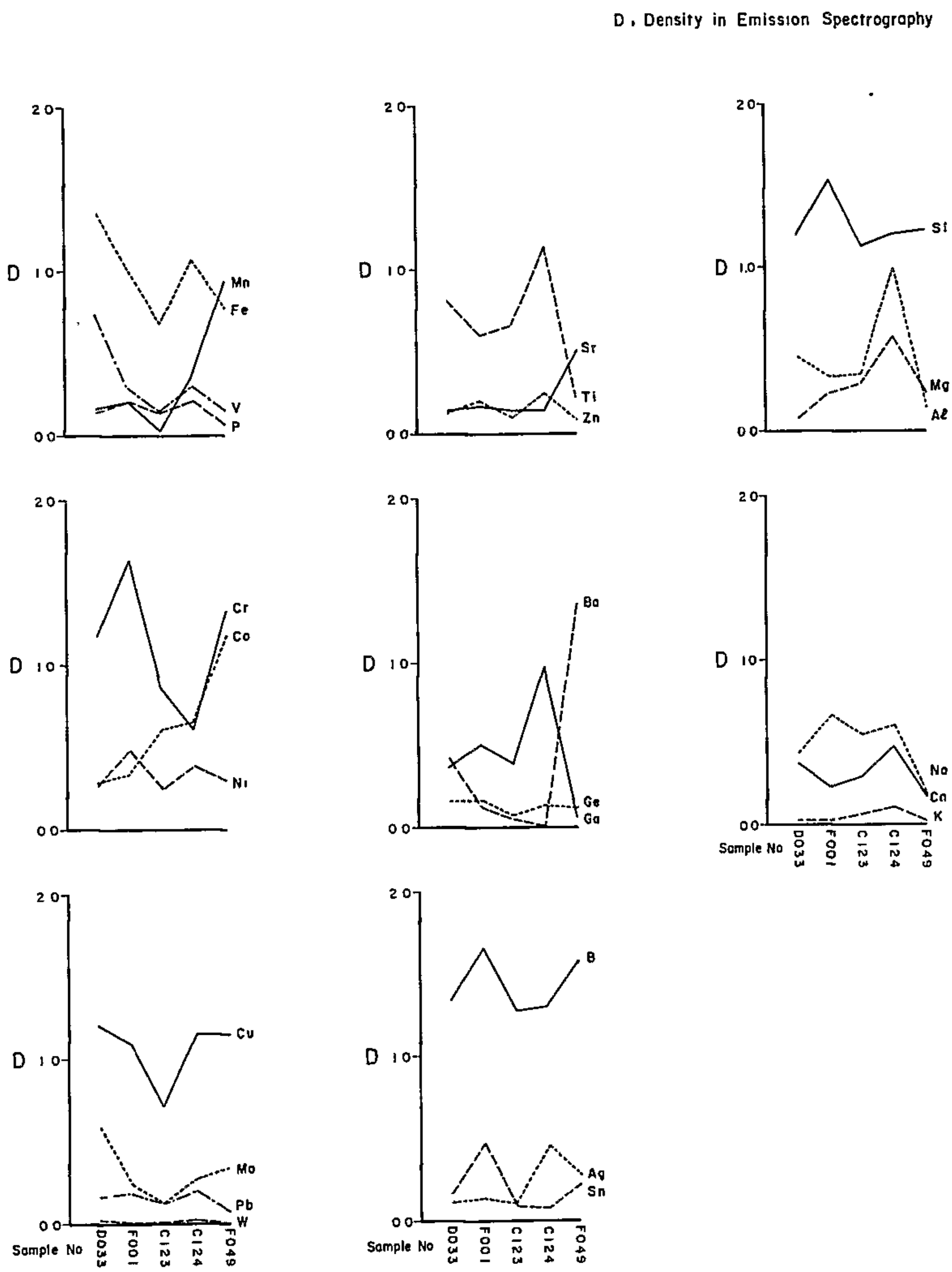

Fig. 30 Trend of Density in Emission Spectrography of Minor Elements in Chert

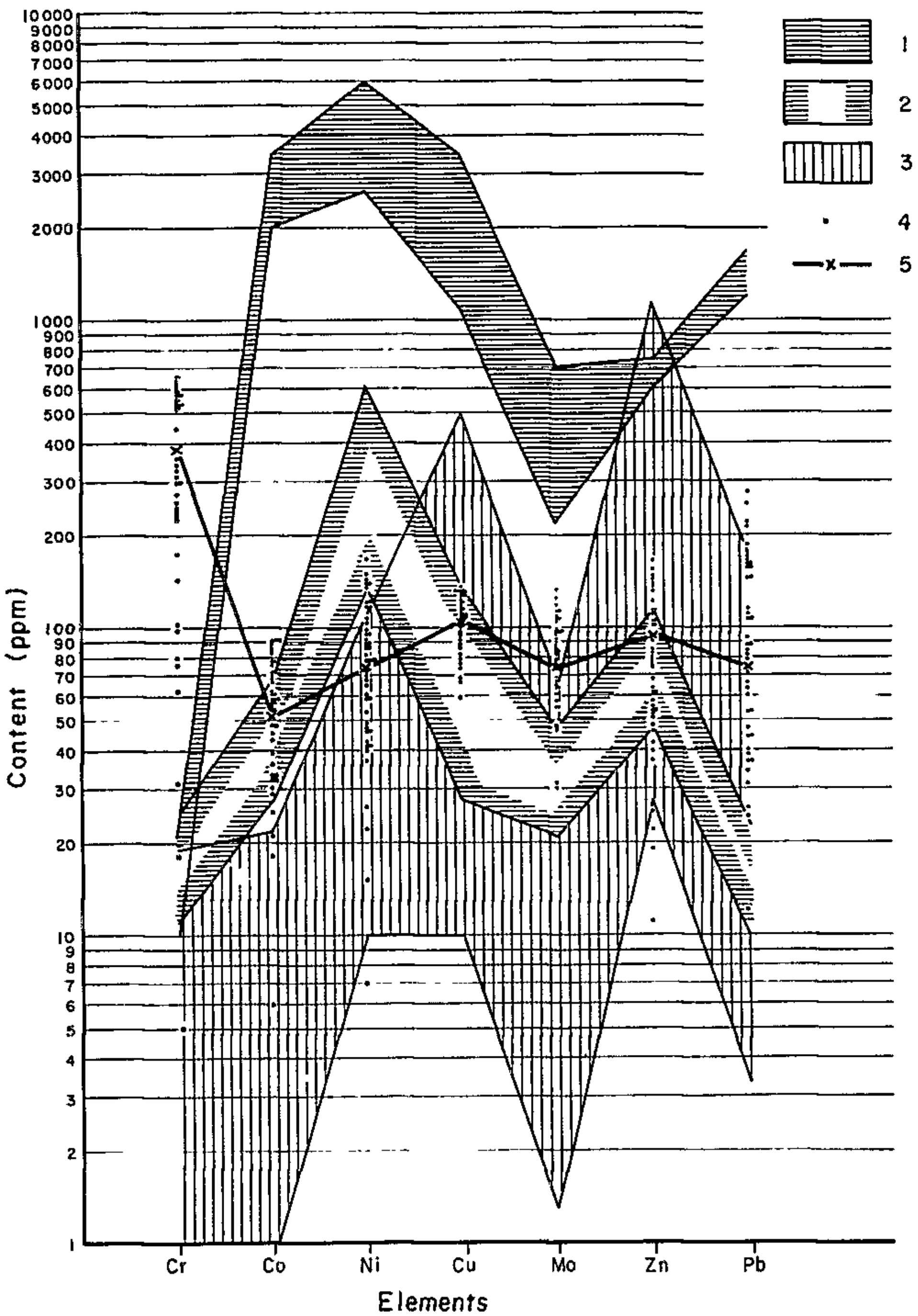

1. manganese ore in recent ocean floor
2 oligocene manganese oxide ore
3. volcanogenic sedimentary manganese ore
4 manganese ore in sur area
5 mean values

Fig. 31 Range of Content of Seven Minor Elements in Manganese Ore

test, which was called as the discharge test of UM−1 style and 2Ω, was performed by getting the preservative time discharging in reality in connection with the 2Ω resister to the dry cell made of the ores in the Sur area. The results are as follows. Reference values are ones used as the raw material of the dry cell nowadays.

	Current	Circuit Voltage	Closed Circuit Voltage	Discharge Ability		
				1.1 V	1.0 V	0.9 V
Ore in Sur Area	4.75 A	1,568 V	1.34 V	30 min.	63 min.	105 min.
Reference Value	6.0 A	1,639 V	1.41 V	53 min.	111 min.	171 min.

All values are below ones of reference. The discharge ability is about 55% of reference values. It was concluded that ores in the Sur area were not suitable for the dry cell.

3−11 Relation between Ore Deposits and Geologic Structure

Manganese ore deposits in this area distribute over whole area of the Halfa Formation. In particular, many deposits distribute at the area of the 16 km northernwest of Awaika (area B of the third year survey), and at the area of the 5 km south of Jaramah (area A of the third year survey). The main geologic structure in two areas are the N−S and E−W systems, respectively. It is considered that the manganese ore deposits were formed under the syngenetic environment, the primary ore deposits were actively controlled by the sedimentation environment, and later the deposits have suffered the diageneses, extensive folding and fault activities. And the distribution of ore deposits and the bonanza have not a close association with folding structure. The relationship between the lava, dyke and sill distributing in the Halfa Formation and the ore deposits was not directly made clear. The veinlets of coarse pyrolusite grains, which fill the cracks in the ore beds and chert, are considered to be the segregation vein during the diagenetic process, and/or the segregation into the cracks originating from the fault and folding. The segregation vein, however, is on the small scale and does not make progress to form the bonanza.

3−12 Genesis of Ore Deposits

The genetical condition of the manganese ore deposits in the Sur area on the bases of the surveyed results and known data was discussed as follows.

The manganese ore deposits in this area occur in the alternating bed of chert and shale of the Halfa Formation and belong to the syngenetic type, being composed of a several intermittent ore beds. The principal ore bodies are the layered ore accompanying the manganese nodular

zone of the low grade.

The manganese ore deposits in the Sur area is considered to be closely associated with the formation of the alternating bed of chert and shale, though there are many theories about the genesis on the alternating bed of chert and shale.

The contents of minor elements in the ore show the same feature as ones in the volcanic sedimentary deposit previously reported by Strakhov (1967). Mn represents the similar variation to Sr and Ba, which were considered to be the elements concentrating in the volcanic sedimentary deposit by Borchert (1970) and Zantop (1980). This, consequently, suggests that the manganese ore deposits in this area was associated with the volcanic activity. It is concluded that the deposit suffered little influence of the metamorphism due to diastrophism referring to the relict of the ore texture at the primary deposition, though the ore bodies were deformed extensively on account of the fault and folding after the time of deposition. It is, however, presumed as that the deposits suffered a little deformation during the diagenesis since there is the presence of both pyrolusite and pyrolusite veinlets which believed at the psuedomorph of manganite and the segregation vein.

Summarily, it is considered that the manganese ore deposits in the Sur area belong to the syngenetic sedimentary type deposits at the formation stage of the alternating bed of chert and shale (Later Jurassic ~ Early Cretaceous), associated with the marine volcanism, and the deposits suffered a little influence of the crustral movement and the diagenesis.

4. Drilling Survey

4–1 General Description

As a part surveyed third year, the drilling survey was conducted to investigate the subsurface extensions of the surface ore beds of the outcrop No.110.

In this survey 17 drill holes were conducted at 8 drilling sites as shown in Fig. 32, 12 holes at 5 sites in the eastern part of the outcrop No.110 and 5 holes at 3 sites in the western part.

According to the geological conditions, down-the-hole percussion method was applied as drilling method. The drilling operation was started on 9th of November and completed on 26th of December in 1982, achieving a total drilled length of 300.00 m.

The lithology of each drill hole was complied by observations of the cuttings collected by every 1-m-length. The cuttings of ore parts were sampled by 0.5- to 1-m-length and the ore samples were analyzed for Mn, MnO_2, SiO_2, and Fe.

It was confirmed that one ore bed extends to the depth of 30 m below surface.

The results is described hereafter.

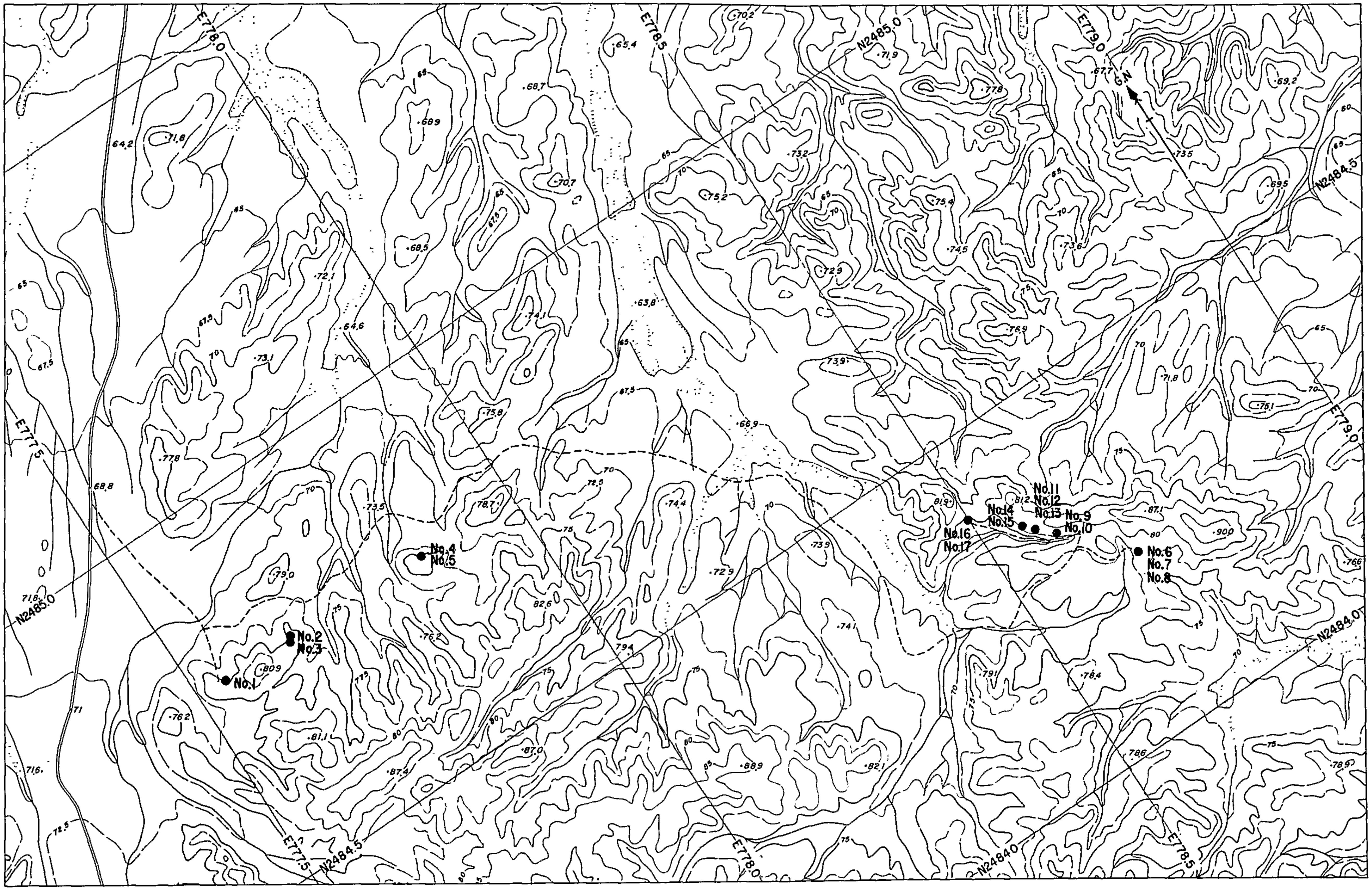

Fig. 32 Location Map of Drilling Holes

0 250M

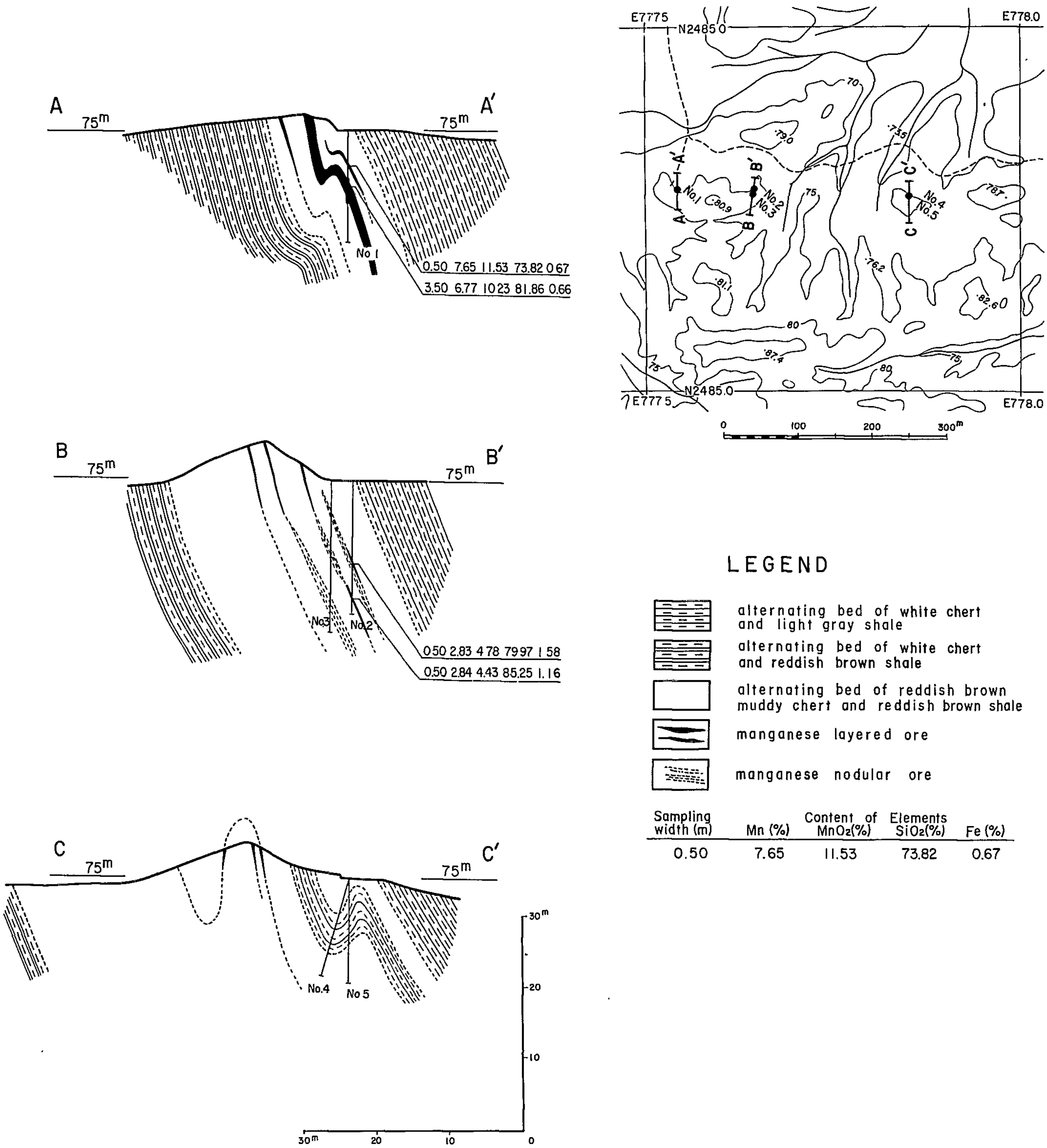

Sampling width (m)	Mn (%)	Content of Elements MnO2(%)	SiO2(%)	Fe (%)
0.50	7.65	11.53	73.82	0.67

Fig. 33—1 Geological Profile of the Drilling Area (No. 1~5)

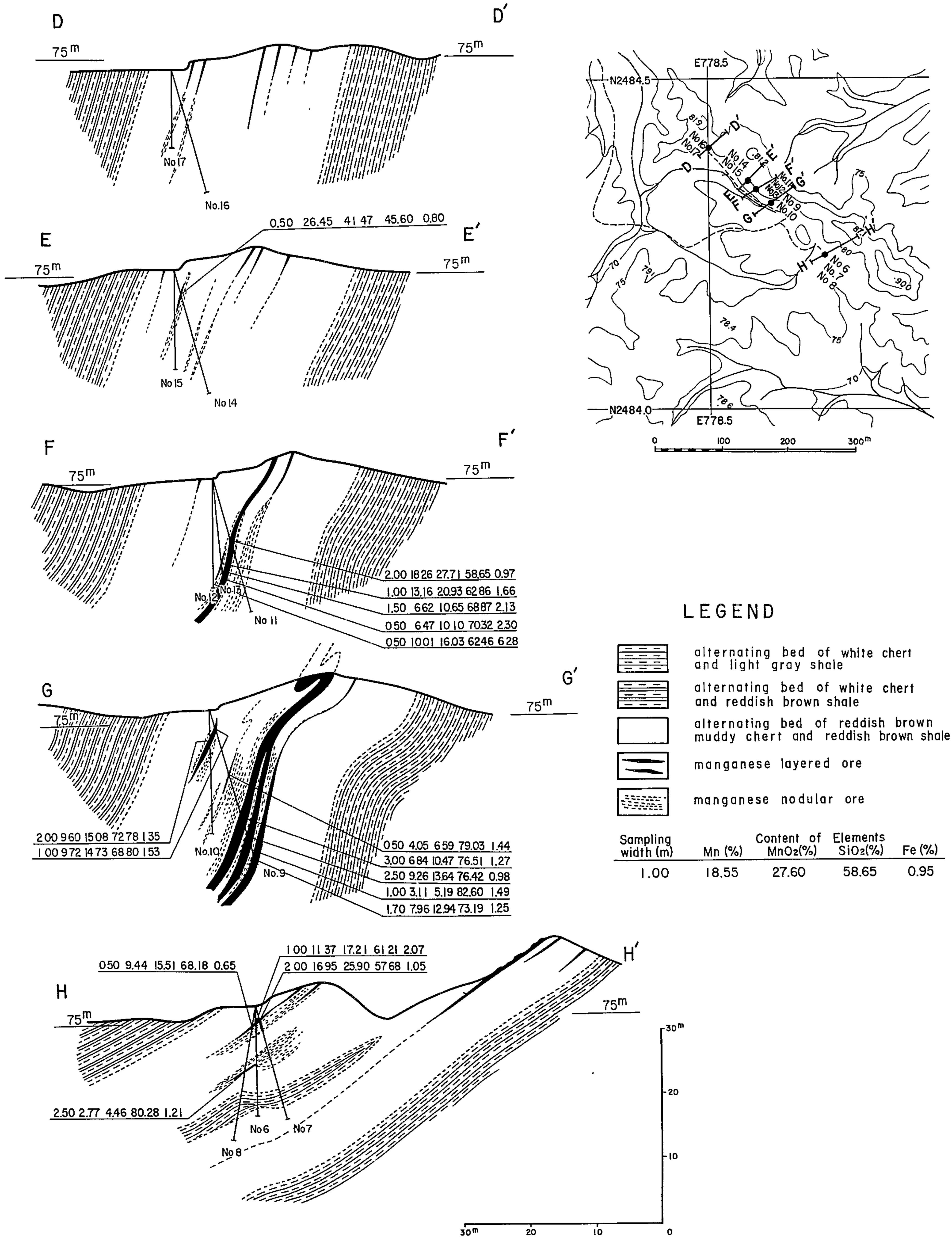

Fig. 33—2 Geological Profile of the Drilling Area (No. 6～17)

No. 1 (15.50m)

No. 2 (18.30m)

No. 3 (20.00m)

No. 4 (14.00m)

No. 5 (14.50m)

No. 6 (17.00m)

No. 7 (18.00m)

No. 8 (21.00m)

No. 9 (24.70m)

No. 10 (19.00m)

No. 11 (21.00m)

No. 12 (16.50m)

No. 13 (15.50m)

No. 14 (19.00m)

No. 15 (15.00m)

No. 16 (19.00m)

No. 17 (12.00m)

red to reddish brown muddy chert and brown shale

white to light gray chert and light gray shale

brown muddy chert and brown shale

black chert and manganese lens

manganese ore with brown muddy chert

manganese ore

ch = chert

Fig. 34 Geological Log and Assay

No. 1

Depth (m)	Core Log	Assay: Sample No.	Width (m)	Mn (%)	MnO2 (%)	SiO2 (%)	Fe (%)	Description
0								0.00-3.00 red ch and white ch
								3.00-4.50 red ch ≫ black ch
		L-1	0.50	7 65	11 53	73 82	0.67	4.50-5.00 manganese ore
5								5.00-6.50 brown ch
		L-2	0.50	5 23	8 04	84.71	0.86	6.50-10.00 manganese ore black colored
		L-3	0.50	7.55	11.46	80.31	0.67	
		L-4	0.50	9 05	14.08	77.01	0.61	
		L-5	0.50	4.94	7.49	83.17	0.88	
		L-6	0 50	5.27	7 70	85 26	0 63	
		L-7	0.50	9 71	14 77	76 61	0 49	
		L-8	0.50	5 65	8.04	85.94	0.47	
10								10.00-11.50 brown ch
								11.50-13.50 red ch and white ch
15								13.50-15.50 red ch and pale brown ch
15.50								

No. 2

Depth (m)	Core Log	Assay: Sample No.	Width (m)	Mn (%)	MnO2 (%)	SiO2 (%)	Fe (%)	Description
0								0.00-4.00 reddish purple ch ≫ white ch
5								4.00-6.00 red ch and white ch
								6.00-8.00 reddish purple ch
								8.00-10.00 red ch and white ch
10								10.00-11.00 brown ch
		L-9	0.50	2.83	4.78	79 97	1.58	11.00-11.50 manganese ore
								11.50-13.00 brown ch ≫ black ch
								13.00-15.50 red ch and white ch
15		L-10	0.50	2.84	4.43	85 25	1.16	15.50-16.00 manganese ore
								16.00-18.30 brown ch > red ch and white ch
18 30								

No. 3

Depth (m)	Core Log	Assay						Description
		Sample No.	Width (m)	Mn (%)	MnO2(%)	SiO2(%)	Fe (%)	
0								0.00-2.00 red to purple ch
								2.00-3.00 red ch ≫ white ch
								3.00-4.00 red ch ≫ black ch
								4.00-5.00 purple ch ≫ white ch > black ch
5								5.00-7.00 red to purple ch and white ch
								7.00-800 dark purple ch and red ch
								8.00-10.00 brown ch ≫ black ch
10								10.00-11.00 dark brown ch with manganese
								11.00-15.00 purple ch > red ch > white ch
15								15.00-19.00 brown ch > black ch
20.00								19.00-20.00 dark brown ch

No. 4

Depth (m)	Core Log	Assay						Description
		Sample No.	Width (m)	Mn (%)	MnO2(%)	SiO2(%)	Fe (%)	
0								0.00-5.00 red ch
5								5.00-6.00 red ch and white ch
								6.00-11.00 white to gray ch
10								11.00-14.00 red ch
14.00								

No. 5

Depth (m)	Core Log	Assay: Sample No.	Width (m)	Mn (%)	MnO_2 (%)	SiO_2 (%)	Fe (%)	Description
0								0.00 - 1.00 red ch and white ch
5								1.00 - 9.00 white ch
10								9.00 - 12.00 white ch and red ch
14.50								12.00 - 14.50 purple to red ch and white ch

No. 6

Depth (m)	Core Log	Assay: Sample No.	Width (m)	Mn (%)	MnO_2 (%)	SiO_2 (%)	Fe (%)	Description
0								0.00 - 1.00 dark purple ch, red ch and white ch
								1.00 - 2.00 dark brown ≫ black ch
		L-11	0.50	11.18	16.98	61.74	2.07	2.00 - 3.00 manganese ore
		L-12	0.50	11.55	17.44	60.68	2.07	
								3.00 - 4.00 red ch and white ch ≫ black ch
5								4.00 - 7.00 brown ch > red ch and white ch
								7.00 - 9.50 brown ch ≫ black ch
10								9.50 - 10.00 red ch
								10.00 - 11.00 red ch and white ch
								11.00 - 14.00 purple ch, red ch and white ch
								14.00 - 15.00 white ch
15								15.00 - 16.00 white ch > red ch
17.00								16.00 - 17.00 grayish brown ch

No. 7

Depth (m)	Core Log	Assay Sample No	Width (m)	Mn (%)	MnO2(%)	SiO2(%)	Fe (%)	Description
0								0.00 – 1.00 dark purple ch, red ch, white ch
								1.00 – 2.00 dark brown ch and red ch
		L 13	1.00	21.04	32.00	49.41	0.88	2.00 – 4.00 manganese ore ≫ red ch
		L 14	1.00	12.86	19.80	65.94	1.21	
5								4.00 – 5.00 red ch ≫ black ch
								5.00 – 6.00 brown ch and red ch
								6.00 – 8.00 brown ch ≫ black ch
								8.00 – 11.00 brown ch
10								11.00 – 12.00 red ch and white ch
								12.00 – 13.00 white ch ≫ red ch
								13.00 – 16.00 white to gray ch
15								16.00 – 18.00 red ch
18.00								

No. 8

Depth (m)	Core Log	Assay Sample No	Width (m)	Mn (%)	MnO (%)	SiO (%)	Fe (%)	Description
0								0.00 – 1.00 dark purple ch, red ch, white ch
								1.00 – 3.00 dark purple ch ≫ black ch
		L 15	0.50	9.44	15.51	68.18	0.65	3.00 – 3.50 manganese ore
								3.50 – 5.00 purple ch and black ch
5								5.00 – 7.50 brown ch ≫ black ch
								7.50 – 8.00 pale brown ch
		L 16	0.50	3.04	5.03	83.23	1.45	8.00 – 10.00 manganese ore ≫ brown ch
		L 17	0.50	2.58	4.10	80.19	1.67	
		L 18	1.00	1.74	2.89	81.48	0.65	
10		L 19	0.50	4.75	7.40	75.04	1.62	10.00 – 10.50 manganese ore
								10.50 – 13.00 red ch
								13.00 – 13.50 red ch > white ch
								13.50 – 15.00 white ch > red ch
15								15.00 – 18.00 white to gray ch
								18.00 – 19.00 red ch > white ch
								19.00 – 20.00 brown to red ch
20								20.00 – 21.00 white ch > red ch
21.00								

No. 9

Depth (m): 0, 5, 10, 15, 20, 24.70, 25

Sample No	Width (m)	Mn (%)	MnO_2 (%)	SiO_2 (%)	Fe (%)
L 20	0.50	11 65	17 25	65.60	1.48
L 21	0.50	7 79	12 20	71 99	1.58
L 22	0 50	4 05	6.59	79 03	1.44
L 23	0 50	9.94	14 98	71.79	0 92
L 24	0.50	5.67	9.20	76.31	1.55
L 25	0 50	4 08	7.10	75.48	2.01
L 26	0.50	8.50	13.22	75.32	1.26
L 27	0 50	7 19	10.97	77.33	1.14
L 28	0 50	5 66	7.32	82.01	0.74
L 29	0 50	4.79	7.54	78 64	1.80
L 30	0 50	6 01	8 46	85 25	0 57
L 31	0 50	8 79	12 54	77.26	0.83
L 32	0.50	21 76	32 22	54.03	0.99
L 33	0 50	4 94	7.45	86 93	0 69
L34	1 00	3 11	5.19	82.60	1.49
L35	1.00	5 99	9 49	77.94	1 26
L36	070	10.88	17.88	66.41	1.23

Description

- 0.00 – 2 00 red ch, white ch > brown ch
- 2.00 – 2.50 brown ch ≫ red ch
- 2.50 – 3.50 manganese ore
- 3.50 – 4 00 brown ch
- 4.00 – 6.50 red ch
- 6.50 – 8.00 brown ch ≫ red ch
- 8.00 – 10.00 brown ch
- 10.00 – 10.50 manganese ore
- 10.50 – 11.50 manganese ore ≫ brown ch
- 11.50 – 16.00 brown ch ≫ black ch
- 16.00 – 19.00 manganese ore
- 19.00 – 19.50 manganese ore ≫ brown ch
- 19.50 – 22.00 manganese ore
- 22.00 – 23.00 manganese ore ≫ brown ch
- 23.00 – 24.70 manganese ore

No. 10

Depth (m): 0, 5, 10, 15, 19.00

Sample No	Width (m)	Mn (%)	MnO_2 (%)	SiO_2 (%)	Fe (%)
L 37	1.00	10 95	17.88	65.30	1.98
L 38	1.00	8 25	12.28	80.25	0.71

Description

- 0.00 – 2.00 red ch and white ch
- 2.00 – 3.00 red ch
- 3.00 – 3.50 brown ch
- 3.50 – 4.00 brown ch ≫ black ch
- 4.00 – 6.00 manganese ore
- 6.00 – 8.00 brown ch ≫ black ch
- 8.00 – 9.00 brown ch ≫ red ch
- 9.00 – 10.00 red ch
- 10.00 – 11.00 brown ch ≫ black ch
- 11.00 – 14.00 brown ch
- 14.00 – 15.00 brown ch ≫ black ch
- 15.00 – 16.00 brown ch
- 16.00 – 17.00 brown ch and black ch
- 17.00 – 19.00 brown ch

No. 11

Depth (m)	Sample No	Width (m)	Mn (%)	MnO2 (%)	SiO2 (%)	Fe (%)	Description
0.00 – 2.00							red ch and white ch
2.00 – 6.00							red ch
6.00 – 8.50							red ch and brown to orange ch
8.50 – 9.50							manganese ore ≫ brown ch
9.50 – 11.50	L 39	1.00	13.52	21.36	63.82	1.43	manganese ore
	L 40	1.00	22.99	34.05	53.48	0.51	
11.50 – 12.50							manganese ore ≫ brown ch
12.50 – 13.50							pale brown ch ≫ black ch
13.50 – 18.00							manganese ore ≫ brown ch
18.00 – 21.00							pale brown ch

No. 12

Depth (m)	Sample No.	Width (m)	Mn (%)	MnO2 (%)	SiO2 (%)	Fe (%)	Description
0.00 – 1.00							red ch
1.00 – 3.00							red ch ≫ white ch
3.00 – 4.00							brown to red ch
4.00 – 5.00							orange ch
5.00 – 7.00							red ch
7.00 – 9.00							orange to red ch
9.00 – 11.00							red ch
11.00 – 13.00							white ch and red ch
13.00 – 14.50							red ch
14.50 – 15.00							red ch ≫ black ch
15.00 – 16.00							brown ch ≫ black ch
16.00 – 16.50	L 41	0.50	10.01	16.03	62.46	6.28	manganese ore ≫ brown ch

No. 13

Depth (m)	Core Log	Assay: Sample No	Width (m)	Mn (%)	MnO_2 (%)	SiO_2 (%)	Fe (%)	Description
0								0.00 – 1.00 purple to red ch and white ch
								1.00 – 2.00 red ch
								2.00 – 4.00 orange to red ch
								4.00 – 5.00 red ch > white ch
5								5.00 – 8.00 red to orange ch
								8.00 – 11.00 brown ch and red ch
10								11.00 – 12.00 red ch
								12.00 – 12.50 red ch and black ch
		L 42	0.50	16.23	26.32	59.27	1.37	12.50 – 13.00 manganese ore ≫ brown ch
		L 43	0.50	10.08	15.53	66.44	1.95	13.00 – 13.50 manganese ore
		L 44	0.50	5.96	9.92	72.46	1.99	13.50 – 15.00 manganese ore ≫ brown ch
15		L 45	1.00	6.95	11.02	67.08	2.20	
15.50		L 46	0.50	6.47	10.10	70.32	2.30	15.00 – 15.50 manganese ore

No. 14

Depth (m)	Core Log	Assay: Sample No	Width (m)	Mn (%)	MnO_2 (%)	SiO_2 (%)	Fe (%)	Description
0								0.00 – 2.50 yellow to orange ch and red ch
								2.50 – 3.00 brown ch ≫ black ch
		L 47	0.50	26.45	41.47	45.60	0.80	3.00 – 3.50 purplish red ch ≫ black ch
								3.50 – 4.00 manganese ore
								4.00 – 5.00 dark brown ch ≫ black ch
5								5.00 – 6.00 brown ch, red ch ≫ black ch
								6.00 – 7.00 grayish brown ch
								7.00 – 9.00 brown ch > red ch and white ch
10								9.00 – 11.00 brown to dark brown ch
								11.00 – 12.00 brown ch ≫ black ch
								12.00 – 13.00 dark brown ch
								13.00 – 14.00 brown ch, red ch and black ch
15								14.00 – 15.00 brown ch, red ch and white ch
19.00								15.00 – 19.00 brown ch

No. 15

Depth (m)	Core Log	Assay: Sample No.	Width (m)	Mn (%)	MnO2 (%)	SiO2 (%)	Fe (%)	Description
0								0.00 – 2.00 orange to red ch
								2.00 – 6.00 red to brownish red ch > white ch
5								
								6.00 – 6.50 red ch
								6.50 – 7.00 *brown ch ≫ black ch*
								7.00 – 9.00 brown ch, red ch, white ch and black ch
10								9.00 – 13.00 brown ch
15 00								13.00 – 15.00 reddish brown ch

No. 16

Depth (m)	Core Log	Assay: Sample No.	Width (m)	Mn (%)	MnO2 (%)	SiO2 (%)	Fe (%)	Description
0								0.00 – 1.00 *dark brown ch ≫ red ch, white ch*
								1.00 – 3.00 dark brown to brown ch
								3.00 – 5.00 brown ch > red ch and white ch
5								5.00 – 6.00 brown ch ≫ red ch and white ch > black ch
								6.00 – 7.00 brown ch, red ch and white ch
								7.00 – 8.00 brown ch > red ch and white ch > black ch
								8.00 – 9.00 brown ch ≫ black ch
10								9.00 – 19.00 brown ch
15								
1900								

No. 17

Depth (m)	Core Log	Assay: Sample No.	Width (m)	Mn (%)	MnO_2 (%)	SiO_2 (%)	Fe (%)	Description
0								0.00 - 1.00 dark brown ch, red ch, white ch
								1.00 - 4.00 dark brown ch and black ch
								4.00 - 5.00 dark brown ch, red ch, white ch, black ch
5								5.00 - 10.00 brown ch > black ch > red ch and white ch
10								10.00 - 12.00 dark brown ch ≫ red ch
12.00								

4–2 Results of Drilling Operation

According to the mode of occurrence of the outcrops, 12 drill holes out of 17 holes were conducted in the eastern part of the outcrop No.110 and remaining 5 holes in the western part. By the drilling survey, 11 holes encountered ore beds. Most of the proven extentions are limitted to a range of less than 20 m below surface. The maximum depth of the proven ore bed is 24.70 m in the No.9 drill hole.

The occurrencies of ore beds in each drill hole are described hereafter. The geology and ore grades are shown in Fig. 34.

Fig. 33–1, 33–2 are the compiled profile from the geological data.

1) No.1 drill hole

Drilled length; 15.50 m, direction; – , inclination; 90°

Ore beds were recognized in two depth intervals(4.50 – 5.00 m, 6.50 – 10.00 m). As shown in the profile, the two ore beds are considered to continue to the outcrops following small-scaled anticlinal and synclinal structures.

2) No.2 drill hole

Drilled length; 18.30 m, direction; – , inclination; 90°

Ore beds were found in two depth intervals (11.00 – 11.50 m, 15.50 – 16.00 m). The two ore beds are, as shown in the profile, not the extensions of the main outcrops but those of north-neighboring 10 cm-thick ore outcrops.

3) No.3 drill hole

Drilled length ; 20.00 m, direction; –, inclination; 90°

No major ore bed was encountered in this hole except minor amount of black chert in three depth intervals (3.00 – 5.00 m, 8.00 – 11.00 m, 15.00 – 20.00 m). These black cherts are likely the downward extensions of the outcropping beds and, farther, the upward continuations of the ore beds found in the No.2 drill hole. Consequently, the ore beds around this drilling site are estimated to be intermittent in dip side as well as in strike side.

4) No. 4 drill hole

Drilled length; 14.00 m, direction; 180°, inclination; 75°

No ore bed was recognized, however, as shown in the profile, a paired anticline and syncline were clearly delineated.

5) No.5 drill hole

Drilled length; 14.50 m, direction; –, inclination; 90°

No ore bed was found, but it was made clear that as shown in the profile the white chert part in this drill hole continues to the white chert part in No.4 drill hole and, farther, to the alternation of light gray chert and shale showing a paired syncline and anticline.

6) No.6 drill hole

Drilled length; 17.00 m, direction; – , inclination, 90°

One ore bed was recognized in the depth interval of 2.00 to 3.00 m. This bed is the extension of the outcrop 7 m north to the drill hole.

7) No.7 drill hole

Drilled length; 18.00 m, direction; 60°, inclination; 75°

One ore bed was found in the depth interval of 2.00 to 4.00 m. This ore bed is the same one found in the No.6 drill hole.

8) No.8 drill hole

Drilled length; 21.00 m, direction; 240°, inclination; 80°

Ore beds were encountered in two depth intervals (3.00 – 3.50 m, 8.00 – 10.50 m). The upper bed is likely the continuation of the ore bed found in the No.6 drill hole: the lower bed to the thin black chert part found in the depth interval of 7.00 to 9.50 m of the No.6 drill hole. The main ore bed might be embedded in deeper part as shown in the profile.

9) No.9 drill hole

Drilled length; 24.70 m, direction; 55°, inclination; 75°

Ore beds were recognized in three depth intervals (2.50 – 3.50 m, 10.0 – 11.50 m, 16.00 – 24.70 m). As shown in the profile, the upper two beds are considered to be small in scale. The lowest bed might be the downward extension of the 2-m-thick outcrop. By this drilling, the major ore bed was confirmed to extend to the depth of 30 m below surface showing fold structures. By the X-ray diffractive analysis and microcopic studies on the ore samples from the deepest ore bed pyrolusite, cryptomelane and manganite were detected. Moreover, a weak X-ray diffraction peak of probable rhodochrosite was detected from one sample.

10) No.10 drill hole

Drilled length; 19.00 m, direction; – , inclination; 90°

One ore bed was recognized in the depth interval of 4.00 to 6.00 m. This bed may be the downward extension of a small-scale outcrop near the drilling site.

The thin black chert parts found in the depth interval of 10.00 to 16.00 m are considered to extend to the ore bed recognized near 10 m depth in the No.9 drill hole.

11) No.11 drill hole

Drilled length; 21.00 m, direction; 60°, inclination; 75°

Ore beds were encountered in two depth intervals (8.50 – 12.50 m, 13.50 – 18.00 m). These beds are estimated to be the underward continuations of the outcrops.

12) No.12 drill hole

Drilled length; 16.50 m, direction; – , inclination; 90°

Although a ore bed was encountered in the depth interval of 16.00 to 16.50 m.

This ore bed is considered to continue to the ore part of the No.11 drill hole as shown in the profile.

13) No.13 drill hole

Drilled length; 15.50 m, direction; 60°, inclination; 85°

A ore bed occurred from the depth of 12.50 m up to the depth of 15.50 m. This ore bed is the probable continuation of the ore bed found in the No.11 drill hole.

14) No.14 drill hole

Drilled length; 19.00 m, direction; 45°, inclination; 75°

One ore bed was recognized in the depth interval of 3.50 to 4.00 m. This bed is estimated to be a small-scale lens. The thin black chert beds are possibly the subsurface extensions of the outcrops.

15) No.15 drill hole

Drilled length; 15.00 m, direction; – , inclination; 90°

No major ore bed was found. The thin black chert in the middle part is considered to be the extension of the ore bed of the No.14 drill hole.

16) No.16 drill hole

Drilled length; 19.00 m, direction; 50°, inclination; 75°

No major ore bed was recognized. The two thin black chert parts may be the continuation of the ore beds on surface.

17) No.17 drill hole

Drilled length; 12.00 m, direction; – , inclination; 90°

No major ore bed was encountered. The thin black chert parts found in the depth from 1.00 to 10.00 m are estimated to continue to those of the No.16 drill hole.

4–3 Summary of Results

By the drilling exploration, it was confirmed that at one site a ore bed extends to the depth of 30 m below the surface. In many places, the surface ore beds grade to thin black chert beds at the levels of 10 to 15 m below surface. The dip-side continuity of most ore beds is estimated poor as well as the strike-side one.

The manganese minerals in the drilled ore samples show almost similar assemblage to that of the outcrops. However, the probable rhodochrosite was detected by X-ray diffraction of one sample.

5. Evaluation of the Ore Deposits

Although many outcrops of manganese ore deposits were found in the Sur area, it may be difficult to develop these deposits because of their small scale and low grade.

The provisional operation costs were considered under the condition in the followings.

(1) The scale of operations

Total tonnage of ore reserves is estimated as 520,000 tons, but if a simple surface mining method will be applied, minable ore reserves should be reduced to 5 meters portion below the surface only, and they would be recalcurated as 86,000 tons. If the mine life is supposed to be of 5 years, daily production rate would be 57 tons of ore (300 operation days a year) and required manpower should be thirty.

(2) Mining costs

Ore beds are mined by hydraulic brakers and a backhoe type power shovel as a manner of

trenching along the ore beds to the depth of 5 meters.

Crude ores digged out by backhoe contain waste rocks because ore beds are thin. Therefore, waste rocks are removed by hand picking. The average grade of the final product may be 20% Mn.

Another required mining equipments are rock drills, a air compressor and a bucket loader. 15 workers are required for mining, hand picking and handling.

The mining costs of the manganese ore deposits may be more than US$20/ton ore, because the mining costs of the Rajmi Mine which has similar operational scale and mining method, are US$20/ton ore and the amount of wast rocks is more than that of the Rajmi Mine.

(3) Transportation costs

The final product is transported to Muscat by trucks. The distance between Muscat and the Rajmi Mine is about 300 kilometers and the transportation costs are US$25/ton ore. The estimated transportation costs of the manganese ore deposits are US$30/ton ore. This figure increase 20 percents over the case of the Rajmi Mine, because the transportation distance is 20 percents longer than that of the Rajmi Mine.

(4) Price of ore

The price of manganese ore is not stable, but the recent price of manganese ore is around US$70/ton ore* in case of 48% Mn ore. Assuming the price of manganese ore is US$70/ton ore, the unit price (1% Mn price) is US$1.46/ton ore. The average grade of the manganese ore is about 20% Mn, so the ore price will be US$29/ton ore.

---

* Year Book of Ferroalloy (1982 in Japanese)

Manganese ore price (FOB) imported from Australia

1981	US$67.296/T (Mn48%)	US$1.402/T (Mn1%)
1980	US$65.28/T (")	US$1.36/T (")
1979	US$57.00/T (")	US$1.1875/T (")

Mining Journal (1982 Dec.)

Manganese ore price

	US$76.8/T (Mn 48%)	US$1.60/T (Mn 1%)

(5) Profitability

The price of ore is US$29/ton ore as mentioned above, and the estimated transportation costs are US$30/ton ore. Therefore, the price of ore can not cover the transportation costs. Furthermore, assuming the mining costs of the manganese ore deposits are similar to the costs of the Rajmi Mine, the total costs of mining operation are US$50/ton ore. Therefore, the development of the manganese ore deposits in the Sur area is not profitable at the present time.

CHAPTER IV. CONCLUSION AND EVALUATION

1. Conclusion

This survey has been conducted in the Salalah area as the first year, and in the Sur area as the second and third year.

1–1 Salalah Area

Geological survey and radiometric survey of the area 1,500 km^2 were carried out and the following conclusion was obtained.

Geology

(1) Stratigraphy in the area was established by the classification of rock facies comparing with geochronologic data. It is clarified that Precambrian rocks particularly correspond to the period of the formation of Arabian shield.

(2) It is clarified that Mirbat Sandstone Formation is shallow sea sediments by the study of the sedimentary structure and sedimentary environment.

(3) Principal geologic structure in the survey area trends NE–SW, NW–SE and N–S. Gneisose structure and its folding axis of Precambrian metamorphic rocks mainly trend NE–SW with N–S. The trend of faults and dykes indicates NW–SE trending, with NE–SW trending in some place.

Ore Deposits

(1) Mineral occurrence in the survey area is very poor and shows very low grade. Pegmatite veins were observed associated with very small amount of chalcopyrite, malachite and pyrite in some place. Some barite-calcite veinlets containing galena crystal were recognized in the Mirbat Sandstone Formation, which are not considered to be economical.

(2) The survey of the sedimentary environment and structure of the Mirbat Sandstone Formation was carried out to clarify the possibility of uranium deposits. As the result of the survey, the Mirbat Sandstone Formation is shallow sea sediment and has no material absorbing uranium. It is concluded that there is slight possibility of uranium deposits existing.

(3) Pegmatite veins observed in Precambrian gneiss are small size and are not economical for the raw material of the ceramic industry. Any minerals containing valuable elements of rare metal were not recognized in pegmatite veins. Barite-calcite veinlets in some parts of the Mirbat Sandstone Formation are not economical.

1–2 Sur Area

Geological survey, including photogeological survey of the area 3,400 km^2, and trenching and drilling surveys in the area were carried out and the following conclusion was obtained.

Geology

(1) Geology of the area is composed of Precambrian basement rocks, Triassic to Early Cretaceous Halfa Formation, Later Cretaceous to Middle Tertiary Limestone Formation and Quaternary sediments.

(2) The Halfa Formation consists of alternating bed of chert and shale, shale, limestone and basic lava, and was divided into the Lower, Middle and Upper memebers. Furthermore, the Middle Member was subdivided into the Red alternating bed, the White alternating bed, the Transitional alternating bed and the Shale bed to clarify the structure of the Halfa Formation and the ore horizon.

(3) The direction of principal structure in the area trends N–S to NNW–SSE indicating the direction of the arrangement of basement rocks, folding axes and faults. The structure of the Halfa Formation is very complicated with many folds and faults, which indicates different direction in each area.

Ore Deposits

(1) Manganese ore deposits are mainly observed in the Red alternating bed of the Middle Member which is the alternating bed of reddish brown chert, reddish brown to pale brown muddy chert and reddish brown to pale brown shale. It is considered that manganese ore deposits is volcanogenic stratiform sedimentary deposits.

(2) Three to six ore horizons were recognized in the Middle Member. By folding of the Halfa Formation many ore outcrops are distributed in wide area.

(3) Geological survey including trenching and drilling survey were carried out in the four selected areas to clarify the occurrence, scale and continuity of ore deposits.

(4) It is clarified that ore deposits are composed of several small discontinuous manganese beds with layered or lenticular shape. Most of the ore deposits dip steeply along the bedding of the alternating bed.

(5) It is recognized by drilling survey that ore beds continue at least 30 meters downward from the outcrop.

(6) Ore consists of pyrolusite as principal ore mineral, shows low grade, 20 to 40% of MnO_2 (average grade of 29.56% MnO_2).

(7) Total ore reserve, assuming ore beds continue 30 meters from the surface, is 520,000 ton with average grade of 29.56% MnO_2. The most of ore outcrops are small scale, and their ore reserve are less than 5,000 ton.

2. **Evaluation**

As the results of the survey of the Salalah area and the Sur area, the following evaluation was obtained.

(1) Stratigraphy and geological structure of the Salalah area were clarified, and it is concluded that there is slight possibility of uranium deposits existing.

(2) Although many manganese outcrops are recognized in the Sur area, it seems that the development of ore deposits is not profitable at the present time because of their small scale, thin bed type, low grade and sporadic distribution.

Reference

Salalah Area

Beydoun, Z.R., 1966, Geology of the Arabian Peninsula – Eastern Aden Protectorate and part of Dhufar. U.S. Geol. Surv. Prof. Papaer, 560–H, P. H1–49, 1970, Southern Arabia and northern Somalia: comperative geology. Phil. Trans. Roy. Soc. Lond. A. 267, p. 267–292.

Brown, G.F. and Jackson, R. O., 1960, The Arabian Shield: Internat, Geol. Cong., 21st, Copenhagen 1960, Rept. 21, Pt. 9, p. 69–77.

Carney, J. N. and Welland, M. J. P., 1974, Geology and mineral resources of the Oman Mountains. Institute Geol. Soc. London Rept. No. 27, p. 1–49.

Daly, R. A., 1933, Igneous rocks and the depth of the earth. p. 9–10, Mcgrow-Hill Book Company, Inc. New York.

Delfour, J., 1975, Volcanism and mineral deposits of the Arabian-Nubian Shield. p. 1–36. Ministry of Petroleum and Mineral Resources, Saudi Arabia B. R. G. M. Saudi Arabia Mission.

El Ramly M. F. and Others, 1971. Tha alkaline rocks of south-eastern Egypt. United Arab Republic Ministry of Industry

Gealey, W. K., 1977, Ophiolite obduction and geologic evolution of the Oman Mountains and adjacent areas. Geol. Soc. America Bull., v.88, p. 1183–1191.

Geukens, F., 1966, Geology of Arabian Peninsula – Yemen. U. S. Geol. Surv. Prof. Paper, 560–B, p. B1–23.

Glennie, K. W. and others, 1974, Geology of the Oman Mountains, Pt. 1 (Text) and Pt. II (Tables and Illustrations). Verh. Konink. Nederlands Geolo. Mijnbowkundig Genootschap, Deel 31, p. 1–423.

Greenwood, J. E. G. M. and Loney, P. E., 1968, Geology and mineral resources of the Trucial Oman Range. Inst. Geol. Sci. London, Unpublished report, p. 1–108

Heremboure, J. and Horstink, J., 1967, Mesozoic nappes in the Oman Mountains, a hypothesis. Unpublished PD (Oman) Report.

Ishihara, S. and others, 1967, Uranium content of Upper Paleozoic slate and Neogene siltstone. Rept. Geol. Surv. Japan, No. 232, p. 221–231.
(in Japanese with English abstract).

Japan International Cooperation Agency 1979, Report on the survey for mineral resources development in The Sulauate of Oman

Kapp, H. and Llewellyn, P. G., 1965, The geology of the Central Oman Mountains.
Unpublished PD (Oman) Report.

Katada, M., 1967, Ryoke metamorphic belt in the northern Kiso district, Nagano prefecture. Rept. Geol. Surv. Japan, No. 223, P. 1–38.
(in Japanese with English abstract)

Lees, G. M., 1928, The geology and tectonics of Oman and of parts of southeastern Arabia. Quart. Jour. Geol. Soc. London, V. 84, p. 585–670.

Miyashiro A., 1979. The Earth Science 16,.Iwanami Shoten, Tokyo (in Japanese)

Mercanton C. H. and others, 1968, Geological Study of DHOFAR, A report of Shell International Petroleum (unpublished)

Perters, Tj. and Kramers, J. D., 1974, Chromite deposits in the ophiolite complex of Northern Oman. Mineal, Deposita, v. 9, p. 253–259.

Powers, R. M. and others, 1966, Geology of the Arabian Peninsula – Sedimentary geology of Saudi Arabia. U. S. Geol. Surv. Prof. Paper, 569–D, p. D1–147.

PENCOL International Ltd. 1979, Water well drilling in the Jebel and Negd Dhofar (unpublished)

Roberts, R. J. and others, 1975, Mineral deposits in western Saudi Arabia. U.S. geol. Surv. Saudi Arabian Project Report 201, p. 1–60.

Saudi Arabia Directorate General of Mineral Resources, 1976, Mineral resources activity 1390–1395 A. H. (1970–1875 A. D.). A report of the first Saudi Arabia Five-Year Development Plan.

Shibata, H., 1968, Description on the rocks of Japan, H, p. 152. Asakura Shoten, Tokyo. (in Japanese)

, 1968, ditto, IV, p. 128, ditto.

Takahashi, K., 1979, geological history and granitoides in Arabian Shield, Institute of geological survey of Japan geology news No. 295. p. 44–55.

, 1979, Metavolcanic formation in Arabian Shield. Institute of geological survey of Japan, geology news No. 279, p. 34–48.

Welland, M. J. P. and Mitchell, A. H. G., 1977, Emplacement of the Oman ophiolite, A mechanism related to subduction and collision. Geol. Soc. America Bull., v. 88, p. 1081–1088.

Sur Area

Bamba, T. (1976) — Ophiolite and related copper deposits of Ergani mining district, southeastern Turkey, Bull. Miner. Res. Expl. Inst. Turkey, 86, p.36–50.

Borchert, H. (1970) — On the ore deposition and geochemistry of manganese, Mineral. Deposita (Berl.) 5, p.300–314.

Carlson, L.E. (1973) — Ras Al-Hadd area, Oman manganese deposit, Granges International Mining.

Carney, J.N. and Welland, M.J.P. (1974) — Geology and mineral resources of the Oman Mountain. Institute Geol. Soc., London Rept. No.27, p.1–49.

Coleman, R.G. and Bailey, E.H. (1974) — Mineral deposits and geology of Northern Oman, U.S.G.S. Project Report, Oman Investigations (IR) OM–1.

Crerar, D.A. and other (1982) — Manganiferous Cherts of the Fraciscan Assemblage I. General Geology, Ancient and Modern Analogues, and Implications for Hydrothermal Convection at Oceanic Spreading Centers, Economic Geology vol. 77. No. 3 p.519–540

Elboushi, I.M. and Zachariah, C. (1979) — Ras Al-Hadd Manganese deposits, The Sultanate of Oman, Mineral department directorate general of petroleum and minerals, Muscat.

Foreman, H.P. (1973) — Radiolaria of Leg 10 with systematics and ranges for the families Amphipyndacidae, Artostrobiidae, and Theoperidae. in Initial Report of the D.S.D.P., 10 Washing D.C. (U.S. Government Printing Office) 407–474

__________ (1977) — Mesozoic Radiolaria from the Atlantic basin and its borderlands. in Development in Paleontology and Stratigraphy 6; stratigraphic micropaleontology of Atlantic basin and borderlands (ed. F.M. Swan) 305–320 Elsevier

Glennie, K.W. and others (1974) — Geology of the Oman Mountains, Pt.I (Text) and Pt.II (Tables and Illustrations). Verh. Konink, Netherland Geolo. Mijnbowkundig Genootscap, Deel 31, p.1–423.

Gealey, W.K. (1977) — Ophiolite obduction and geologic evolution of the Oman Mountains and adjacent area, Geol. Soc. America Bull. V.88, p.1183–1191.

Graham, G.M. (1980) — Structure and sedimentology of the Hawasina Window, Oman Mountains, Unpub. report, Department of Earth Science, The Open Univ. p.1–422.

Hewett. D.F. (1966) — Stratified deposits of the oxides and carbonates of manganese, Econ. Geol. vo.61 No.3, p.431–461.

Iijima, A. (1982) — Siliceous sediments, Earth vol.4 No.8, p.478–484. (in Japanese)

JICA (1979) — Report on the survey for mineral resources development in the Sultanate of Oman.

JICA and MMAJ (1981) Report on geological survey of the Sultanate of Oman (Sur area) Phase 2

Krauskopt, K.B. (1979) Introduction to geochemistry, 2nd ed., New York, McGraw Hill p.617.

Pessagno, E.A. Jr (1977a) Upper Jurassic radiolaria and radiolarian biostratigraphy of the California Coast Ranges. Micropaleontology, 23. 56–113.

__________ (1977b) Lower Cretaceous radiolarian biostratigraphy of the Great Valley Sequence and Franciscan Complex, California Coast Ranges. Cushman Foundation for foraminiferal Research, Sep. Pub. No. 15, Washington.

Pettijohn, F.J. (1957) Sedimentary rocks, Harpper and Brothers, New York, N.Y.

Reinhardt, B.W. and Glennie, K.W. (1969) Some observation on mineral resources in the Oman Mountains, Koninklijke/Shell Exploration En Produktie Laboratorium, Rijswijk, The Netherland.

Roy, S. (1976) Ancient manganese deposits, in Wolf, K.H., ed., Handbook of stratabound and stratiform ore deposits. : Amsterdam, Elsevier Sci. Pub. Co. V7, p.395–476.

Schaaf, A., (1981) Late Early Cretaceous radiolaria from Deep Sea Drilling Project Leg. 62.
Initial Reports of the Deep Sea Drilling Project, 62, Washington (U.S. Government Printing Office)

Shooji, R. (1971) Petrology of sedimentary rocks, Asakura-shoten, p.1–285 (in Japanese).

Strakhov, N.M. and others (1967) Behavior of minor elements in sedimentary manganese mineralization, Bulletin of Geological Survey of Japan, vol.19, No.5 (Translated in Japanese by Moritani, T., 1968).

Zantop, H. (1980) Trace elements in volcanogenic manganese oxides and iron oxides, The San Francisco Manganese deposit, Jalisco, Mexico, Econ. Geol. vol. 76, No.3, p.545–555.

Watanabe, T., Yui, S. and Kato, A. (1970) Bedded manganese deposits in Japan, a Review, Tatsumi, T. (editor), volcanism and ore genesis, Tokyo Univ. Press, Tokyo, p.119–142.

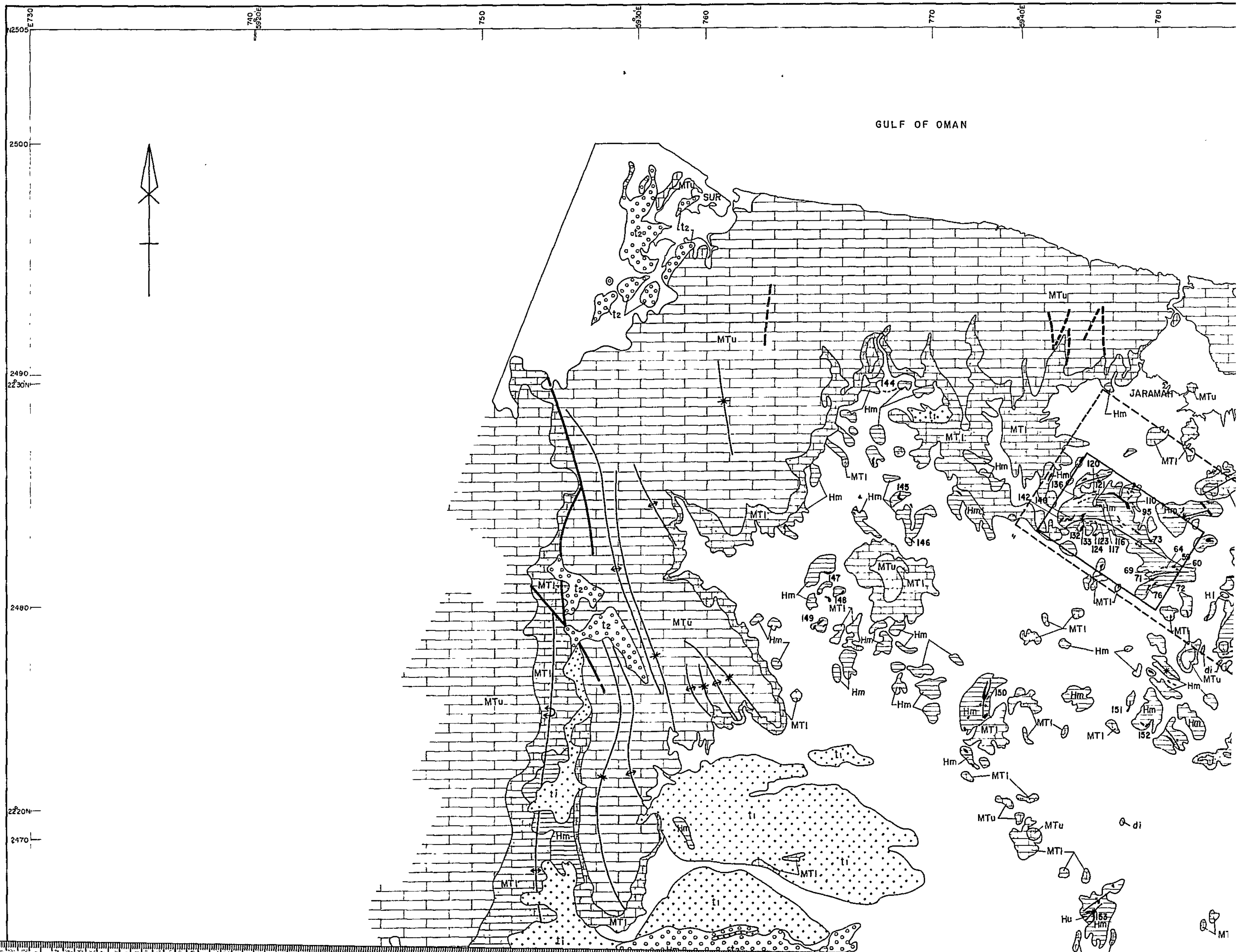

N2505
E730
740
59°20'E
750
59°30'E
760
770
59°40'E
780
2500
2490
22°30'N
2480
22°20'N
2470
GULF OF OMAN
SUR
JARAMAH
MTu
MTl
t2
ti
Hm
Hu
HI
di
144
145
146
147
148
149
150
151
152
153
120
121
136
142
140
132
133
123
124
116
117
110
95
73
64
59
60
69
71
72
76

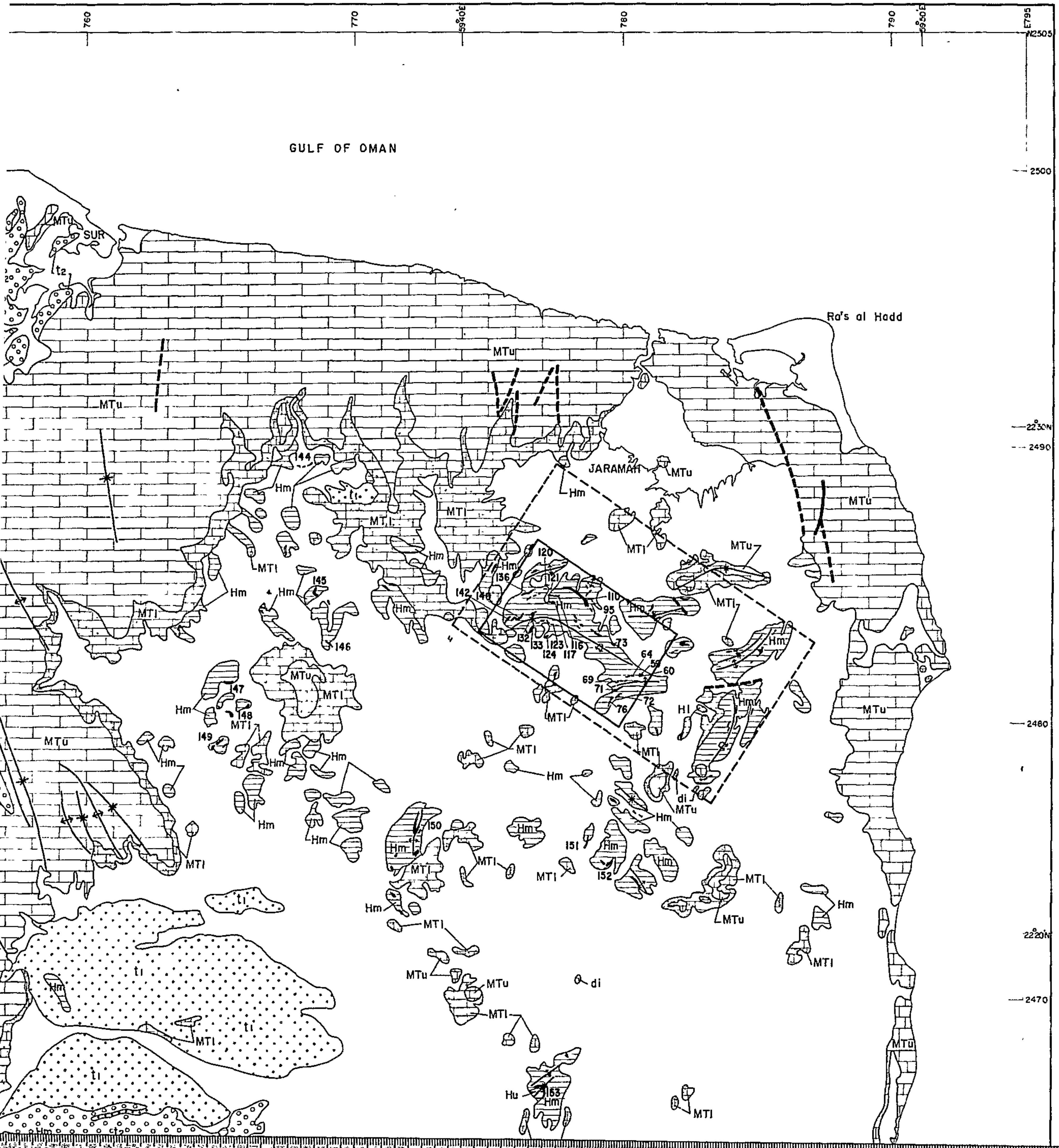

PL. 1

GEOLOGICAL SURVEY OF THE SULTANATE OF OMAN

Distribution Map of Manganse Outcrops of the Sur Area

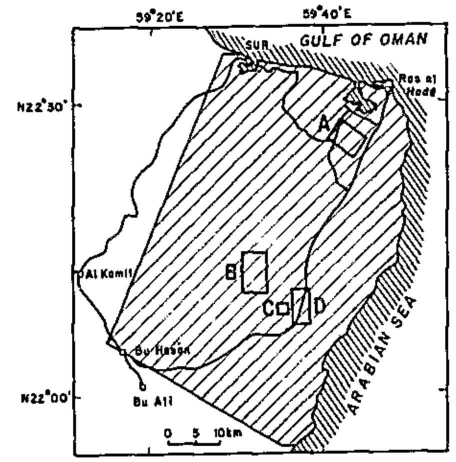

JAPAN INTERNATIONAL COOPERATION AGENCY
METAL MINING AGENCY OF JAPAN

March 1983

Prepared by Bishimetal Exploration Co., Ltd.

SCALE 1:100,000

0 — 5 — 10 KM

LEGEND

Quaternary		W		wadi sediments and talus sediments
		t2		terrace deposits (higher)
		t1		terrace deposits (lower)
Late Cretaceous ~ Middle Tertiary: Maastrichtian ~ Tertiary Limestone	Upper	MTu		limestone
		MTb		basalt lava
	Lower	MTl		sandy limestone, calcareous sandstone
Triassic ~ Early Cretaceous (Hawasina sediments): Halfa Formation	Upper	Hu		alternation of shale and limestone
	Middle	Hm		alternation of chert and shale
	Lower	Hl		alternation of chert and shale (chert<shale)

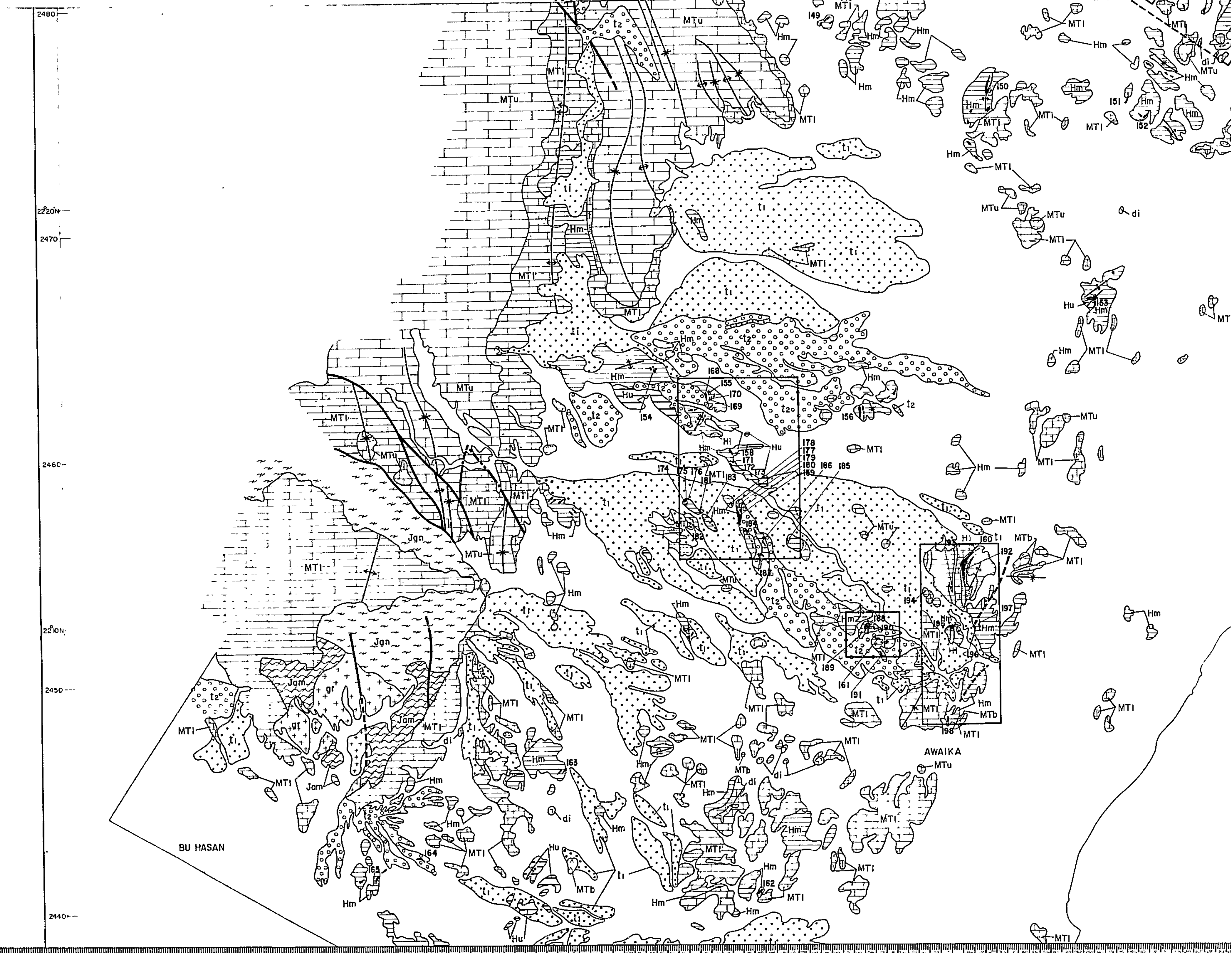

2480
2470
2460
2450
2440
MTu
MTl
Hm
Hu
t1
t2
Jgn
Jam
gr
di
MTb
AWAIKA
BU HASAN

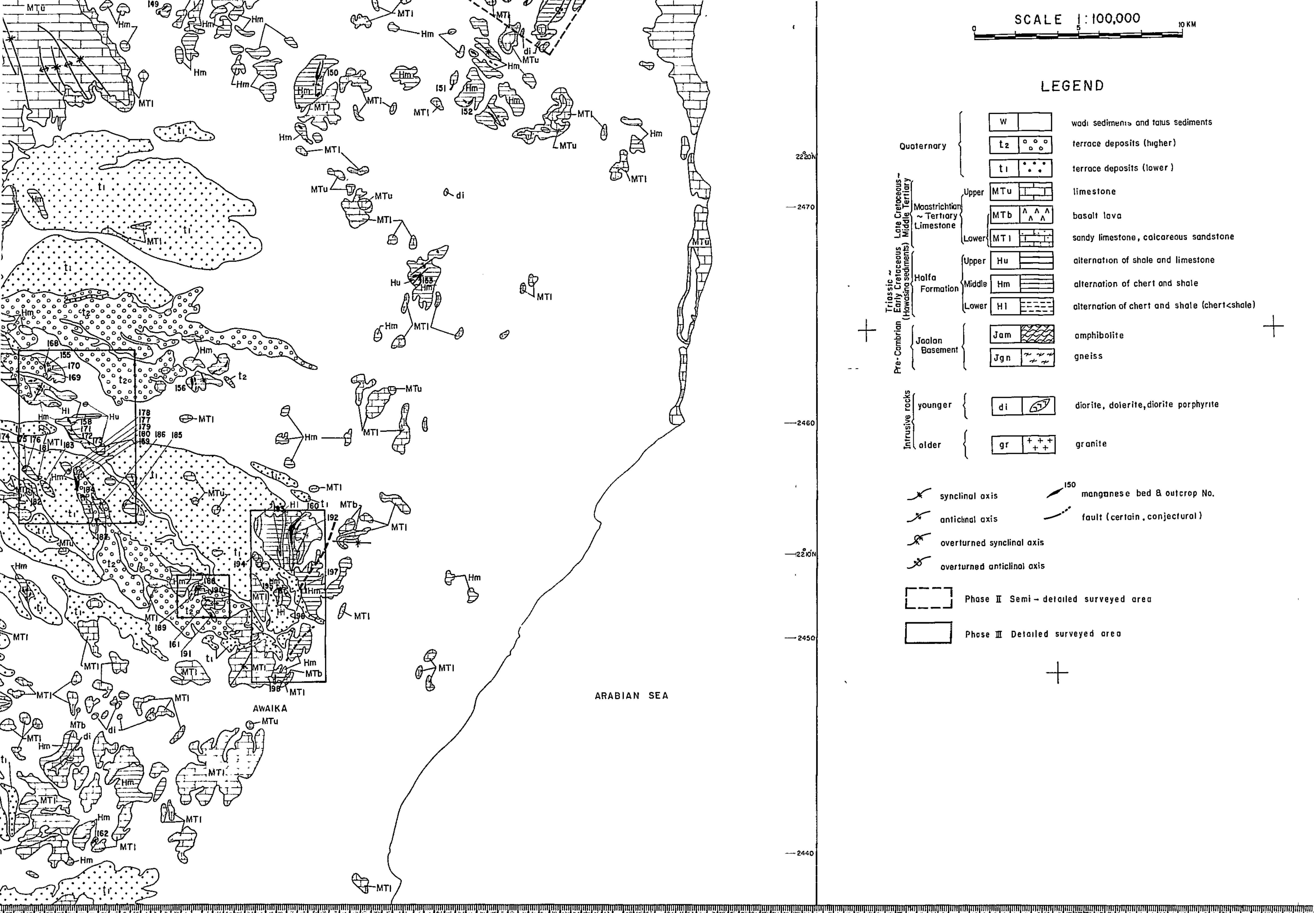

SCALE 1:100,000
0
5
10 KM
LEGEND
Quaternary
W wadi sediments and talus sediments
t2 terrace deposits (higher)
t1 terrace deposits (lower)
Late Cretaceous ~ Middle Tertiary
Maastrichtian ~ Tertiary Limestone
Upper MTu limestone
MTb basalt lava
Lower MTl sandy limestone, calcareous sandstone
Triassic ~ Early Cretaceous (Hawasina sediments)
Halfa Formation
Upper Hu alternation of shale and limestone
Middle Hm alternation of chert and shale
Lower Hl alternation of chert and shale (chert<shale)
Pre-Cambrian
Jaalan Basement
Jam amphibolite
Jgn gneiss
Intrusive rocks
younger di diorite, dolerite, diorite porphyrite
older gr granite
synclinal axis
anticlinal axis
overturned synclinal axis
overturned anticlinal axis
150 manganese bed & outcrop No.
fault (certain, conjectural)
Phase II Semi-detailed surveyed area
Phase III Detailed surveyed area
ARABIAN SEA
AWAIKA
22°20'N
22°10'N
2470
2460
2450
2440

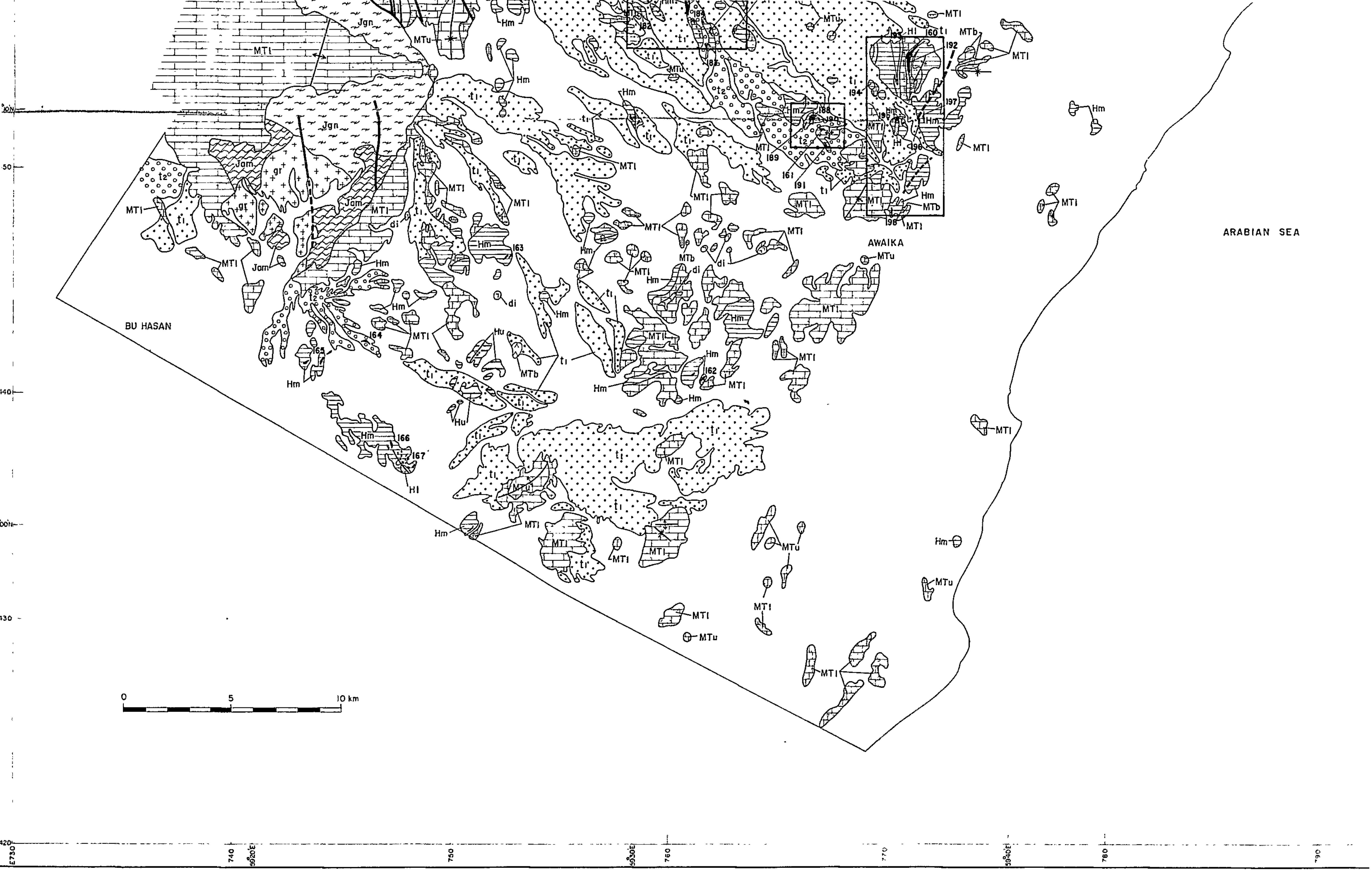
ARABIAN SEA
AWAIKA
BU HASAN
MTl
MTu
MTb
Hm
Hl
Hu
Hmz
Jgn
Jam
gr
di
t1
t2
0
5
10 km
50
440
430
420
E730
740
5920E
750
5930E
760
770
5940E
780
790

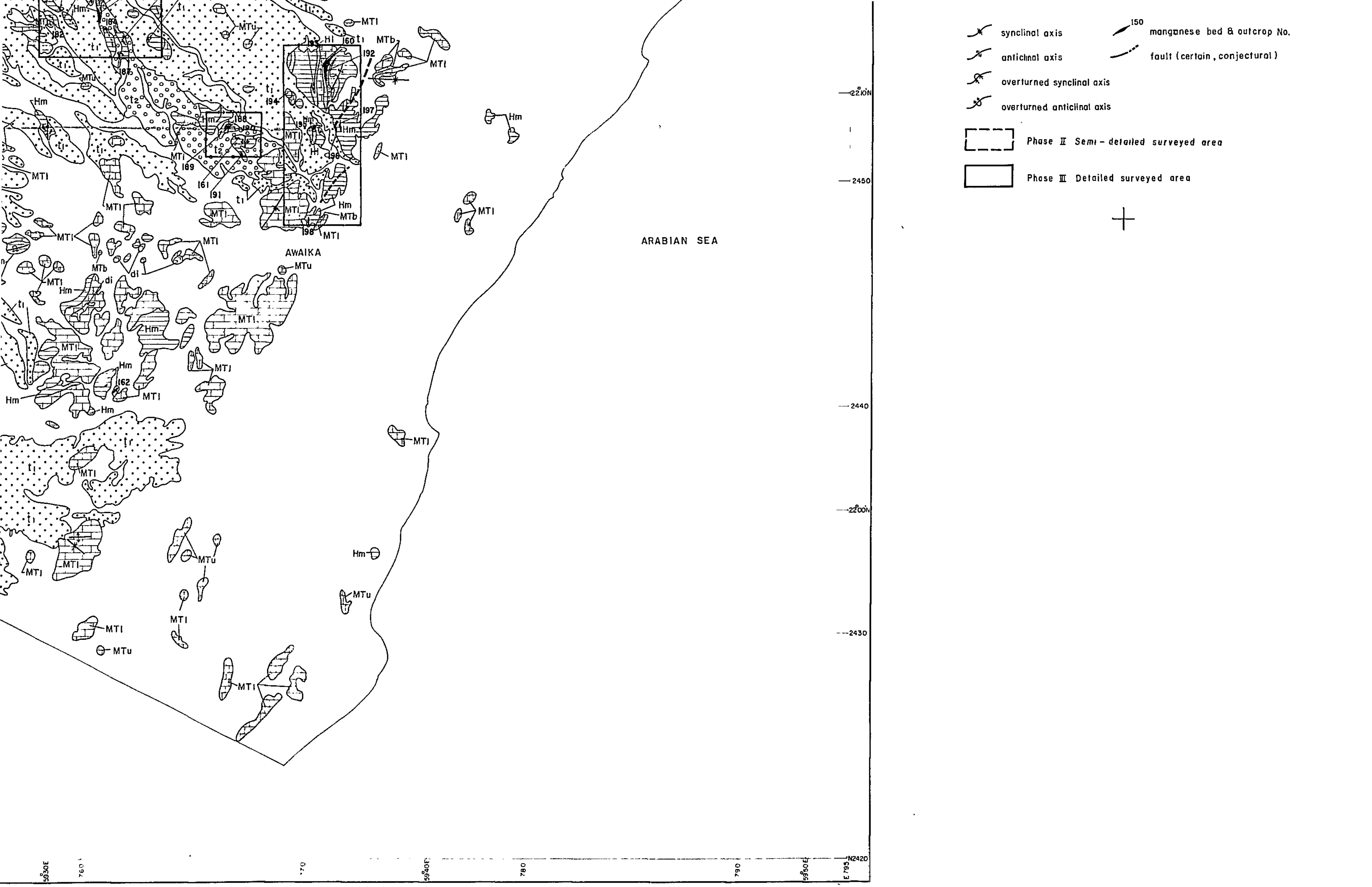
synclinal axis
anticlinal axis
overturned synclinal axis
overturned anticlinal axis
150 manganese bed & outcrop No.
fault (certain, conjectural)
Phase II Semi-detailed surveyed area
Phase III Detailed surveyed area
ARABIAN SEA
AWAIKA
MTl
MTu
MTb
Hm
Hl
t1
t2
di
22°10'N
22°00'N
2450
2440
2430
N2420
5930E
760
770
5940E
780
790
5950E
E795